Receptor-like protein-mediated sensing of cysteine-rich patterns in plants

Dissertation

der Mathematisch-Naturwissenschaftlichen Fakultät

der Eberhard Karls Universität Tübingen

zur Erlangung des Grades eines

Doktors der Naturwissenschaften

(Dr. rer. nat.)

vorgelegt von

Yuankun Yang

aus Shandong, China

Tübingen

2023

Gedruckt mit Genehmigung der Mathematisch-Naturwissenschaftlichen Fakultät der Eberhard Karls Universität Tübingen.

Tag der mündlichen Qualifikation:	29.11.2023
Dekan:	Prof. Dr. Thilo Stehle
1. Berichterstatter/-in:	PD Dr. Andrea Gust
2. Berichterstatter/-in:	Prof. Dr. Rosa Lozano-Durán

1 Abstract

1.1 English version

Plants deploy pattern recognition receptors (PRRs) to detect microbe or damaged-self-derived molecular patterns, thereby responding to biotic stresses. *Arabidopsis* Lysine-Rich Repeat Receptor Like Protein (LRR-RLP) RLP30 contributes to immunity against the necrotrophic fungus *Sclerotinia sclerotiorum* by recognizing a so far unknown pattern within Sclerotinia Culture Filtrate Elicitor 1 (SCFE1).

Here we identify the RLP30-ligand as a small cysteine-rich protein (SCP) that occurs in many fungi and oomycetes. RLP30 specifically binds SCP and forms a tripartite complex with co-receptor kinases SOBIR1 and BAK1 to mediate signaling. RE02 (Response to VmE02), an LRR-RLP non-homologous to RLP30, mediates SCP recognition in *Nicotiana benthamiana*. However, RLP30 and RE02 share little sequence similarity and respond to different parts of the native/folded protein. Moreover, some Brassicaceae other than *Arabidopsis* also respond to a linear SCP peptide instead of the folded protein, suggesting that SCP is an eminent immune target that led to the convergent evolution of distinct immune receptors in plants.

Surprisingly, RLP30 shows a second ligand specificity for a SCP nonhomologous protein secreted by bacterial Pseudomonads. Stable and ectopic expression of RLP30 in *Nicotiana tabacum* thus not only results in quantitatively lower susceptibility to fungal and oomycete pathogens, but also to bacterial infection, demonstrating that detection of immunogenic patterns by *Arabidopsis* RLP30 is involved in defense against pathogens from three microbial kingdoms. Our study therefore reveals an intricate network of plant immune recognition: a single PRR can monitor immune alerts derived from three microbial kingdoms and distinct immune-sensing mechanisms for one molecular pattern exist in Brassicaceae and Solanaceae.

Formerly, pattern-triggered immunity (PTI) on the plant surface and intracellular effector-triggered immunity (ETI) have been regarded as two separate branches of the plant immune system. However, it is now known that both pathways are interconnected and interdependent. As shown for other *Arabidopsis* RLPs, RLP30-mediated immune signaling depends on the lipase-like proteins EDS1 (enhanced disease susceptibility 1) and PAD4 (phytoalexin-deficient 4) and helper NLR (helper nucleotide-binding LRR receptor, RNL) ADR1, further solidifying the fact that PTI mediated by RLPs requires ETI components in *Arabidopsis*. However, EDS1 and RNLs are dispensable for SCP-triggered defenses in *N. benthamiana*, suggesting that the dependence of RLP signaling on EDS1-RNL modules is not conserved in *Arabidopsis* and *N. benthamiana*. Instead, the coiled coil-type helper NLR (CNL) NRCs (NLR Required for Cell death) are involved in the hypersensitive cell death induced by SCP and a few other RLP-ligands. In addition, nicotinamide, which inhibits TIR (Toll-interleukin 1 receptor) enzymatic activity, abolishes RLP-mediated cell death in *N. benthamiana*, implicating that a TNL (TIR-NLR receptor) and its derived small signaling molecules are required for RLP signaling. We thus speculate that a TNL-CNL tandem regulates RLP signaling in *N. benthamiana*.

1.2 German version

Pflanzen nutzen Mustererkennungsrezeptoren (PRRs), um molekulare Muster mikrobieller Herkunft oder von verändertem „Selbst“ zu erkennen und so auf biotischen Stress zu reagieren. *Arabidopsis* Lysine-Rich Repeat Receptor Like Protein (LRR-RLP) RLP30 trägt zur Immunität gegen den nekrotrophen Pilz *Sclerotinia sclerotiorum* bei, indem es ein bisher unbekanntes molekulares Muster im *Sclerotinia Culture Filtrate Elicitor* 1 (SCFE1) erkennt.

Hier identifizieren wir den RLP30-Liganden als ein kleines Cystein-reiches Protein (SCP), das in vielen Pilzen und Oomyceten vorkommt. RLP30 bindet spezifisch SCP und bildet zur Signalübertragung einen dreiteiligen Komplex mit den Co-Rezeptorkinasen SOBIR1 und BAK1. RE02 (*Response to VmE02*), ein LRR-RLP das nicht homolog zu RLP30 ist, vermittelt die SCP-Erkennung in *Nicotiana benthamiana*. RLP30 und RE02 weisen jedoch nur geringe Sequenzähnlichkeit auf und reagieren auf unterschiedliche Teile des nativen/gefalteten SCP-Proteins. Darüber hinaus reagieren einige Brassicaceae, außer Arabidopsis, auch auf ein lineares SCP-Peptid anstelle des gefalteten Proteins, was darauf hindeutet, dass SCP als wichtiges *Target* zur konvergenten Evolution unterschiedlicher Immunrezeptoren in Pflanzen führte.

Überraschenderweise zeigt RLP30 eine zweite Ligandenspezifität für ein nichthomologes SCP-Protein, das von bakteriellen Pseudomonaden sekretiert wird. Die stabile und ektopische Expression von RLP30 in *Nicotiana tabacum* führt entsprechend nicht nur zu einer quantitativ geringeren Anfälligkeit gegenüber Pilzen und Oomyceten, sondern auch gegenüber Bakterien. Die Erkennung immunogener Muster durch Arabidopsis RLP30 ist also an der Abwehr von Krankheitserregern aus drei mikrobiellen Reichen beteiligt. Unsere Studie deckt daher ein komplexes Netzwerk der pflanzlichen Immunerkennung auf: Ein einziger PRR kann molekulare Muster von drei Mikrobenreichen erkennen, und in Brassicaceae und Solanaceae gibt es unterschiedliche Immunerkennungsmechanismen für ein und dasselbe molekulare Muster.

Bisher wurden die mustergesteuerte Immunität (PTI) auf der Pflanzenoberfläche und die intrazelluläre effektorgesteuerte Immunität (ETI) als zwei getrennte Zweige des pflanzlichen Immunsystems betrachtet. Mittlerweile ist jedoch bekannt, dass beide Wege miteinander verbunden und voneinander abhängig sind. Wie für andere Arabidopsis-RLPs gezeigt, hängt die RLP30-vermittelte Immunantwort von den Lipase-ähnlichen Proteinen EDS1 (*Enhanced Disease Susceptibility* 1) und PAD4 (*Phytoalexin Deficient* 4) sowie dem Helfer-NLR (Nukleotid-bindender LRR-Rezeptor, RNL) ADR1 ab. Dies bestätigt, dass die durch RLPs vermittelte PTI auch ETI-Komponenten in *Arabidopsis* benötigt. In *N. benthamiana* werden EDS1 und RNLs für die SCP-ausgelöste Immunantwort allerdings nicht gebraucht, anscheinend ist also die für Arabidopsis RLPs beobachtete Abhängigkeit von EDS1-RNL-Modulen nicht in *N. benthamiana* konserviert. Stattdessen sind die Coiled-Coil-Helfer-NLR (CNL) NRCs (*NLR Required for Cell Death*) am durch SCP und einigen anderen RLP-Liganden ausgelösten hypersensitiven Zelltod beteiligt. Darüber hinaus verhindert der TIR (Toll-Interleukin-1-Rezeptor)-Inhibitor Nicotinamid den RLP-vermittelten Zelltod in *N.*

benthamiana, so dass für die RLP-vermittelte Signalweiterleitung wahrscheinlich ein TNL (TIR-NLR-Rezeptor) und die entsprechend generierten kleinen Signalmoleküle erforderlich sind. Wir spekulieren daher, dass die RLP-Signalübertragung in *N. benthamiana* über ein TNL-CNL-Tandem reguliert wird.

2 Introduction

2.1 The plant innate immune system

Plants are exposed to complex environments and are constantly challenged by a plethora of potential pathogens such as bacteria, fungi, oomycetes and viruses. However, plants have evolved a two-tiered innate immune system to fend off harmful infections. Pattern recognition receptors (PRRs) at the plasma membrane perceive pathogen/damage/microbe/herbivore-associated molecular patterns (PAMPs/DAMPs/MAMPs/HAMPs) to initiate pattern-triggered immunity (PTI). Host-adapted microbes secrete effectors to shut down PTI-associated immune responses, which results in effector-triggered susceptibility (ETS). In resistant plants effectors are sensed by intracellular nucleotide binding leucine-rich repeat receptors (NLRs) to induce what is typically referred to as effector-triggered immunity (ETI). The interaction between PTI, ETS, and ETI was incorporated into the widely cited “zig-zag-zig” intellectual framework[1,2].

2.2 PTI

PRRs containing leucine-rich repeat (LRR) ectodomains are divided into receptor-like kinases (hereafter referred to as RLK) or receptor-like proteins (hereafter referred to as RLP) based on the presence or absence of a cytoplasmic kinase domain. Due to the lack of functional cytoplasmic domains, immunity-related RLPs usually cooperate with the adapter Suppressor of Brassinosteroid Insensitive 1 (BRI1)-Associated Kinase (BAK1)-Interacting Receptor Kinase 1 (SOBIR1) in a ligand-independent manner, and upon pattern sensing recruit members of the SERK (Somatic Embryogenesis Receptor Kinase) family such as Brassinosteroid Insensitive 1 (BRI1)-Associated Kinase (BAK1)[3]. RLPs/SOBIR1/BAK1 tertiary complexes are proposed to be functionally equivalent to RLKs/BAK1 heteromeric complexes to jointly transmit intracellular immune signals[3]. Upon PAMP perception by cognate PRRs, numerous signaling events are initiated, including production of reactive oxygen species (ROS), mitogen-activated protein kinase (MAPK) cascades, callose deposition, and transcriptional programming, together culminating in PTI[4].

2.2.1 RLP-mediated immunity

Multiple RLPs from Brassicaceae and Solanaceae have been identified to sense patterns from pathogens and herbivores.

In *Arabidopsis*, the LRR-RLPs RLP1, RLP23, RLP30, RLP32 and RLP42 have been described to be capable of sensing an enigmatic MAMP (eMax) conserved in different *Xanthomonas* species, Nep1-like proteins (NLPs) from various bacteria, oomycetes, and fungi, proteobacterial Translation Initiation Factor 1 (IF1), *Sclerotinia sclerotiorum* filtrate elicitor1 (SCFE1) and fungal polygalacturonases (PGs), respectively[5–9]. Nlp20, a conserved 20 amino acid (aa) fragment from NLPs, IF1 and pg13, a conserved 9-amino-acid fragment within PGs, directly bind to their corresponding RLPs and induce SERK recruitment to form triple complexes for immune activation[5,6,9]. In addition, RLPs are also involved in resistance

to pathogens in other Brassicaceae. *Brassica napus* resistance to *Leptosphaeria maculans* is determined by BnLepR3/BnRLM2-mediated recognition of AvrLm1/AvrLm2[10,11].

In tomato, the LRR-RLPs Cf2, Cf4, and Cf9 confer resistance to *Cladosporium fulvum* (Cf) by recognizing their corresponding avirulence (Avr) genes encoding the Cys-rich proteins Avr2, Avr4, Avr5, and Avr9, respectively[12,13]. In addition to Cf/Avr pairs, other RLP/PAMP pairs have been identified in tomato plants. The first discovered and most extensively studied Trichoderma PAMP known as ethylene inducing xylanase (EIX) elicits plant defenses in responsive tomato plants. However, the response to EIX in tomato cultivars is controlled by a dominant locus, which contains two RLPs, SlEIX1 and SlEIX2. Although both receptors are able to bind the EIX elicitor, only SlEIX2 is responsible for EIX-triggered defense[14]. SlEIX1 acts as a decoy receptor and attenuates SlEIX2-mediated EIX perception in a BAK dependent manner[15]. In addition to microbial pathogens, tomato RLPs are also involved in defense against parasitic plants. For example, the LRR–RLP CuRe1 perceives the peptide Crip21 derived from a Cuscuta glycine-rich cell wall protein[16].

Interestingly, *Nicotiana tabacum* has been reported to sense EIX by an unknown receptor, whereas *Nicotiana benthamiana*, which is closely related to *N. tabacum*, lacks the receptor for EIX recognition[14]. However, NbEIX2, an ortholog of SlEIX2 in *N. benthamiana*, was recently found to mediate cell death and defense responses induced by the EIX-like protein (VdEIX3) from *Verticillium dahliae*[17]. Strikingly, inconsistent with immune-related RLPs in *Arabidopsis* or Cf proteins in tomato, neither SlEXI2 nor NbEIX2-mediated immunity is dependent on the co-receptor BAK1, and NbEXI2-mediated cell death even does not require SOBIR1[15,17]. Other examples for RLPs in solanaceous plants are RXEG1, RE02 and REL in *N. benthamiana* which sense glycoside hydrolase 12 protein XEG1 from *Phytophthora sojae*, small cysteine-rich protein VmE02 from *Valsa mali*, and elicitins from *Phytophthora infestans*, respectively[18–20]. RXEG1, the so far only LRR-RLP whose crystal structure was reported, binds to its ligand XEG1 through an amino-terminal and a carboxy-terminal loop-out region (RXEG1(ID)) to further facilitate its association with the co-receptor BAK1[21]. Moreover, the binding of RXEG1 to the active site of XEG1 inhibits XEG1 endoglucanase activity and impairs its virulence function in *Phytophthora* infection of *N. benthamiana*[21].

In other plant species, cowpea (Vigna unguiculata) inceptin receptor (INR) confers responses to the 11-amino acid inceptin peptide in caterpillar oral secretions which is cleaved from the chloroplastic ATP synthase during caterpillar herbivory[22]. Moreover, the wild potato receptor elicitin receptor ELR mediates the broad-spectrum recognition of elicitin proteins from *Phytophthora* spp. Importantly, transfer of ELR into cultivated potato resulted in enhanced resistance to *P. infestans*[23].

2.2.2 RLK-mediated immunity

In *Arabidopsis*, receptor like kinases (RLKs) are classified into 44 subfamilies based on their kinase domains[24]. As the largest subfamily of RLKs, LRR-RLKs are also the most thoroughly characterized RLKs in plants. Two well-studied immunity-related LRR-RLKs in *Arabidopsis* are Flagellin Sensing 2 (FLS2) and Elongation Factor-Tu Receptor (EFR), which are involved

in antibacterial immunity by perceiving the conserved 22-amino acid peptide (flg22) derived from bacterial flagellin and the bacterial peptide epitope elf18 derived from bacterial Elongation Factor Tu (EF-Tu), respectively[25,26]. Upon binding their specific PAMP ligands, LRR-RLKs form heteromeric receptor complexes with co-receptors of the SERK family such as BAK1 for activation of intracellular immune signaling and induction of defense responses[27].

Although flagellin is sensed by a large number of plants, the immunogenic epitopes necessary for recognition and the cognate receptors vary among plant species. For instance, tomato encodes FLS2 but also an additional flagellin receptor, Flagellin-Sensing 3 (FLS3), which senses another flagellin epitope flgII-28 that is distinct from flg22[28]. Other well-studied bacterial peptides are RaxX21 and csp22 derived from the RaxX tyrosine-sulphated protein and the cold shock protein, which are perceived by the rice RLK XA21 and the tomato RLK CORE, respectively[29,30]. Both receptors require the co-receptor BAK1 to trigger signal transduction.

Plants also employ LRR-RLKs to perceive damage-associated molecular patterns (DAMPs) from damaged or infected tissues. Damage-activated metacaspases cleave precursor PROPEPs to generate PEPs (AtPep1, AtPep2 and AtPep3) that are perceived by the RLKs PEPR1 and PEPR2 in *Arabidopsis*[31,32]. Similarly, multiple phytocytokines are also upregulated during immunity. For instance, two pathogen-induced endogenous peptides PIP1 and PIP2 are processed in the apoplast before being recognized by RLK7 [33]. In addition, the *Arabidopsis* RLK MIK2 participates in the perception of the phytocytokine SCOOP peptides and SCOOP-like peptides from Fusarium, suggesting that MIK2 is involved in both self and fungal recognition[34,35]. Finally, systemin, an 18 amino acid peptide from Solanaceae, is sensed by the RLKs SYR1 and SYR2 to induce immunity against insect herbivory[36].

2.2.3 Other types of receptor-mediated immunity

While the majority of characterized PRRs feature an LRR-type extracellular ectodomain (ECD), many other types of PRRs have been identified in plants. The lysin-motif (LysM)-Containing Receptor-Like Kinase 5 (LYK5) is a major chitin receptor in *Arabidopsis* and associates with the LysM-RLK Chitin Elicitor Receptor Kinase 1 (CERK1) to form a chitin-induced complex for regulating antifungal immunity[37,38]. In rice, the glycosylphosphatidylinositol (GPI)-anchored LysM receptor-like protein (RLP) OsCEPIB rather than OsCERK1 directly binds chitin, whereas OsCERK1 acts as a co-receptor to initiate chitin-induced signaling via its cytoplasmic kinase domain[39,40]. Plant PRRs have been shown to perceive a range of extracellular self-molecules. For example, quinone, ATP, and NAD^+ are sensed by CARD1, DORN1, and LecRK-1.8 in *Arabidopsis*, respectively[41–43]. The G-lectin Receptor Kinase Lipooligosaccharide-specific reduced elicitation (LORE) recognizes bacterial 3-OH-FAs (Medium-chain 3-hydroxy fatty acids)[44]. The two non-LRR type PRRswall-associated kinase AtWAK1/2 are proposed to recognize plant cell wall-derived oligogalacturonides (OGs) and pectin[45]. Besides, the wheat (*Triticum aestivum*) TaWAK detects SnTox1 (host-selective toxin1) from the necrotrophic fungal pathogen *Parastagonospora nodorum*[46].

2.3 ETI

To counter pathogen attack, in addition to receptors on the cell surface, plants also deploy intracellular nucleotide-binding/leucine-rich repeat receptors (NLRs). Recognition of pathogen-derived effectors by NLRs leads to effector-triggered immunity (ETI) which provides robust defense responses that are often associated with an induced cell death, called the hypersensitive response (HR)[1,47]. A typical NLR is composed of three domains: a variable N-terminal domain, a conserved nucleotide-binding (NB) domain and a C-terminal LRR domain[48]. NLRs are subdivided into three main groups based on their N-terminal domains: those containing a TIR (Toll/interleukin-1 receptor and resistance) domain (TNLs), those with an N-terminal CC (coiled-coil) domain (CNLs) or those with an CC (coiled-coil) domain related to RPW8 (resistance to powdery mildew 8) (RNLs, also known as helper NLRs)[48].

In general, while the CC or TIR domain acts as the signaling moiety, the NB domain controls the 'on' and 'off' signaling states of the NLR by binding adenosine diphosphate (ADP) or adenosine triphosphate (ATP), respectively[48]. The LRR domains of TNLs are responsible for effector-specific recognition. As a central event in ETI activation, the intracellular effector recognition is performed by plant NLR proteins either directly through physical interactions or indirectly through intermediate partners.

2.3.1 TNL-mediated immunity

So far, the most well-studied TNLs with known crystal structures are RPP1 (Recognition of *Peronospora parasitica* 1) and Roq1(Recognition of XopQ 1) identified in *Arabidopsis thaliana* and *Nicotiana benthamiana*, respectively. While RPP1 confers resistance against the downy mildew pathogen *Hyaloperonospora arabidopsidis* through recognition of the effector ATR1, Roq1 associates with the recognized effector XopQ from *Xanthomonas* and its close homolog HopQ1 from *P. syringae* and is involved in antibacterial immunity[49,50].

Cryo-electron microscopy (cryo-EM) studies on Roq1-XopQ and RPP1-ATR1 complexes showed that the LRR domain of these two TNLs participates in direct binding of their ligands during pathogen perception. TNL activation upon ligand recognition results in an exchange of ADP to ATP in the NB domain and the formation of a tetrameric structure, termed a “resistosome”. The four LRR domain-effector complexes spread out at one end, while the NB domain oligomerizes at the center, thereby driving the TIR domain to self-associate at the other end of the cylinder[51,52]. The tetrameric resistosome formation of TNLs induces an NADase enzymatic function of the TIR domains and exposes its NADase catalytic sites in the interface[53]. The activated TNLs initiates the degradation of NAD+/NADP+ and the hydrolysis of DNA/RNA substrates, leading to the production of (cyclic-)ADP-ribose ((c)ADPR) isomer products and the synthesis of 2’,3’- cAMP/cGMP, respectively[54].

Subsequently, TNL-activated disease resistance and cell death largely depend on the EDS1 (enhanced disease susceptibility 1) family, including EDS1, PAD4 (phytoalexin Defect 4) and SAG101 (senescence-associated Gene 101). EDS1 directly associates with PAD4 or SAG101 to form two core immune regulatory modules of the heterodimer structure to regulate

immune signaling[55]. While pRibAMP/ADP binds to EDS1/PAD4 complexes, ADPr-ATP/di-ADPR binds to EDS1/SAG101 complexes. In both cases, small molecule binding leads to a conformational change in the EDS1 complex and results in downstream immune output[56,57].

2.3.2 CNL-mediated immunity

The first cryo-electron microscopy (EM) structure of plant CNLs is *Arabidopsis* ZAR1 (HopZ-activated resistance) which is indirectly involved in the recognition of the *Xanthomonas campestris* effector AvrAC through the two receptor-like cytoplasmic kinases RKS1 and PBL2. RKS1 constitutively associates with the LRR domain of ZAR1. PBL2 is uridylated by AvrAC and is recruited to the RKS1–ZAR1 complex to activate ZAR1[58]. In contrast to ROQ1 and RPP1 each forming a tetrameric resistosome that resembles a four-leaf clover, activated ZAR1 forms a pentameric resistosome, which functions as a calcium-permeable channel on the plasma membrane through its CC domain, leading to Ca^{2+} ion flux that is required for the hypersensitive cell death[59,60].

Recently, the cryo-EM structure of wheat CNL Sr35 in complex with the effector AvrSr35 from wheat stem rust pathogen was reported[61]. Effector binding to the LRR domain of Sr35 leads to the formation of a pentameric Sr35-AvrSr35 complex (Sr35 resistosome) which shares striking structural similarity with the *Arabidopsis* ZAR1 resistosome, including arginine cluster in the LRR domain and Ca^{2+} channel activity, which suggests the evolutionary conservation of CNL-resistosomes in plants[62].

2.3.3 RNL-mediated immunity

So far, all characterized TNLs and some CNLs in *Arabidopsis thaliana* function as effector sensors that require the presence of RNLs (also termed helper NLRs) to activate full immunity. In *Arabidopsis*, there are two helper NLR families: ACTIVATED DISEASE RESISTANCE (ADRs) and N REQUIREMENT GENE (NRGs)[63]. These two functionally redundant helper families have specific functions in downstream signaling of sensor NLRs. While ADR1s are predominantly involved in mediating resistance (including SA accumulation, transcriptional reprogramming and restriction of pathogen growth), NRG1s function mainly in cell death induction. However, in some specific cases, RLRs can rescue each other, such as ADR1 mediates RPS1/RPS4-mediated cell death in *Arabidopsis* when NRG1s and the salicylate pathway are disrupted[64,65]. Interestingly, NRG1 has already been shown to mediate resistance against tobacco mosaic virus and *Pseudomonas syringae* infections in *N. benthamiana*, since knockdown of ADR1 does not affect resistance responses[66].

EDS1-PAD4 and EDS1-SAG101 heterodimers work together with ADR1 and NRG1, respectively, forming two parallel signalling pathways[55]. It has been demonstrated that the EDS1-SAG101-NRG1 module is responsible of inducing cell death mediated by TNLs and some CNLs, whereas the EDS1-PAD4-ADR1 module provides basal immunity mediated by both TNLs and CNLs in *Arabidopsis*[67]. However, immunity activated by all TNLs tested so far in *N. benthamiana* is associated with the EDS1-SAG101-NRG1 module, while there is currently no evidence that the EDS1–PAD4–ADR1 module is required for activation of

immunity in *N. benthamiana*[68]. Similar to CNL-resistosomes as Ca^{2+} cation channels, both activated helper NLRs form high-weight complexes to promote Ca^{2+} influx via self-association and ultimately cause cell death[69].

In Solanaceae, initiation of immune signaling by sensor NLRs generally dependents on a series of downstream helper NLRs which are called NRCs (NLRs required for cell death)[70]. Sensor NLRs and NRCs constitute a unique and complex signaling network architecture in Solanaceae to mediate immunity against a wide array of plant pathogens including bacteria, oomycetes, nematodes, aphids and viruses[71]. Like ADR1 and NRG1, NRCs are also functionally redundant in mediating cell death and disease resistance[71]. NRCs contain a key signature known as the MADA motif at their N-terminus, which is essential for the induction of cell death. The MADA motif is functionally conserved in CLRs (e.g. ZAR1 and Sr35) and NRCs, suggesting that the "cell death switch mechanism" of ZAR1 resistosome might also apply for NRCs[72]. Indeed, recent studies suggest that sensor NLRs perceive their corresponding effectors and promote downstream NRC assembly into pentameric NRC-resistosomes[73].

2.4 PTI-ETI crosstalk

Although PRR- and NLR-activated immunity have been long-considered as separate pathways due to their distinct activation mechanisms, PTI and ETI share many similar downstream outputs, including an induction of a ROS burst, Ca^{2+} influx, MAPK phosphorylation and transcriptional reprogramming, which suggests that there is an inextricable relationship between PTI and ETI. Recently, four papers published in Nature collectively revealed the existence of intricate interactions between PTI and ETI[74]:

On the one hand, PRRs in the PTI pathway are required for the full activation of ETI. Specifically, cell death triggered by the effectors AvrRpt2, AvrPphB, and AvrRps4 delivered by *P. syringae* pv. *tomato* (*Pst*) DC3000 is markedly impaired in *Arabidopsis* PRR mutants *fls2 efr cerk1* (fec triple mutant) and PRR-coreceptor mutants *bak1 bkk1 cerk1* (bbc triple mutant)[75,76]. In addition, *fls2 efr* and *bak1-5 bkk1-1* double mutants also show higher susceptibility to *Pst* DC3000:AvrRps4 infection[75]. Moreover, PRRs and the RLCK BIK1 are required for ROS production during ETI[75,76]. Together, these results suggest that ETI-mediated antibacterial immunity requires PTI components.

On the other hand, PTI activation also requires key players of the ETI pathway. While both EDS1- PAD4 and EDS1-SAG101 modules are essential for ETI, however, only EDS1 and PAD4 are required for PTI, as ethylene and ROS accumulation, salicylic acid (SA) production, callose deposition, and resistance to *Pst* DC3000 induced by nlp20 were greatly reduced in *eds1* and *pad4* mutants compared to wild-type plants[77]. The helper NLR ADR1 that works together with EDS1-PAD4 is also required for nlp20-induced PTI. Indeed, nlp20-induced defense responses are compromised in *adr1* triple mutants[77,78]. Altogether, these data demonstrate that the EDS1/PAD4/ADR1 node participates in RLP-mediated immunity, and SOBIR1 as a bridge connects RLPs and this node[79].

Besides, ETI and PTI can potentiate each other to generate stronger defense responses against pathogen infections[76]. Flg22 treatment results in much stronger cell death caused by AvrRpt2 in *Arabidopsis*. ETI activation can also induce higher expression of many PTI regulators, such as BAK1, BIK1 (Botrytis–induced kinase 1), XLG2 (Extra large G-protein 2), and AGB1 (Arabidopsis GTP Binding Protein). In agreement with these data, both the TNL RPS4- and the CNL RPS2-activated ETI can increase and prolong the production of PTI-ROS[76]. In addition, the coactivation of PTI and ETI leads to more callose deposition and higher expression of PTI-marker genes[75].

2.5 Aim of the work

The *Arabidopsis* Receptor-Like Protein 30 (RLP30) has already been shown to mediate basal resistance to the fungus *Sclerotinia sclerotiorum,* but the identity of the proteinaceous PAMP detected by RLP30 remained open. The aims of this work were (1) the identification of RLP30 ligand(s), (2) the recognition mechanism of this ligand in different plant families, (3) assessing the potential of RLP30 for crop improvement, (4) exploring RLP signaling in Brassicaceae and Solanaceae.

3 Materials and Methods

3.1 Materials

3.1.1 Plant Materials

Arabidopsis plants were grown in soil for 7-8 weeks in a growth chamber under short-day conditions (8 h photoperiod, 22°C, 40%–60% humidity). *Arabidopsis* natural accessions have been previously described, mutant lines and derived complemented transgenic lines used in this study are listed in Supplementary Table 1.

Solanaceae and *Brassica* plants were grown in a greenhouse at 23 °C under long-day conditions of 16 h of light and 60–70% humidity. Mutant lines of *N. benthamiana* used in this study are listed in Supplementary Table 2.

3.1.2 Chemical and Kits

Chemicals in standard purity were ordered from Carl Roth (Karlsruhe), Sigma-Aldrich (US), Thermo Fisher Scientific (Karlsruhe) and Merck (Darmstadt).

Phusion DNA Polymerase (F530S), Restriction enzymes, T4 ligase (EL0011) and Gibson Assembly Cloning Kit (E5510S) were purchased from Thermo Fisher Scientific (St. Leon-Rot) and NEB (Beverly, USA).

Hi Yield® Gel/PCR DNA Fragment Extraction Kit (HYDF300) and Hi Yield® Plasmid Mini Kit (30 HYPD300) were ordered from Süd-Laborbedarf Gauting (Gauting).

Primary antibodies were purchased from Abcam (α-6xHis (ab18184) and α-RFP(ab185921)), SICGEN (α-GFP (AB0020)), SIGMA (α-HA (H3663) and α-myc (M4439)), Agrisera (α-SOBIR1 (AS16 3204) and α-BAK1 (AS121858)) and Cell Signaling Technology (α-p42/44 (AS121858)).

3.1.3 Genes and Peptides

The genes encoding the elicitors (SCP^{Ss}, SCP^{Bc} ,SCP^{Pi} and $SCP^{C\text{-}S}$ mutants) were synthesized by GenScript (China). RE02, EIX1 and EIX2 were cloned from the genomic DNA of *N. benthaminana* and tomato using primers listed in Supplementary Table 3.

The peptides (flg22, nlp20, and SCP^{Ss}C3C5) were synthesized by GenScript and prepared as 10 mM stock solutions in 100 % dimethyl sulfoxide (DMSO) and diluted in water to the desired concentration before use.

3.1.4 Constructs

The constructs used in this study were constructed by gateway, Golden Gate cloning or Gibson assembly methods, and listed in Supplementary Table 4. All these constructs can be found in the plasmid list of Andrea Gust group.

3.2 General molecular biology methods

3.2.1 Cloning

All primers used for cloning or sequencing are listed in Supplementary Table 3.

For expression of SCP^{Ss} in *N. benthamiana* leaves, the SCP^{Ss} and SCP cysteine-to-serine (SCP$^{C\text{-}S}$) mutant sequences were cloned into the pBIN-plus vector with a C-terminal GFP tag using Gibson Assembly (NEB).

For recombinant protein expression in *Pichia pastoris* KM71H (Multi-Copy Pichia Expression Kit Instructions, Thermo Fisher Scientific), constructs encoding *SCP^{Ss}*, *SCP^{Bc}*, *SCP^{Pi}*, truncated *SCP^{Ss}* versions and cysteine-to-serine replacements (all without signal peptide and Stop codon) were cloned into the secretory expression plasmid pPICZalphaA (Thermo Fisher Scientific). Individual cysteine-to-serine replacements in SCP^{Ss} were amplified from synthetic genes (gBlocks, Integrated DNA Technologies) using primers extended by restriction sites *Eco*RI and *Bam*HI (Table 5) and cloned into pPICZalphaA.

For the generation of transgenic *rlp30-2* lines expressing *p35S::RE02-GFP*, *p35S::EIX1-GFP* or *p35S::EIX2-GFP*, the coding sequences of RE02, EIX1 or EIX2 extended by *Bsa*I cleavage sites (via PCR, primer sequences listed in Table 4) was cloned into the pGEM®-T vector (Promega). The cauliflower mosaic virus 35S promoter, RE02, EIX1 or EIX2 coding sequences and GFP-tag were assembled via golden gate cloning in the vector LII_F_1-2_-_BB10c[8].

For 35S-promoter-driven stable expression of RLP30-YFP in *rlp30-2* mutants or RLP30-RFP and SOBIR1-GFP in *N. tabacum L*. var. Samsun NN, RLP30 and SOBIR1 coding sequences were first cloned into pCR™8/GW/TOPO™ (Thermo Fisher Scientific) and subsequently fused via Gateway cloning to a C-terminal YFP (pB7YWG2), RFP (pB7RWG2) or GFP (pK7FWG240)[5], respectively. Primers used are also listed in Table 4.

For 35S-promoter-driven transient protein expression in *N. benthamiana or N. tabacum*, coding sequences of respective genes were amplified using the primers listed in Table 4, cloned into pCR™8/GW/TOPO™ (Thermo Fisher Scientific) and subsequently recombined via Gateway cloning into pGWB5 (C-terminal GFP-tag), pGWB14 (C-terminal HA-tag), or pGWB17 (C-terminal Myc-tag)[5]. Likewise, a pENTR/D-Topo (Thermo Fisher Scientific) clone containing the coding sequence for *NbSOBIR1* and *SlSOBIR1* was recombined with pGWB14. Transient protein expression in *Nicotiana* and constructs for *AtSOBIR1-HA*, *BAK1-myc* and *RLP23-GFP* have been previously described[5].

3.2.2 Transformation of bacteria

For transformation of chemically competent *E. coli* DH5α, 50 ul of competent cells were mixed with 200 ng of plasmid DNA and incubated on ice for 30 minutes. After heat incubation at 42°C for 30 s, the cells were incubated on ice for 2 min. 600 µl LB medium was added to the *E. coli* cells and incubated for 1 hour at 37°C with shaking at 220 rpm. 100 µl of the cell mixture was spread on selective LB agar plates and incubated at 37°C for overnight.

For the transformation of competent *A. tumefaciens* cells GV3101, 50 µl of cells and 200 ng of plasmid DNA were mixed and transferred to a pre-cooled electroporation cuvette, then incubated on ice for 10 min. The cells were pulsed once with 1500V via the Electroporator 2510 (Eppendorf), and 1 ml LB medium was added to the cuvette. The cells were transferred to a fresh Eppendorf tube and incubated at 28°C for 1-2 hours at x rpm. 100 µl of the cell mixture was spread on selective LB agar plates and incubated at 28°C for 2 days.

3.2.3 VIGS and qRT-PCR

For virus-induced gene silencing (VIGS), a 300 bp fragment of *RE02* was amplified using primers listed in Table 5 and cloned into vector pYL156[47] (*TRV2::RE02*), the *TRV2::GUS* control construct has been previously described[42]. Agrobacterium-mediated VIGS was performed as described[42]. Gene silencing was verified by measuring *RE02* versus *NbActin* transcript levels using quantitative RT-PCR with primers listed in Table 3. RT-qPCR analysis in transgenic RLP30-RFP- and AtSOBIR1-GFP-expressing tobacco lines *#49* and *#55* was performed as previously described using gene specific primers for *NtPR1* and *NtPDF1.2* and *NtACT9* as house-keeping gene as listed in Supplementary Table 3.

3.3 Plant immune response assays

3.3.1 Ethylene

Determination of the accumulation of ethylene assay were performed as previously described[5]. In brief, ethylene production was induced in three leaf pieces floating on 0.5 ml 20 mM MES buffer pH 5.7 and the indicated elicitors. After incubation for 4 h, 1 ml air was drawn from sealed assay tubes and the ethylene content was measured by gas chromatography (GC-14A, Shimadzu).

3.3.2 ROS burst

ROS accumulation was measured in one leaf piece per well placed in a 96-well plate (Greiner BioOne) containing 100 µl of a solution with 20 µM luminol derivative L-012 (Wako Pure Chemical Industries) and 20 ng ml^{-1} horseradish peroxidase (Applichem)[77]. Luminescence was measured in 2 min intervals both before (background) and for up to 60 min after PAMP or mock treatment using a Mithras LB 940 luminometer (Berthold Technologies).

3.3.3 MAPK

For MAPK activity assays, treated leaf material was harvested after indicated times and frozen in liquid nitrogen. Proteins were extracted with 20 mM Tris-HCl pH 7.5, 150 mM NaCl, 1 mM EDTA, 1 % Triton X-100, 0.1 % SDS, 5 mM DTT, Complete Protease Inhibitor Mini, EDTA-free (Roche), PhosStop Phosphatase Inhibitor Cocktail (Roche), separated via 10 % SDS-PAGE, and transferred to nitrocellulose[77]. Activated MAPKs were detected by protein blotting using the rabbit anti-phospho-p44/42-MAPK antibody (Cell Signalling Technology, 1:1000 dilution).

3.3.4 Pathogen infections

Leaves of 6- to 8-week-old *Arabidopsis* plants were primed by leaf infiltration with 1 µM nlp20, 1 µM SCP^{Ss} or SCP-like^{Psp}, or water (mock treatment) and after 24 h inoculated with *Pseudomonas syringae pv*. tomato DC3000 (*Pst* DC3000) by leaf infiltration with a final cell density of 10^4 colony-forming units (CFU) per ml 10 mM $MgCl_2$. Bacterial populations were determined 3 d after infiltration *N. tabacum* plants were likewise infected with *P. syringae pv*. tabaci at a final cell density of 10^5 CFU/ml and harvested after 4 days[77].

For fungal infection, spores of *B. cinerea* isolate B05.10 or SCP^{Bc} depletion mutant ΔSCP^{Bc}/Bcplp1 (lines 45 and 46)[81] were diluted to a final concentration of 5 x 10^6 spores per ml in potato dextrose broth and 5-µl drops were used for leaf inoculation. Lesion sizes were determined after 2 d by determining the average lesion diameter.

N. tabacum leaves inoculated with 0.8 cm fresh mycelial plugs of *Phytophthora capsici* grown on V8 juice agar were clipped and kept in the dark in plastic boxes to obtain high humidity. Lesion diameters were measured at 48 hpi using UV light[17].

3.4 Biochemical methods

3.4.1 SCP^{Ss} identification

Partially purified SCFE1 fractions from *S. sclerotiorum* strain 1946 were purified as described[18]. The most active fractions from eight rounds of fungal culture and the two-step cation-exchange chromatography purification protocol were pooled and dialysed overnight in 2 l 25 mM MES, pH 7.0, at 4°C in a dialysis membrane (ZelluTrans, nominal MWCO: 3.5; 46mm, Roth), afterwards vacuum-filtrated through a cellulose acetate membrane (Ciro Manufacturing Corporation, pore size: 0.2µm) and loaded with a flow rate of 1ml/min onto a Source 15S 4.6/100PE column (GE Healthcare) equilibrated with buffer A (50 mM MES, pH 5.4). After washing with buffer A, bound proteins were eluted with a linear gradient of buffer B (500 mM KCl, 50 mM MES, pH 5.4; 0-50 % in 15 column volumes) and 500 µl fractions were collected using automated fractionation.

LC-MS/MS sample preparation: Three elicitor-active (B11 to B13, Supplementary Fig. 1b), and two inactive (B9 and B15) fractions of SCFE1 (in 50 mM MES buffer pH 7.0 with varying concentration of KCl, depending on the elution time point) were selected for proteomics analysis. For each fraction a sample volume of 88 µl was used, which corresponded to a total protein content per fraction from 3.9 µg (B9) to 16.0 µg (B13), as determined using the BCA protein assay kit (Thermo Fisher Scientific). All samples were reduced (10 mM DTT, 30 min, 30°C) and carbamidomethylated (55 mM CAA, 30 min, room temperature). Digestion of proteins was carried out by addition of trypsin (proteomics grade, Roche) at a 1/50 enzyme/protein ratio (w/w) and incubation at 37°C overnight. Digests were acidified by addition of 0.5 % (v/v) formic acid, and desalted using self-packed StageTips (three disks per micro-column, ø 1.5mm, C18 material, 3M Empore). The peptide eluates were dried to completeness and stored at -80°C. For LC-MS/MS analysis all samples were resuspended in

11 µl 0.1 % formic acid in HPLC grade water and 5 µl sample per measurement was injected into the mass spectrometer.

LC-MS/MS data acquisition: LC-MS/MS measurements were performed on a nanoLC Ultra1D+ (Eksigent, Dublin, CA) coupled online to a Q-Exactive HF-X mass spectrometer (Thermo Fisher Scientific). Peptides were loaded onto a trap column (ReproSil-pur C18-AQ, 5 µm, Dr. Maisch, 20 mm × 75 µm, self-packed) at a flow rate of 5 µl/min in 100 % solvent A (0.1 % formic acid in HPLC grade water). Subsequently, peptides were transferred to an analytical column (ReproSil Gold C18-AQ, 3 µm, Dr. Maisch, 400 mm × 75 µm, self-packed) and separated using a 50 min linear gradient from 4 % to 32 % of solvent B (0.1 % formic acid in acetonitrile and 5 % (v/v) DMSO) at 300 nl/min flow rate. Both nanoLC solvents contained 5 % (v/v) DMSO to boost the nanoESI response of peptides. The eluate from the analytical column was sprayed via a stainless-steel emitter (Thermo Fisher Scientific) at a source voltage of 2.2 kV into the mass spectrometer. The transfer capillary was heated to 275°C. The Q-Exactive HF-X was operated in data-dependent acquisition (DDA) mode, automatically switching between MS1 and MS2 spectrum acquisition. MS1 spectra were acquired over a mass-to-charge (m/z) range of 350–1400 m/z at a resolution of 60,000 using a maximum injection time of 45 ms and an AGC target value of 3e6. Up to 18 peptide precursors were isolated (isolation window 1.3 m/z, maximum injection time 25 ms, AGC value 1e5), fragmented by high-energy collision-induced dissociation (HCD) using 26 % normalized collision energy and analyzed at a resolution of 15,000 with a scan range from 200 to 2000 m/z. Precursor ions that were singly charged, unassigned, or with charge states > 6+ were excluded. The dynamic exclusion duration of fragmented precursor ions was 25 s.

LC-MS/MS data analysis: Peptide identification and quantification was performed using MaxQuant (version 1.5.3.30)[36]. MS2 spectra were searched against a *Sclerotinia sclerotiorum* protein database (assembly accession number PRJNA348385, 11130 protein sequence entries, https://www.ncbi.nlm.nih.gov/bioproject/PRJNA348385/), supplemented with common contaminants (built-in option in MaxQuant). Carbamidomethylated cysteine was set as fixed modification and oxidation of methionine and N-terminal protein acetylation as variable modifications. Trypsin/P was specified as proteolytic enzyme. Precursor tolerance was set to 4.5 ppm, and fragment ion tolerance to 20 ppm. Results were adjusted to 1 % false discovery rate (FDR) on peptide spectrum match (PSM) and protein level employing a target-decoy approach using reversed protein sequences. The minimal peptide length was defined as 7 amino acids, the “match-between-run” function was enabled (default settings). To assess and quantitatively compare the concentrations of the detected proteins the “intensity based absolute quantification” (iBAQ)[37] algorithm was employed. The detected 22 proteins were further filtered and prioritized according to the following characteristics: 1) good correlation between the elicitor activity profile and the measured mass spectrometric protein intensity over the five investigated SCFE1 fractions; 2) presence of a predicted signal peptide sequence (using the SignalP v.6.0 server)[38]; 3) protein molecular weight in the range between 10 to 30 kDa; 4) high cysteine content relative to protein length; 5) detection of at least two unique peptides per protein (Supplementary Table 5).

3.4.2 Protein expression and purification

For SCP expression in the plant apoplast, *Agrobacterium tumefaciens* strain GV3101 carrying pBIN-plus-SCP^{Ss} was infiltrated into leaves of 4-6-week-old *N. benthamiana* plants. At 48 hours post agro-infiltration leaves were vacuum-infiltrated with 0.5 M NaCl, 0.4 M Na_2HPO_4 and 0.4 M NaH_2PO_4 and the apoplastic wash-fluid containing SCP^{Ss} (SCP^{Ss}-AWF) was collected by centrifugation at 1500 g for 20 min and 4°C.

Protein purification from *P. pastoris* culture medium (SCP^{Ss}, SCP^{Bc}, SCP^{Pi}, truncated SCP^{Ss} versions and cysteine-to-serine replacements) was achieved by affinity chromatography on 5 ml HisTrapFF column (GE Healthcare; equilibrated in 20 mM Tris-HCl, 200 mM NaCl, pH 8.0), following washing (20 mM Tris-HCl, 200 mM NaCl, 20 mM imidazole, pH 8.0) and elution (buffer gradient 0-500 mM imidazole in equilibration buffer). Recombinant protein expression was verified by concentration determination using the Bradford method and by Western Blot analysis using the anti-His antibody (dilution 1:1000, Abcam).

3.4.3 Transient protein expression and co-immunoprecipitations.

For transient protein expression in *N. benthamiana* or *N. tabacum*, *A. tumefaciens* strain GV3101 carrying binary vectors were inoculated in LB supplemented with appropriate antibiotics and grown at 28˚C until saturation. The cells were harvested by centrifugation at 2500 g, RT for 5 min and then resuspended in infiltration buffer (10 mM $MgCl_2$, 150 µM acetosyringone) to the appropriate OD600 prior to infiltration into 4-week-old *N. benthamiana* or *N. tabacum* leaves. Cell death phenotypes were observed at 2–4 d.

For SCP^{Ss}-binding assays, native SCP^{Ss}-Myc (pGWB17) or Cys-to-Ser replacement mutants together with RLP30-GFP (pGWB5) from different *Arabidopsis* accessions was transiently co-expressed in *N. benthamiana*. For SCP^{Ss}-induced BAK1 recruitment assays, RLP30-GFP or RLP23-GFP together with SOBIR1-HA and BAK1-myc were transiently co-expressed in *N. benthamiana*. Alternatively, *rlp30-2*/RLP30-YFP transgenic *Arabidopsis* plants were used to perform the BAK1 recruitment experiment. On day 2, leaf material transiently expressing desired proteins was harvested. 200 mg ground leaf material (from *N. benthamiana* transiently expression or from stable Arabidopsis lines) was subjected to protein extraction and immunoprecipitation using GFP-Trap beads (ChromoTek) (Ref or details). Proteins were detected by immunoblotting with tag-specific antibodies raised against epitope tags GFP (dilution 1:5000), HA (dilution 1:3000), Myc (dilution 1:5000, all Thermo Fisher Scientific), anti-SOBIR1 (dilution 1:000, Agrisera) or anti-BAK1 (dilution 1:000, Agrisera) followed by staining with secondary antibodies coupled to horseradish peroxidase and ECL (Cytiva).

3.4.4 SCP-like purification from Pseudomonas spp.

Pseudomonas strains (*Pseudomonas syringae* pv*. tomato* DC3000, *Pseudomonas syringae* pv*. phaseolicola* 1448A, *Pseudomonas protegens* Pf-5, *Pseudomonas fluorescens* SBW25, *Pseudomonas stutzeri* DSM10701, kindly obtained from Prof. Harald Groß, University of Tübingen) were grown in baffled flasks (200 ml medium in 1 l flask) in liquid PDB medium (24 g/l Potato Dextrose Broth, Duchefa) for 12 h at 21°C with 210 rpm shaking. The culture

medium was centrifuged at 6000 rpm for 20 min and then vacuum-filtrated through a filter paper (MN 615, Macherey-Nagel) and subjected to a two-step cation exchange chromatography protocol using an ÄKTA Explorer FPLC system (GE Healthcare) kept at 4°C. In a first step, the culture filtrate was loaded onto HiTrap SP FF column(s) (GE Healthcare) equilibrated in buffer A (50 mM MES, pH 5.4) at a flow rate of up to 15 ml/min. After washing with buffer A, a 100 % elution step with buffer B (500 mM KCl, 50 mM MES, pH 5.4) was performed at a flow rate of 1-2 ml/min and the elution peak was monitored with OD280nm, OD254nm and OD214nm and collected manually. The collected eluate was dialysed against 2 l 25 mM MES, pH 5.4, overnight at 4°C in a dialysis membrane (ZelluTrans, nominal MWCO: 3.5; 46 mm, Roth), afterwards vacuum-filtrated through a cellulose acetate membrane (Ciro Manufacturing Corporation, pore size: 0.2 µm) and loaded with a flow rate of 1 ml/min onto a Source 15S 4.6/100PE column (GE Healthcare) equilibrated with buffer A. After washing with buffer A the bound proteins were eluted with a linear gradient of buffer B (0 to 50 % in 10 column volumes) and 500 µl fractions were collected using automated fractionation.

3.5 Phylogeny reconstruction.

Full length protein sequences, obtained from Ngou *et al*., (2022)[48] (a) and BLAST searches[49] on Phytozome[50] (b) or Uniprot[51] (c), of *A. thaliana*(a,b), *B. rapa*(a), *M. tunculata*(b), *V.vinifera*(b), *S. lycopersicum*(a,b), *S. tuberosum*(b), *N. benthamiana*(a), *N. sylvestris*(c) and *A. trichopoda*(b) were aligned using MAFFT[52] (--localpair --maxiterate 10000 --reorder). The phylogenetic tree was constructed using IQTree[53] (-T AUTO -m TEST -b 50 -con). This work was supported by the BMBF-funded de.NBI Cloud within the German Network for Bioinformatics Infrastructure (de.NBI).

4 Results

4.1 SCP^{Ss} triggers immunity in *Arabidopsis*

4.1.1 Identification of the RLP30 ligand form *Sclerotinia sclerotiorum*

In an earlier publication the *Arabidopsis* RLP30 has been shown to detect a proteinaceous elicitor secreted by *Sclerotinia sclerotiorum*, originally termed SCFE1[7]. To identify the immunogenic pattern in the supernatants of fungal cultures, our former colleague Dr. Christina Steidele (Technische Universität München) used a two-step separation on cation exchange chromatography and monitored RLP30-dependent induction of the plant stress hormone ethylene (Fig. 1a,b). Mass spectrometric analysis of the trypsin fragments obtained with the purified, ethylene-inducing fractions revealed the presence of a small cysteine-rich protein according to the following characteristics: 1) peptides were detectable in SCFE1 in three independent LC-MS/MS analyses, 2) presence of a signal peptide and 3) a molecular mass between 15 to 22 kDa (Supplementary Table 5). SCP^{Ss} is a small cysteine-rich protein of 147 amino acids without any known protein domains and contains 8 cysteine residues (Fig. 1c). To confirm SCP^{Ss} as the ligand of RLP30, the SCP^{Ss} protein was heterologously expressed in *N. benthamiana* or *Pichia pastoris* (Fig. 1d,e), with C-terminal GFP or His tags, respectively.

Both forms were found to induce ethylene production in *Arabidopsis* Col-0 wild-type plants but not in the *rlp30-2* mutant (Fig. f,g), ruling out that contaminations occurring during the purification procedure or SCP^{Ss}-copurifying proteins are responsible for the RLP30-dependent defense response. His-tagged SCPSs, affinity purified via His-Trap columns, triggered ethylene production in Col-0 plants at nanomolar concentrations with a half-maximal induction (EC50) at ~26 nM (Fig. 2a).

To further verify the activity of SCP^{Ss} as a PAMP, a series of PTI events induced by SCP^{Ss} were tested. In contrast to *rlp30-2* mutants, Col-0 wild-type plants and *rlp30-2* mutants complemented with RLP30 (hereafter *rlp30-2*/RLP30-YFP) responded to the SCP^{Ss} preparations with typical PAMP responses such as induction of reactive oxygen species (ROS) and activation of mitogen-activated protein kinases (MAPK) (Fig. 2b,4a). Importantly, SCP^{Ss} treatment could prime plants for subsequent infection. Leaves of wild-type Col-0 and *rlp30-2*/RLP30-YFP plants pretreated with SCP^{Ss} showed significantly less colonization by the necrotrophic fungus *Botrytis cinerea* as well as the bacterial pathogen *Pseudomonas syringae pv.* tomato (*Pto*) DC3000, whereas *rlp30-2* mutants failed to restrict pathogen infection upon SCP^{Ss} pretreatment (Fig. 2c,d).

4.1.2 SCP^{Ss} associates with functional RLP30

To assess whether SCP^{Ss} can be found in complex with RLP30, co-immunoprecipitation assays were performed with extracts from *N. benthamiana* leaves that were transiently co-transformed with myc-tagged SCP^{Ss} and with either GFP-tagged RLP30 or the GFP-tagged nlp20 receptor RLP23[19] as control. SCP^{Ss}-myc co-precipitated specifically with RLP30 but not with the structurally related RLP23 (Fig. 3b). Several *Arabidopsis* accessions that were found

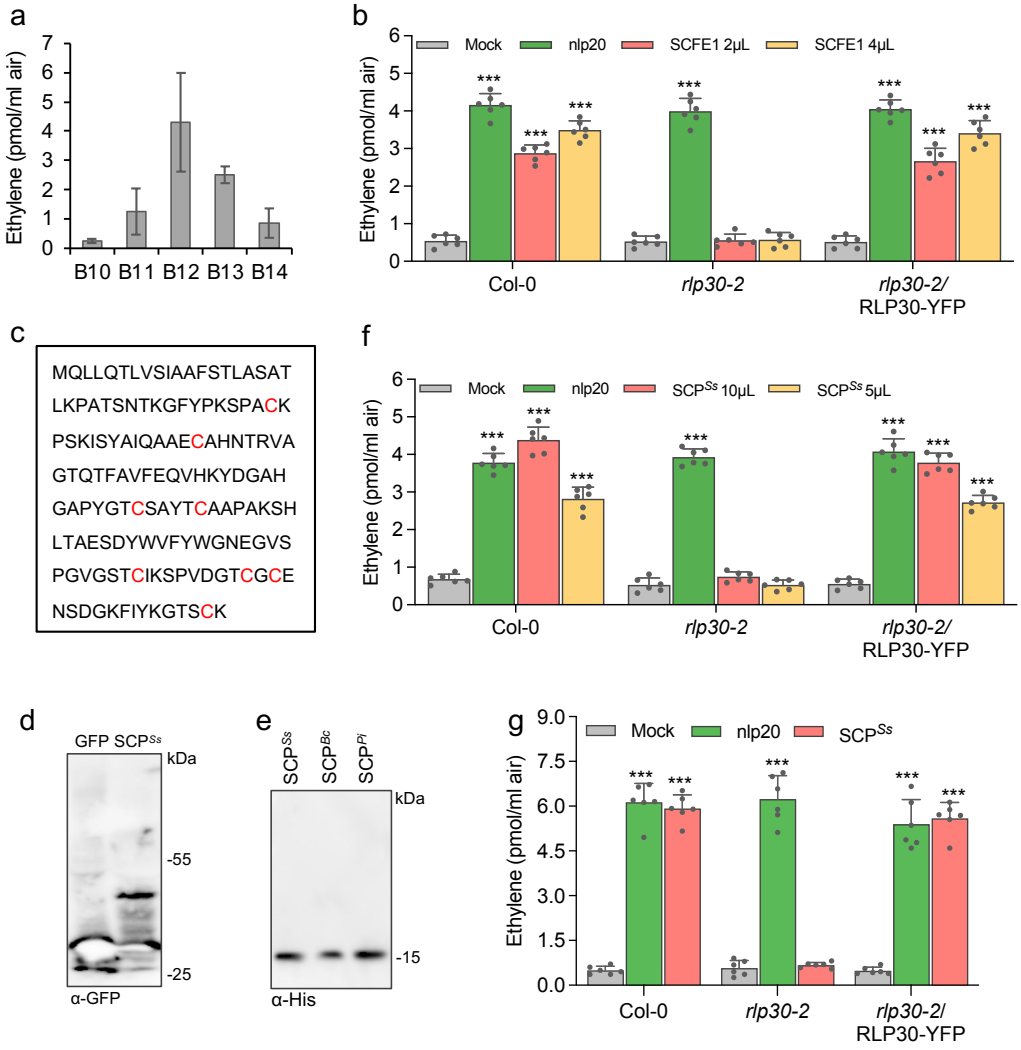

Fig. 1. Identification of an Arabidopsis defense-stimulating protein in the S. sclerotiorum SCFE1 preparation.

a, Ethylene accumulation in Col-0 wild-type plants treated with indicated SCFE1 fractions. **b,** Ethylene accumulation in Col-0 wild-type plants, *rlp30-2* mutants or an *rlp30-2* line complemented with a *p35S::RL30-YFP* construct 4 h after treatment with water (mock), 1 µM nlp20, or 2 or 4 µl per 500 µl assay volume of a SCFE1 preparation. **c,** Amino acid sequence of SCP^{Ss} with the eight cysteine residues depicted in red. **d,e,** Western Blot analysis of SCP from *S. sclerotiorum* (SCP^{Ss}), *B. cinerea* (SCP^{Bc}), or *P. infestans* (SCP^{Pi}) produced in the *N. benthamiana* apoplast (**d**) or purified from *P. pastoris* (**e**) using anti-GFP or anti-His antibodies, respectively. **f,** Ethylene accumulation in Col-0 wild-type plants or *rlp30-2* mutants and complementation line 4 h after treatment with GFP purified from *N. benthamiana* apoplasts (mock), 1 µM nlp20, or given volumes per 500 µl assay volume of SCP^{Ss} purified from *N. benthamiana* apoplasts. **g,** Ethylene accumulation in *Arabidopsis* Col-0 wild-type plants, *rlp30-2* mutants, or an *rlp30-2* line complemented with a *p35S::RL30-YFP* construct 4 h after treatment with water (mock), 1 µM nlp20, or 1 µM *P. pastoris*-expressed SCP^{Ss}. Data points are indicated as dots (n = 6 for a; n = 6 for e) and plotted as box plots (centre line, median; bounds of box, the first and third quartiles; whiskers, 1.5 times the interquartile range; error bar, minima and maxima). Statistically significant differences (**b,f,g**) from mock treatments in the respective plants are indicated (two-sided Student's t-test, ***$P \leq 0.001$). Each experiment was repeated three times with similar results.

to exhibit no response to *S. sclerotiorum* extracts carry SNPs in their *RLP30* genes leading to single amino acid changes[18]. In an extended screen with 77 accessions, we identified futher accessions that did not respond to SCP^{Ss} and that carried point mutations in *RLP30* (Fig. 3a and Supplementary Fig. 1a). We next tested the altered RLP30 versions occurring in these insensitive accessions in a co-precipitation assay for binding of SCP^{Ss}. While most receptor versions, except RLP30 from Sq-1 and Lerik1-3, were expressed in *N. benthamiana*, none of them precipitated SCP^{Ss} (Fig. 3c). Thus, the single amino acid substitutions in different parts of the LRR domain, which are specific to SCP^{Ss}-responsive RLP30 variants, such as L307R in Mt-0, R433G in Lov-1 and Lov-5, R433L in ICE111, N561Y in Bak-2, G563V in Br-0, S654Y in Sq-1, and F760 in Gu-0 (Supplementary Fig. 1a), respectively, all affect RLP30/SCP^{Ss} complex formation and, likely, are responsible for the non-functionality of these mutated receptors.

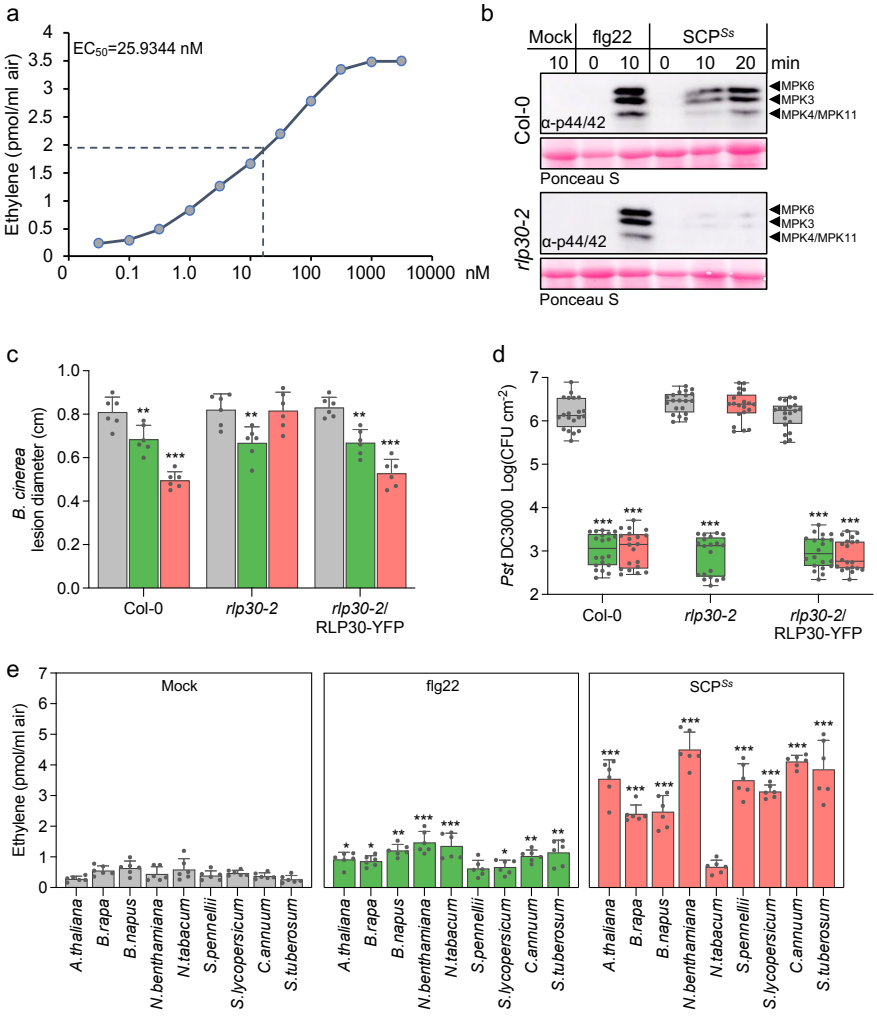

Fig. 2. Recombinant SCPSs induces PTI responses.

a, Determination of EC_{50} values using ethylene accumulation in *Arabidopsis* Col-0 wild-type plants after treatment with increasing concentrations of recombinant SCP^{Ss} (produced in *Pichia*). EC_{50} values and curve fit were calculated using EC_{50} Calculator. **b,** MAPK activation in *Arabidopsis* Col-0 wild-type plants or *rlp30-2* mutants treated for the times indicated with water (mock), 0.1 µM flg22, or 1 µM SCP^{Ss}. MAPK activation was detected by immunoblot using phospho-p44/p42 antibodies, equal loading was verified by staining of the membrane with

Ponceau S Red. Experiments were repeated three times with similar results. **c,** *B. cinerea* infected area as determined by lesion diameter on day 2 after 24 h-treatment of Col-0 wild-type plants, *rlp30-2* mutants or the *rlp30-2/RLP30-YFP* complementation line with water (mock), 1 µM nlp20, or 1 µM SCP^{Ss}. **d,** Bacterial growth in plants pre-treated with water (mock), 1 µM nlp20, or 1 µM SCP^{Ss} 24 h before infiltration of *Pst* DC3000. Bacteria (colony forming units, CFU) were quantified in extracts of leaves 3 days after inoculation. **e,** Ethylene accumulation in plants of the Brassicaceae and Solanaceae family 4 h after treatment with water (mock), 1 µM flg22, or 1 µM SCP^{Ss}. Data points are indicated as dots (n = 6 for **c,e**; n = 20 for **d**) and plotted as box plots (centre line, median; bounds of box, the first and third quartiles; whiskers, 1.5 times the interquartile range; error bar, minima and maxima). Statistically significant differences from mock treatments in the respective plants are indicated (two-sided Student's t-test, $^{**}P \leq 0.01$, $^{***}P \leq 0.001$). All assays were performed at least three times with similar results.

4.1.3 SCP^{Ss} triggers immunity in Brassicaceae and Solanaceae

Unlike most other known patterns recognized by RLPs, which function in either Brassicaceae or Solanaceae[6,8,9,13,14], SCP^{Ss} did not only elicit ethylene production in *Arabidopsis* and related *Brassica species*, but also in solanaceous plants such as *N. benthamiana*, tomato, pepper, and potato (Fig. 2e). Interestingly, *N. tabacum* did not respond to SCP^{Ss}.

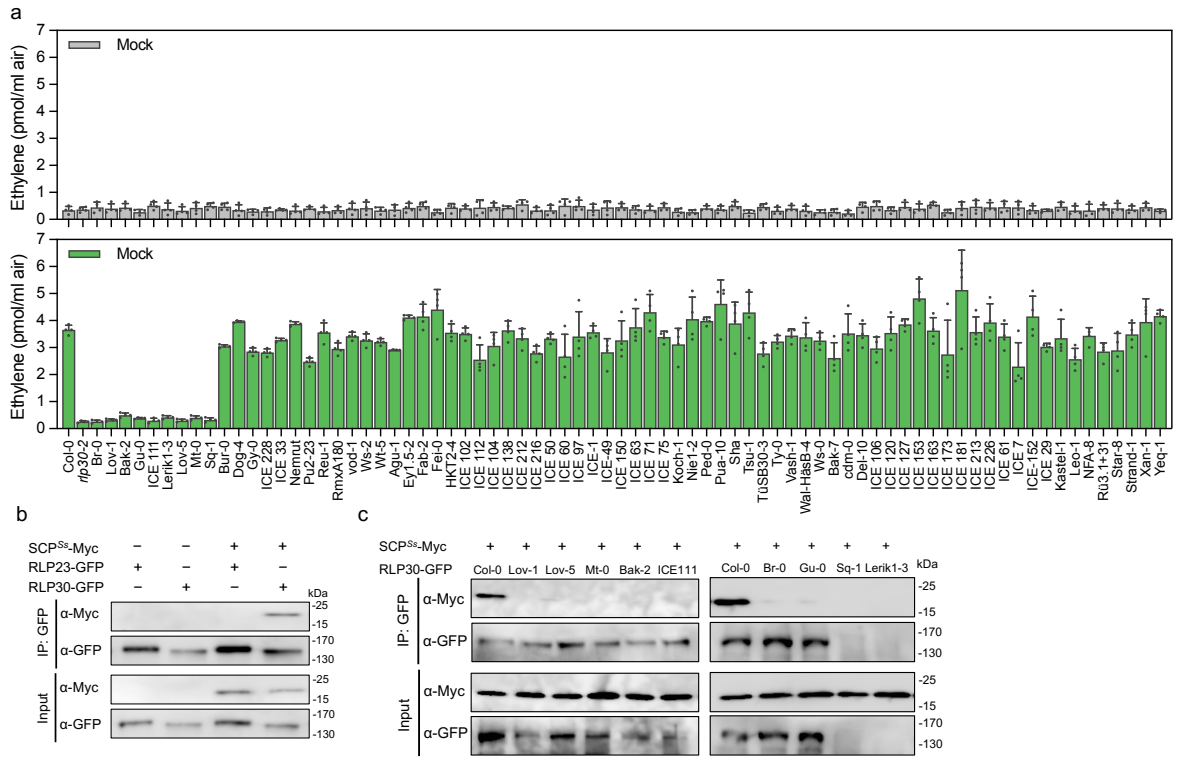

Fig. 3. SCP^{Ss} binds to functional RLP30.

a Natural variation in SCP^{Ss} sensitivity among *Arabidopsis* accessions. 77 *Arabidopsis* accessions were tested for ethylene accumulation upon water (mock) or SCP^{Ss} (1 µM) treatment. Data points are indicated as dots (n = 3) and plotted as box plots (centre line, median; bounds of box, the first and third quartiles; whiskers, 1.5 times the interquartile range; error bar, minima and maxima). The experiment was repeated twice with similar results. **b,c,** Ligand-binding assay in *N. benthamiana* transiently co-expressing SCP^{Ss}-myc and either RLP30-GFP from different *Arabidopsis* accessions or RLP23-GFP. Proteins extracted from *N. benthamiana* leaves expressing

indicated protein combinations (Input) were used for co-immunoprecipitation with GFP-trap beads (IP:GFP) and immunoblotting with tag-specific antibodies. The experiment was repeated three times with similar results.

4.1.4 SCP^{Ss}-induced immunity requires the co-receptors SOBIR1 and BAK1

Immunity-related RLPs function similarly to RLKs by forming a bipartite receptor with the adaptor kinase SOBIR1 in a ligand-independent manner. After sensing molecular patterns, the RLP/SOBIR1 pair recruits the co-receptor BAK1 into a tertiary complex, as was shown for RLP30-SOBIR1 and BAK1 after SCFE1 treatment[5]. To test whether SCP^{Ss} binding to RLP30 induces the formation of a RLP30-SOBIR1-BAK1 complex, we conducted co-immunoprecipitation assays in *rlp30-2*/RLP30-YFP transgenic *Arabidopsis* plants as well as in transiently transformed *N. benthamiana* plants. The association of RLP30 and SOBIR1 was confirmed independently of SCP^{Ss} elicitation. In contrast, formation of RLP30-SOBIR1-BAK1 complexes were observed solely in SCP^{Ss}-treated transgenic *Arabidopsis* and *N. benthamiana* plants, whereas treatment with nlp20, the ligand of RLP23, failed to induce BAK1 recruitment (Fig. 4a,b). To assess whether SOBIR1 and BAK1 participate in SCP^{Ss}-induced immunity, *sobir1-12* and *bak1-5 bkk1* mutants were tested for ethylene and ROS production elicited by SCP^{Ss}. Both mutant lines were defective in responding to SCP^{Ss} and nlp20 compared to wild-type plants (Fig. 4c,d).

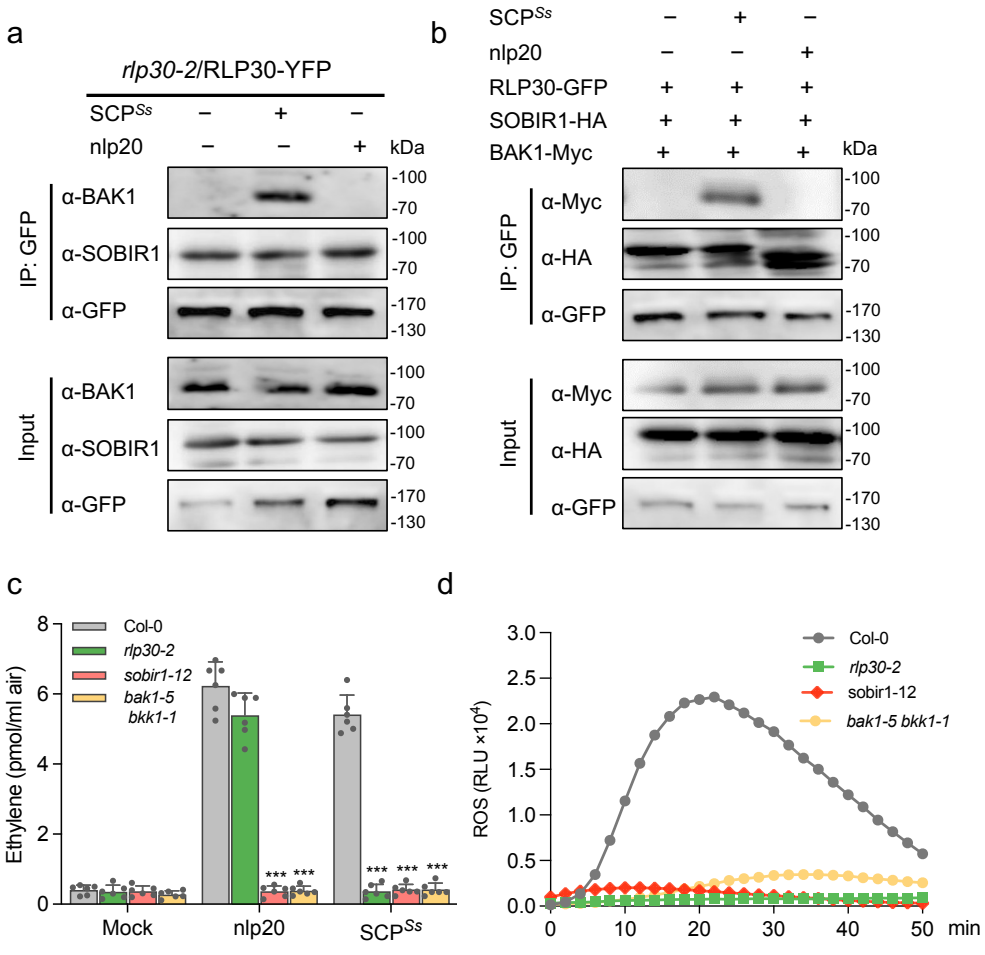

Fig. 4. The co-receptors SOBIR1 and BAK1 are required for SCP^{Ss}-triggered immunity.

a, Ligand-induced BAK1 recruitment assay in stable RLP30-YFP transgenic plants treated with 1 µM SCP^{Ss} or 1 µM nlp20 as indicated. Leaf protein extracts (Input) were used for co-immunoprecipitation with GFP-trap beads (IP:GFP) and immunoblotting with SOBIR1 and BAK1 antibodies. **b,** Ligand-induced BAK1 recruitment assay in *N. benthamiana* transiently co-expressing RLP30-GFP, SOBIR1-HA and BAK1-Myc and treated with 1 µM SCP^{Ss} or 1 µM nlp20 as indicated. Leaf protein extracts (Input) were used for co-immunoprecipitation with GFP-trap beads (IP:GFP) and immunoblotting with tag-specific antibodies. **c,** Ethylene accumulation in *Arabidopsis* Col-0 wild-type plants, *rlp30-2* mutants, *sobir1-12* mutants or *bak1 bkk1-5* mutants 4 h after treatment with water (mock), 1 µM nlp20, or 1 µM *P. pastoris*-expressed SCP^{Ss}. Data points are indicated as dots (n = 6) and plotted as box plots (centre line, median; bounds of box, the first and third quartiles; whiskers, 1.5 times the interquartile range; error bar, minima and maxima). Statistically significant differences from Col-0 plants in the respective plants are indicated (two-sided Student's t-test, $^{**}P \leq 0.01$, $^{***}P \leq 0.001$). **d,** ROS production in leaf pieces of *Arabidopsis* Col-0 wild-type plants, *rlp30-2* mutants, *sobir1-12* mutants or *bak1 bkk1-5* mutants treated with 2 µM SCP^{Ss}. Given are relative light units (RLU) ± SD (n=6). All assays were performed at least three times with similar results.

Collectively, our results demonstrate that SCP^{Ss}, as the active component of SCFE1, induces plant immunity by specifically binding to functional RLP30 to form a tripartite complex with SOBIR1 and BAK1 in *Arabidopsis*, and that SCP^{Ss}-perception mechanisms exists in members of the Brassicaceae and Solanaceae families.

4.2 RLP30 detects SCPs from fungi and oomycetes

Querying the SCP^{Ss} protein sequence against the NCBI database using BLASTP resulted in identification of homologous proteins in fungi and oomycetes[18]. No homologs in bacteria or plants were found, indicating evolutionary conservation of SCP^{Ss} among fungi and oomycetes. SCP^{Ss} and homologs typically contain a predicted signal peptide, seven conserved motifs (R1 to R7) and eight conserved cysteine residues (Supplementary Fig. 2a), however, the absence of previously characterized protein domains hampers the prediction of their specific biological functions. While some SCPs have been reported to function as virulence factors with multiple strategies, deletion of the SCP^{Ss}-homolog in *B. cinerea* (*SCP^{Bc}/Bcplp1*) or its homolog *VmE02* in *V. mali* did not alter pathogenicity on various plant species (Supplementary Fig. 2b), suggesting that these proteins either do not contribute significantly to virulence or act redundantly with others during infection[80,81].

To assess whether SCP^{Ss} homologs from other fungal and oomycete species display RLP30-dependent elicitor activity, homologs from *Botrytis cinerea* (SCP^{Bc}) and *Phytophthora infestans* (SCP^{Pi}) were produced in *P. pastoris* (Fig. 1e). Similar to SCP^{Ss}, SCP^{Bc} and SCP^{Pi} induced the production of ethylene and MAPK activation in wild-type and *rlp30-2*/RLP30-YFP plants, but not in *rlp30-2* mutants (Fig. 5a,b). Additionally, the *sobir1-12* and *bak1–5/bkk1-1* genotypes showed largely abolished PTI responses to SCP^{Ss} homologs (Fig. 5a,b). Moreover, nine SCP^{Ss} -insensitive accessions also failed to respond to SCP^{Bc} and SCP^{Pi}, further confirming that SCP^{Ss} homologs induce immunity in an RLP30-dependent manner (Fig. 5c). Together, these data demonstrate that SCP^{Ss} homologs, common among fungi and oomycetes, are perceived by the RLP30/SOBIR1/BAK1 receptor complex in *Arabidopsis*.

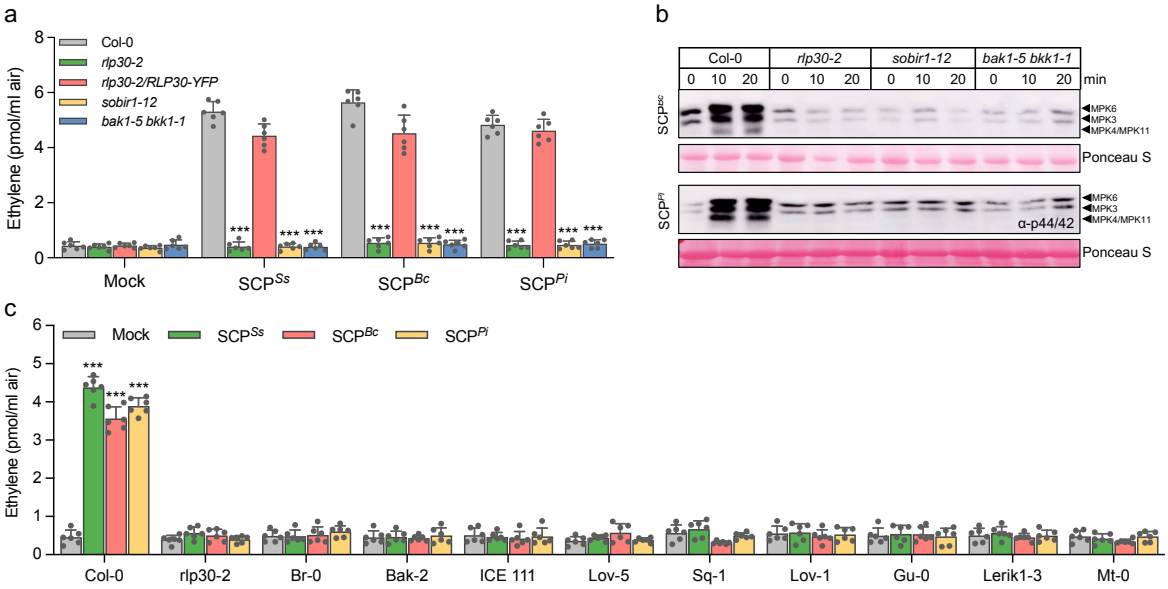

Fig. 5. SCP^{Ss} is conserved in fungi and oomycetes.

a, Ethylene accumulation in *Arabidopsis* wild-type plants (Col-0) or indicated mutants 4 h after treatment with water (mock), 1 µM nlp20, 1 µM SCP^{Ss}, or homologs from *B. cinerea* (*Bc*) and *Phytophthora infestans* (*Pi*). **b,** MAPK activation in *Arabidopsis* Col-0 wild-type plants or *rlp30-2, sobir1-12 and bak1-5 bkk1-1* mutants treated with 1 µM SCP^{Bc} or SCP^{Pi} for the times indicated. MAPK activation was detected by immunoblot using phospho-p44/p42 antibodies, equal loading of Ribulose-1,5-bisphosphate-carboxylase/oxygenase (Rubisco) was verified by staining of the membrane with Ponceau S Red. **c,** Ethylene accumulation in *Arabidopsis* wild-type plants (Col-0), or various SCP^{Ss}-insensitive accessions 4 h after treatment with water (mock), 1 µM SCP^{Ss}, SCP^{Bc}, or SCP^{Pi}. Data points are indicated as dots (n = 6) and plotted as box plots (centre line, median; bounds of box, the first and third quartiles; whiskers, 1.5 times the interquartile range; error bar, minima and maxima). Statistically significant differences from mock treatments or Col-0 plants in the respective plants are indicated (two-sided Student's t-test, ***$P \leq 0.001$). The experiments were repeated three times with similar results.

4.3 SCP^{Ss}-perception in *Solanaceae*

4.3.1 *N. benthamiana* RE02 is a receptor for SCP^{Ss}

SCP^{Ss} recognition systems are present in both Brassicaceae and Solanaceae (Fig. 2e), yet, reciprocal sequence similarity searches suggest absence of RLP30 from Solanaceae. The *N. benthamiana* receptor-like protein RE02 (Response to VmE02) was recently identified to mediate the perception of VmE02, a cysteine-rich PAMP derived from *V. mali* with 55% identity to SCP^{Ss} [12,22]. To compare the ligand specificity of RE02 with RLP30, *RE02* expression in *N. benthamiana* was targeted by virus-induced gene silencing (VIGS), resulting in almost complete loss of SCP^{Ss}-induced ethylene production, whereas *N. benthamiana* plants inoculated with the *TRV:GUS* control construct were not affected (Fig. 6a,b). Similarly, a stable knockout of RE02 (*RE02*-Cas9, from Lili Huang'lab, China) in *N. benthamiana* resulted in complete insensitivity to SCP^{Ss} (Fig. 6c). In contrast, leaves of *RE02*-Cas9 plants either transiently transformed with *RE02*-GFP or *RLP30*-GFP exhibited clear SCP^{Ss} sensitivity (Fig. 6c,d). Likewise, stable expression of *RE02*–GFP also reconstituted the

responsiveness to SCP^{Ss} in *Arabidopsis rlp30-2* mutants (Fig. 6e,f). Hence, SCP^{Ss} recognition is mediated by RE02 in *N. benthamiana.*

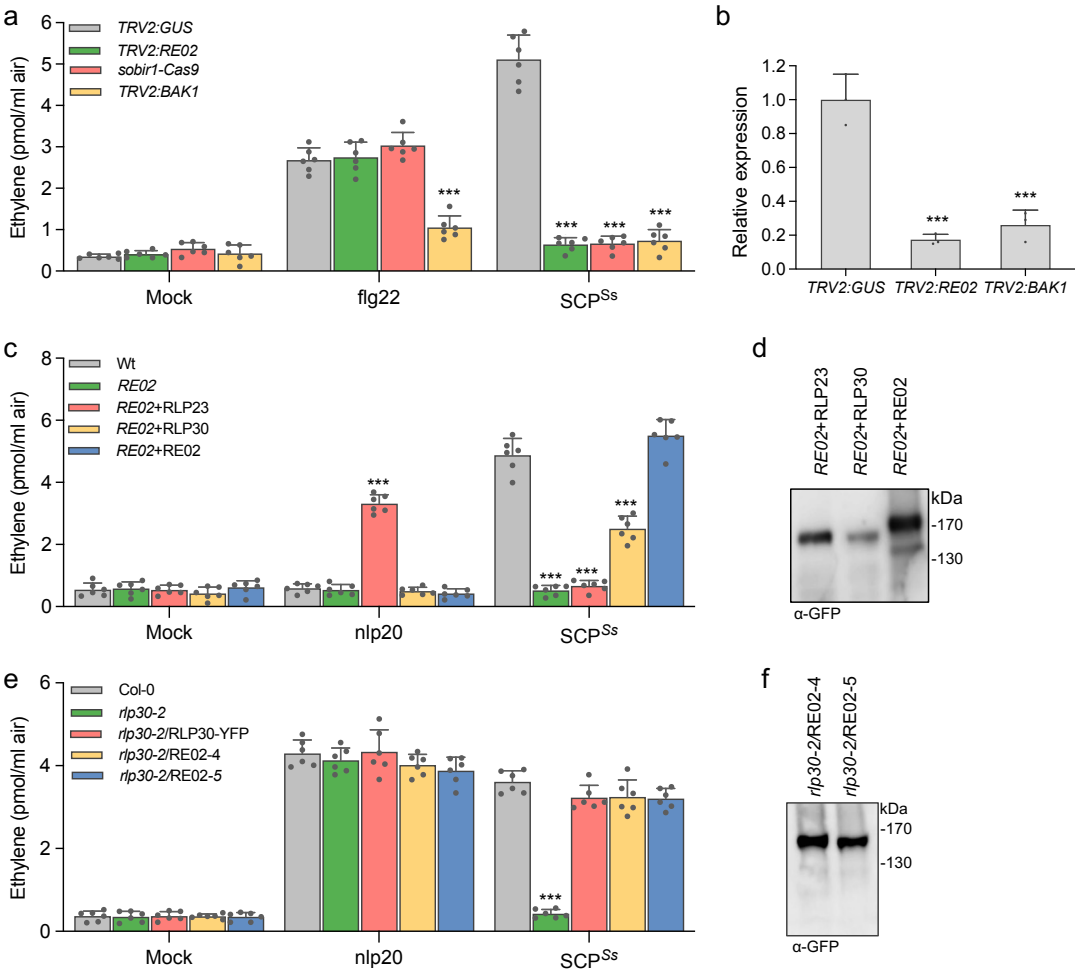

Fig. 6. SCP^{Ss} are sensed RE02 in *N. benthamiana.*

a, Ethylene accumulation in *NbSOBIR1* CRISPR, *RE02* and *NbBAK1* silencing plants. The *TRV2:GUS* construct was used as a control. Ethylene production was measured 4 h after treatment with water (mock), 1 μM flg22, or 1 μM SCP^{Ss}. **b,** RT-qPCR analysis of relative expression of *RE02* and *NbBAK1* in corresponding VIGS-silenced *N. benthamiana* leaves using gene-specific primers. Expression of *RE02* or *NbBAK1* was normalized to the levels of *NbActin* transcript and is presented relative to the *TRV2:GUS* control which was set to 1. **c,** RE02 knockout *N. benthamiana* plants (*RE02*-Cas9) were transiently transformed with *RLP23-GFP*, *RLP30-GFP*, or *RE02-GFP*, respectively. The *RE02*-Cas9 plants were used as a control. Ethylene production was measured 4 h after treatment with water (mock), 1 μM nlp20, or 1 μM SCP^{Ss}. **d,** Western Blot analysis on protein extracts from *RE02*-Cas9 plants transiently expressing GFP-tagged RLP23, RLP30, or RE02 using an anti-GFP antibody. **e,** Ethylene accumulation in *Arabidopsis rlp30-2* mutants or lines stably expressing RLP30-YFP or RE02-GFP (line 4 and 5) 4 h after treatment with water (mock), 1 μM nlp20, or 1 μM SCP^{Ss}. **f,** Western Blot analysis on protein extracts from two independent *Arabidopsis rlp30-2* lines stably expressing *p35S::RE02-GFP* using an anti-GFP antibody. Data points are indicated as dots (n = 6) and plotted as box plots (centre line, median; bounds of box, the first and third quartiles; whiskers, 1.5 times the interquartile range; error bar, minima and maxima). Statistically significant differences from control treatments are indicated (two-sided Student's t-test, *P ≤ 0.05, ***P ≤ 0.001). Each experiment was repeated three times with similar results.

Moreover, a CRISPR/Cas9 line of *NbSOBIR1/NbSOBIR1-like* (From Matthieu H A J Joosten's lab, Wageningen) and *N.benthamiana* plants silenced for *NbBAK1* (*TRV2:BAK1*) proved entirely insensitive to SCP^{Ss} treatment in the ethylene assay (Fig. 6a,b). Together these results demonstrate that RE02 mediates SCP^{Ss}-induced immunity by cooperating with NbSOBIR1 and NbBAK1 in *N. benthamiana*.

4.3.2 EIX1/2 are not responsible for SCP^{Ss} recognition in tomato

Tomato plants are also SCP^{Ss}-responsive (Fig. 1d), and phylogeny analysis of RE02 revealed *S. lycopersicum* EIX2 as a potential RE02 homolog[18]. EIX2 is an RLP type receptor shown to sense ethylene-inducing xylanase (EIX)[14]. SlEIX1, another tomato homolog with high similarity to RE02, negatively regulates EIX2-mediated xylanase perception[15]. To determine whether these two RE02 homologs from tomato could confer SCP^{Ss}-sensitivity, we stably expressed *p35S::EIX1*-GFP or *p35S:: EIX2*-GFP in *rlp30-2* mutants. However, whereas *EIX2*-transgenic *rlp30-2* plants were able to respond to xylanase treatment, thus confirming EIX2 functionality in *Arabidopsis*[17], SCP^{Ss}-induced ethylene production could not be restored in *rlp30-2* mutants expressing EIX1 or EIX2 (Fig.7a). Further, leaves of *RE02*-Cas9 plants, transiently transformed with either EIX1-GFP or EIX2-GFP did not exhibit SCP^{Ss} sensitivity (Fig.7b). Thus, our data suggest that SCP^{Ss} perception in tomato does not rely on EIX1/2.

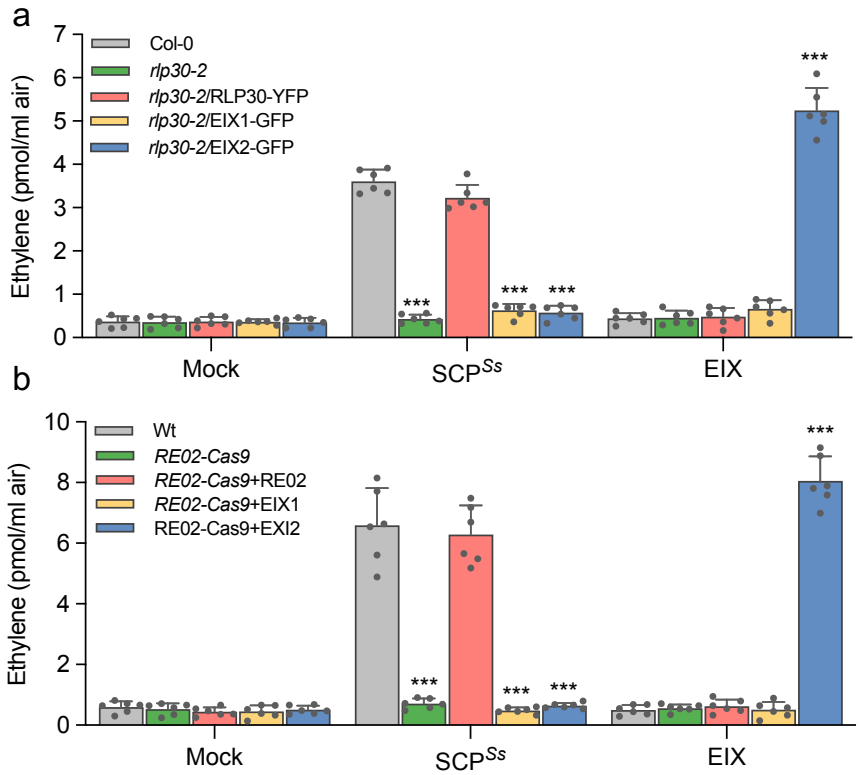

Fig. 7. EIX1 and EIX2 are not the receptors for SCP^{Ss} recognition in tomato.

a, Ethylene accumulation in *Arabidopsis rlp30-2* mutants or *rlp30-2* lines stably expressing RLP30-YFP, EIX1-GFP (line 1 and 2) or EIX2-GFP (line 1 and 2) 4 h after treatment with water (mock), 1 μM nlp20, or 1 μM SCP^{Ss}. **b,** RE02 knockout *N. benthamiana* plants (*RE02*-Cas9) were transiently transformed with *RE02-GFP*, *EIX1-GFP*, or *EIX2-GFP*, respectively. The *RE02*-Cas9 plants were used as a control. Ethylene production was measured 4

h after treatment with water (mock), 1 µM nlp20, or 1 µM SCP^{Ss}. Data points are indicated as dots (n = 6) and plotted as box plots (centre line, median; bounds of box, the first and third quartiles; whiskers, 1.5 times the interquartile range; error bar, minima and maxima). Statistically significant differences from wild-type plants are indicated (two-sided Student's t-test, ***$P \leq 0.001$). Each experiment was repeated three times with similar results.

4.4 Distinct perception of SCP^{Ss} in Brassicaceae and Solanaceae

LRR-type immune receptors typically sense conserved and immunogenic peptide fragments of PAMPs rather than entire proteins[5,6]. Immunogenic activity of SCP^{Ss} is sensitive to treatment with DTT (Fig. 8a,b), suggesting that perception by the RLPs RLP30 and RE02 depends on the tertiary structure of SCP^{Ss}. The SCP^{Ss} protein is predicted to form four disulfide bonds (DB), most likely connecting cysteine residues C1 and C4, C2 and C3, C5 and C8 and C6 and C7, respectively (Fig. 8a). To examine the importance of disulfide bonds for SCP^{Ss} elicitor activity, we individually replaced each of the 8 cysteine residues with serine and expressed these mutant proteins in *P. pastoris* (Fig. 8c). Replacing individual cysteine residues in SCP^{Ss} with serine leads to loss of activity and RLP30 complex formation in *Arabidopsis* for all eight substitutions (Fig. 8d,e). When testing the individual Cys substitutions for ethylene-inducing activity in *N. benthamiana* or tomato, we observed that only the four N-terminal Cys residues, forming the bonds C1-C4 and C2-C3, were required for activity, while replacement of the other four Cys residues did not affect the activity (Fig. 8d and Supplementary Fig. 3a). Hence, whereas RLP30 only senses intact SCP^{Ss}, RE02-mediated perception requires only part of the SCP^{Ss} tertiary structure.

To determine the minimal structural requirements for SCP^{Ss} activity, the truncated versions C1C5 and C3C8 were assessed for their elicitor activity (Fig. 8a). Consistent with the results of the individual cysteine replacements, the truncated form C1C5, but not C3C8, was active in tomato and *N. benthamiana* but not in *Arabidopsis* (Fig. 9a and Supplementary Fig. 3b). In *N. benthamiana,* C1C5 could trigger ethylene production with an EC50 of ~50.55 nM, thus displaying a similar activity as entire SCP^{Ss} (Fig. 9b). C1C4, a variant of the protein further truncated from both the N- and the C-terminus but still comprising the first four Cys residues, proved inactive in *Arabidopsis* but also in *N. benthamiana* and tomato (Fig. 9a,b and Supplementary Fig. 3b), indicating that in addition to the disulfide bonds also amino acids flanking the C1C4 peptide are important for immunogenic activity in solanaceous plants. Thus, SCP^{Ss} is one of the very few identified ligands whose tertiary structure is important for PAMP activity similar to IF1-recognition by RLP32[9]. Intriguingly, in *B. napus, B. rapa,* and *B. oleracea* all SCP^{Ss} mutants exhibited elicitor activity comparable to the wild-type SCP^{Ss} (Fig. 8d and Supplementary Fig. 3a), indicating that in these Brassicaceae species SCP^{Ss}-immunogenic activity is independent of cysteine-bridges and, thus, of its tertiary structure. Hence, at least two distinct SCP^{Ss}-perception systems are present in Brassicaceae, one responding to intact SCP^{Ss} protein (as in *Arabidopsis*), and the other one responding to a SCP^{Ss}-derived peptide (as in *Brassica ssp.*). As both C1C5 and C3C8 displayed activity in Brassicaceae (Fig. 9a,b and Supplementary Fig. 3b), we generated the 36-amino-acid peptide C3C5 spanning the overlapping region of C1C5 and C3C8 (Fig. 8a). Surprisingly, C3C5 was found to be nearly

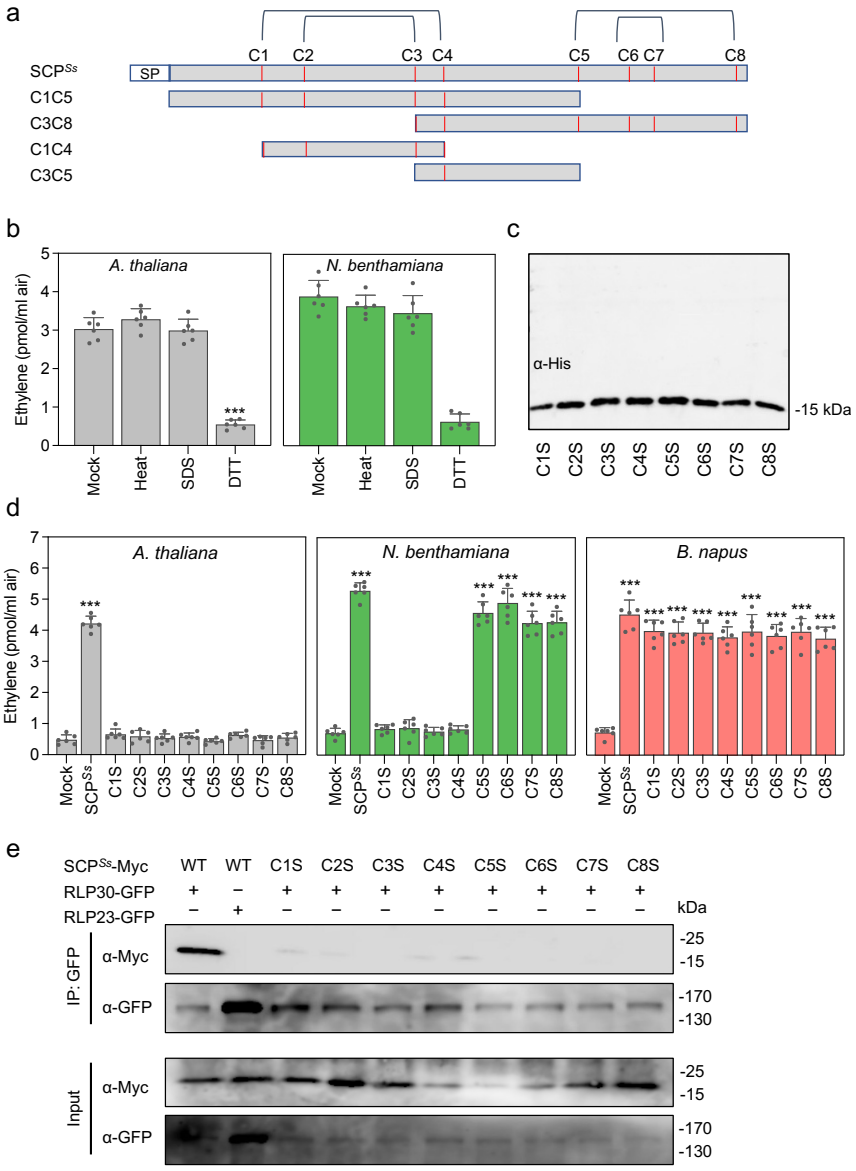

Fig. 8. Different requirements for cysteines in SCP^{Ss} for its immunogenic activity in Brassicaceae and Solanaceae.

a, Schematic representation of SCP^{Ss} and derived truncations C1C5, C3C8, C1C4 and C3C5. Cysteine (C) residues are numbered and indicated as red lines, predicted disulphide bridges (DB, http://clavius.bc.edu/~clotelab/DiANNA/) are shown on top. SP, signal peptide. **b,** Ethylene accumulation in *A. thaliana* Col-0 or *N. benthamiana* plants treated with 1 µM water-treated SCP^{Ss} (mock), or SCP^{Ss} that was pre-treated for 1h at 95°C (heat), 1 % SDS, or 100 µM DTT. **c,** Western Blot analysis of SCP^{Ss} with individual cysteine to serine mutations purified from *P. pastoris* using anti-His antiserum. **d,** Ethylene accumulation in *A. thaliana* Col-0, *N. benthamiana* or *B. napus* wild-type plants after 4 h treatment with water (mock), 1 µM SCP^{Ss}, and SCP^{Ss} with individual cysteine to serine mutations (C1S to C8S, according to cysteine numbering shown in **a**). Data points are indicated as dots (n = 6 for b; n = 6 for c) and plotted as box plots (centre line, median; bounds of box, the first and third quartiles; whiskers, 1.5 times the interquartile range; error bar, minima and maxima). Statistically significant differences from mock treatments in the respective plants are indicated (two-sided Student's t-test, ***P ≤ 0.001). **e,** Ligand-binding assay in *N. benthamiana* transiently expression SCP^{Ss}-myc and SCP-Cys mutations

with RLP30-GFP or RLP23-GFP. Proteins extracted from *N. benthamiana* leaves expressing indicated protein combinations (Input) were used for co-immunoprecipitation with GFP-trap beads (IP:GFP) and immunoblotting with tag-specific antibodies. The experiment was repeated three times with similar results.

as active as intact SCP in *B. napus, B. rapa,* and *B. oleracea* (Fig. 9a,b and Supplementary Fig. 3b), indicating that this SCP^{Ss}-fragment is sufficient to trigger immune responses in *Brassica* species. We therefore demonstrate that unlike RLP30-mediated recognition of intact SCP^{Ss} in *Arabidopsis*, *Brassica* species can sense a small SCP^{Ss} epitope that is distinct from the disulfide-bond containing peptide perceived in Solanaceae.

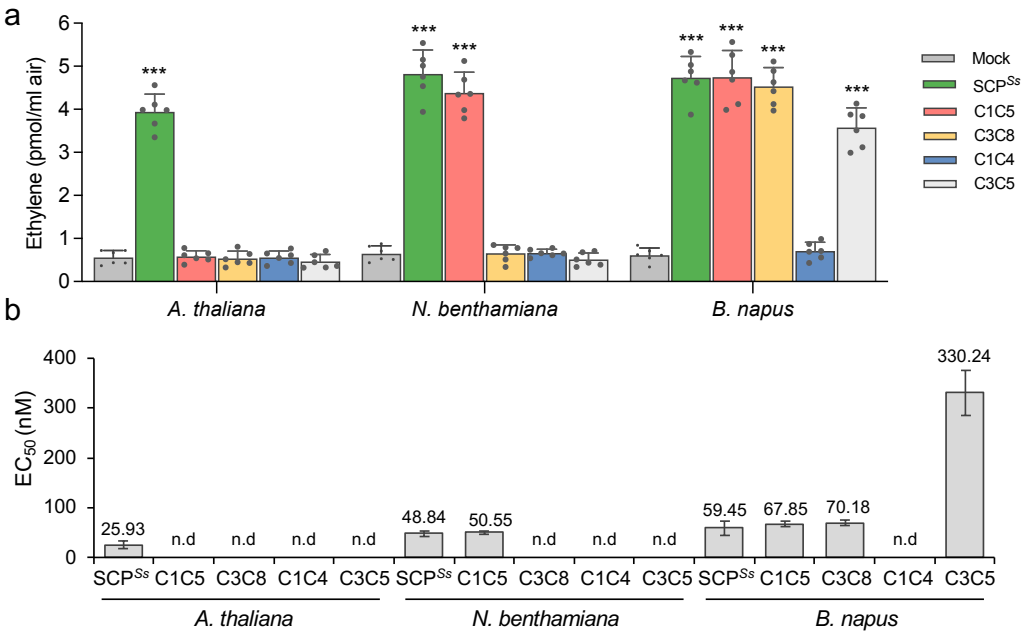

Fig. 9. SCP^{Ss} sensing differs in Brassicaceae and Solanaceae. a, c, Ethylene accumulation in *A. thaliana* Col-0, *N. benthamiana* or *B. napus* wild-type plants after 4 h treatment with water (mock), 1 µM SCP^{Ss}, and SCP^{Ss} truncations depicted in **Fig. 8a**. Data points are indicated as dots (n = 6 for b; n = 6 for c) and plotted as box plots (centre line, median; bounds of box, the first and third quartiles; whiskers, 1.5 times the interquartile range; error bar, minima and maxima). Statistically significant differences from mock treatments in the respective plants are indicated (two-sided Student's t-test, ***$P \leq 0.001$). **b,** Determination of EC_{50} values of SCP^{Ss} and the various SCP^{Ss} truncations using ethylene accumulation in *A. thaliana*, *N. benthamiana*, or *B. napus* plants after treatment with increasing concentrations of recombinant SCP^{Ss} versions (produced in *Pichia*) or synthetic C3C5 (n.d, activity not detectable). Each experiment was repeated three times with similar results.

4.5 RLP30 senses *Pseudomonas*-derived PAMPs

4.5.1 SCP-like^{Psp} has similar function with SCP^{Ss}

Intriguingly, *rlp30* mutants have been found to be more susceptible to bacterial infection with *P. syringae* pv. *phaseolicola* (*Psp* 1448A)[25]. We thus wondered whether RLP30 might also recognize a PAMP from *Pseudomonads*, despite the apparent absence of SCP^{Ss} homologs in bacteria[18]. Using the chromatographic enrichment protocol established for SCFE1 from S. *sclerotiorum*[7], Dr. Christina Steidele purified a RLP30-dependent elicitor-containing fraction

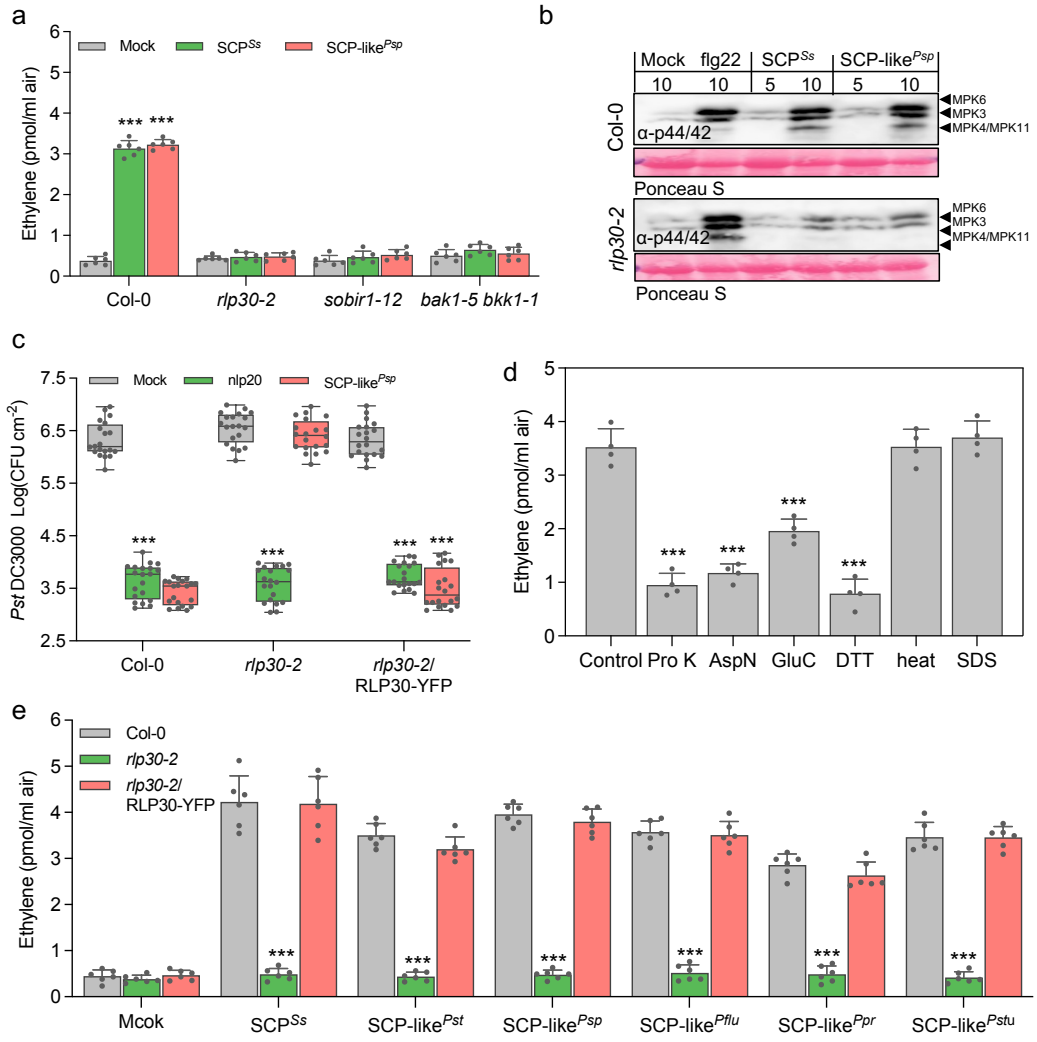

Fig. 10. *Pseudomonads* produce a RLP30-dependent elicitor activity.

a, Ethylene accumulation in Col-0 wild-type plants, indicated mutants 4 h after treatment with water (mock), 1 µM SCP^{Ss} or 1.5 µg/ml SCP-like from *P. syringae* pv. *phaseolicola (Psp).* **b,** MAPK activation in *Arabidopsis* Col-0 wild-type plants or *rlp30-2* mutants infiltrated for the indicated times with 0.1 µM flg22, 1 µM SCP^{Ss}, or 1.5 µg/ml SCP-like^{Psp}. MAPK activation was detected by immunoblot using phospho-p44/p42 antibodies, equal loading was verified by staining of the membrane with Ponceau S Red. **c,** Bacterial growth in Col-0 wild-type plants, *rlp30-2* mutants, or the *rlp30-2/RLP30-YFP* complementation line treated with water (mock), 1 µM nlp20, or 1.5 µg/ml SCP-like^{Psp} 24 h before infiltration of *Pst* DC3000. Bacteria (colony forming units, CFU) were quantified in extracts of leaves 3 days after inoculation. **d,** Ethylene accumulation in Col-0 wild-type plants incubated for 4 h with water (mock), or 1.5 µg/ml SCP-like^{Psp} treated for 4 h with 100 nM Proteinase K (Prot K), AspN, GluC, DTT, 1h at 95°C (heat), or 1 % SDS. **e,** Ethylene accumulation in Col-0, *rlp30-2* and *rlp30-2*/RLP30-YFP plants 4 h after treatment with water (mock), 1 µM SCP^{Ss} or 1.5 µg/ml SCP-like from *Pseudomonas syringae* pv. *tomato (Pst)*, *P. syringae* pv. *phaseolicola (Psp)*, *P. fluorescens (Pflu)*, *P. protegens (Ppr)*, and *P. stutzeri (Pstu)* (SCP-like fractions produced by Dr. Christina Steidele). Data points are indicated as dots (n = 6 for a,d,d,e c; n = 20 for c) and plotted as box plots (centre line, median; bounds of box, the first and third quartiles; whiskers, 1.5 times the interquartile range; error bar, minima and maxima). Statistically significant differences are indicated (two-sided Student's t-test, ***$P \leq 0.001$). Each experiment was repeated three times with similar results.

from *Psp* 1448A culture medium (Fig. 10a). This elicitor-active fraction was termed SCP-like^{Psp} for “SCP like elicitor from *P. syringae* pv. *phaseolicola* (*Psp*)”.

SCP-like^{Psp} triggered typical immune responses such as ethylene production, the phosphorylation of mitogen-activated protein kinases, as well as enhanced resistance to *Pst* DC3000 in *Arabidopsis* wild-type plants and RLP30-YFP complementation lines, whereas *rlp30-2* mutants proved insensitive to SCP-like^{Psp}-treatment (Fig. 10b,c).

SCP-like^{Psp} also induced ethylene biosynthesis in *fls2 efr* and *rlp32-2* mutants, indicating that activity was not due to the well-established bacterial PAMPs flagellin, EF-Tu or IF1 (Fig. 11a). In contrast, SCP-like^{Psp} had no activity in the mutant *rlp30*-2, in nine of the SCP^{Ss}-insensitive accessions, and in the *sobir1-12* and *bak1-5 bkk1-1* mutants (Fig. 10a and Fig. 11b), suggesting that perception of SCP-like^{Psp} involves all the components required for perception of SCP^{Ss}.

So far, our attempts to determine the molecular identity of SCP-like^{Psp} were not successful. However, much like SCP^{Ss}, the immunogenic activity of SCP-like^{Psp} was sensitive to treatment with DTT and proteases, but resistant to heat and SDS treatment, suggesting that it is likely also a protein stabilized by disulfide bridges (Fig. 10d).

4.5.2 SCP-like^{Psp} is conserved in *Pseudomonas* species

To determine whether SCP-like^{Psp} activity is conserved in *Pseudomonas,* we enriched SCP-like containing fractions from other *Pseudomonas* strains. As shown in Fig. 10e, SCP-like^{Psp} was present in all tested *Pseudomonas* strains, including *P. syringae pv. tomato* DC3000, *P.phaseolicola*, *P. fluorescens*, *P. protegens* and *P. stutzerii*. All purified SCP-like fractions were shown to trigger RLP30-dependent ethylene accumulation. Taken together, our results suggest that RLP30 is involved in *Pseudomonas* resistance by sensing a conserved *Pseudomonas*-conserved pattern.

4.5.3 RLP30 and RE02 differ in perception of SCP-like

SCP-like^{Psp} showed activity in *A. thaliana*, *B. rapa,* and *B. oleracea*, species of the *Brassicaceae* family that perceive SCPs and thus encode RLP30 homologs (Fig. 11c). Interestingly, none of the species from the Solanaceae family tested showed responsiveness to bacterial SCP-like^{Psp} (Fig. 11c). These species included *N. benthamiana, S. pennellii, S. lycopersicum, S. tuberosum and C. annuum* with functional SCP^{Ss} perception, indicating that RE02 and solanaceous homologs do not respond to SCP-like^{Psp}. Ectopic expression of RLP30 in *N. benthamiana* conferred sensitivity to SCP-like^{Psp}, but not to nlp20 which required expression of RLP23 (Fig. 11d). Thus, RLP30, but not RE02, senses patterns from three microbial kingdoms.

4.6 RLP30 expression in *N. tabacum* confers increased resistance to bacterial, fungal and oomycete pathogens

Since RLP30 has the property of sensing PAMPs from microorganisms of three kingdoms, we envisaged to confer broad-spectrum disease resistance by introducing RLP30 into SCP^{Ss}-

insensitive crop plants. We selected *N. tabacum* as crop due to its lack of endogenous immune sensor systems for SCPs (SCP^{Ss} and SCP homologs) and SCP-like^{Psp} (Fig. 2e,11c and Extended Data Fig. 3a). We observed that *N. tabacum* plants transiently expressing RLP30-GFP were responsive to SCP^{Ss} and SCP-like^{Psp}, albeit with only a moderate increase in production of ethylene (Supplementary Fig. 3a,b). We wondered whether this might be due to a partial incompatibility of RLP30 with the endogenous tobacco SOBIR1. Indeed, co-expression of RLP30 with *At*SOBIR1 in *N. tabacum* established higher responses to SCP^{Ss} and SCP-like^{Psp}, whereas plants co-transformed with *RLP30* and *NbSOBIR1* or *SlSOBIR1* showed responses as plants without additional SOBIR1 (Supplementary Fig. 3a,b).

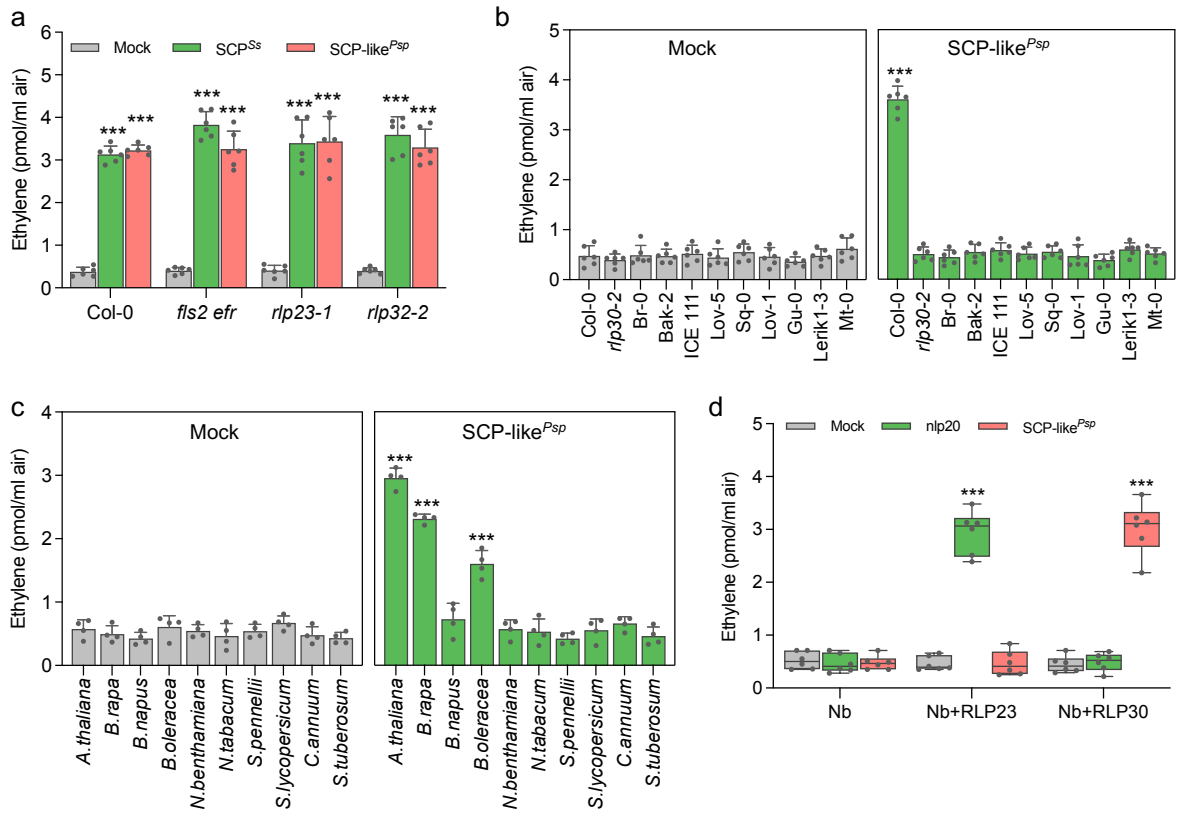

Fig. 11. RLP30 and RE02 differ in perception of SCP-like^{Psp}. a,b, Ethylene accumulation in Col-0 wild-type plants, indicated mutants or SCP^{Ss}-insensitive accessions 4 h after treatment with water (mock), 1 µM SCP^{Ss} or 1.5 µg/ml SCP-like^{Psp}. **c,** Ethylene accumulation in Col-0 wild-type plants or indicated plants of the Brassicaceae and Solanaceae family 4 h after treatment with water (mock), or 1.5 µg/ml SCP-like^{Psp}. **d,** Ethylene accumulation in *N. benthamiana* (*Nb*) plants transiently expressing RLP23-GFP or RLP30-GFP and treated for 4 h with water (mock), 1 µM nlp20, or 1.5 µg/ml SCP-like^{Psp}. Data points are indicated as dots (n = 6 for a,b,d; n = 4 for c) and plotted as box plots (centre line, median; bounds of box, the first and third quartiles; whiskers, 1.5 times the interquartile range; error bar, minima and maxima). Statistically significant differences are indicated (two-sided Student's t-test, ***$P \leq 0.001$). Each experiment was repeated three times with similar results.

Thus, *p35S::RLP30-RFP* together with the *p35S::AtSOBIR1-GFP* construct were introduced into *N. tabacum* by *Agrobacterium*-mediated transformation. Two stable transgenic lines (*#49* and *#55*, lines generated by Dr. Christina Steidele) were selected based on detectable expression of RLP30 and *At*SOBIR1 (Supplementary Fig. 3c). Neither of the two transgenic

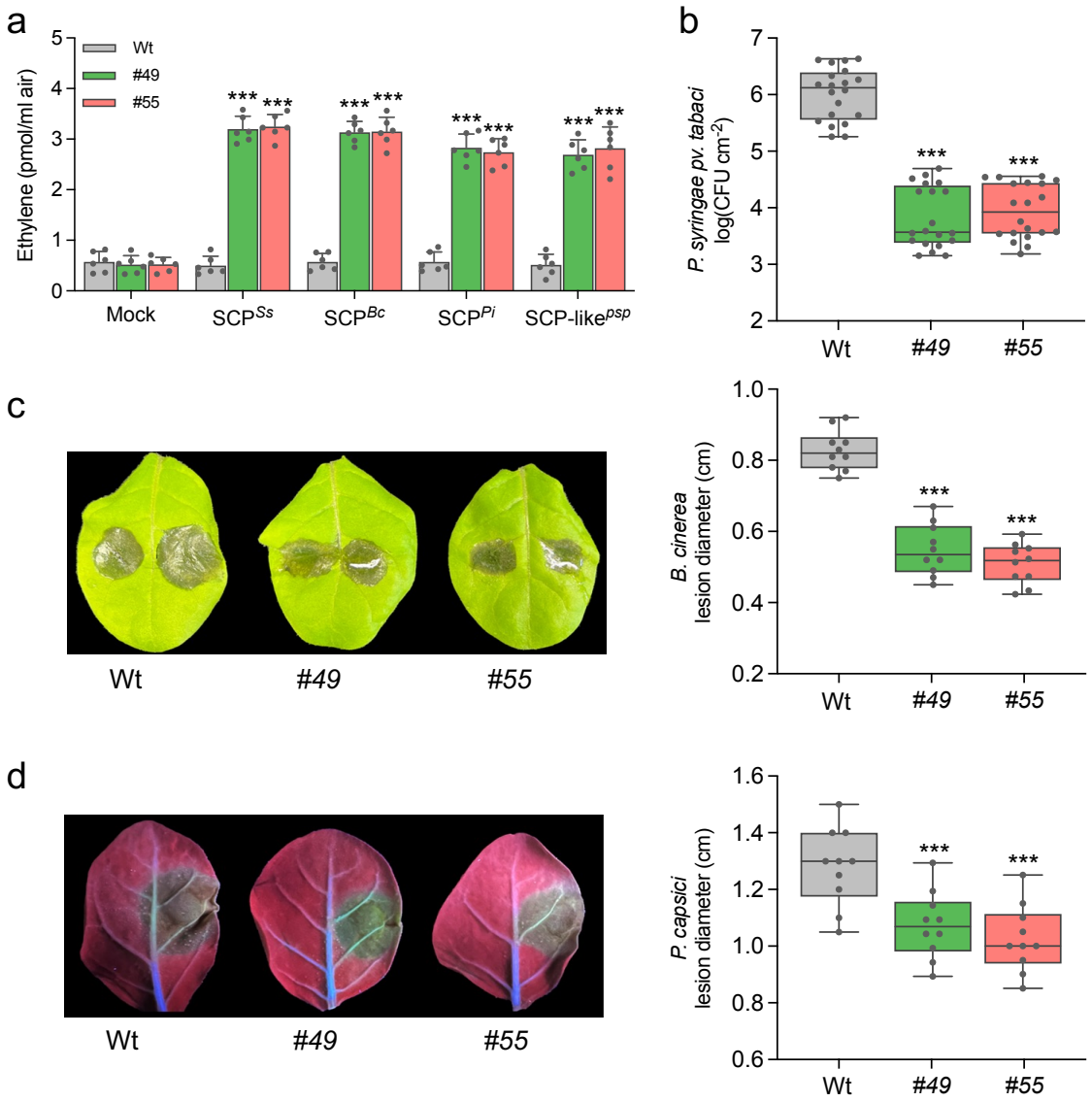

Fig. 12. RLP30 expression in *N. tabacum* confers increased resistance to pathogens.

a, Ethylene accumulation in *N. tabacum* wild-type plants (Wt) or two transgenic lines (*#49* and *#55*) stably expressing RLP30-RFP and SOBIR1-GFP after 4 h treatment with water (mock), 1 µM SCP from indicated sources, or 1.5 µg/ml SCP-like^{Psp}. **b,** Bacterial growth of *P. syringae* pv. *tabaci* in *N. tabacum* wild-type plants (Wt) or transgenic *RLP30/SOBIR1* lines (#49 and #55). Bacteria (colony forming units, CFU) were quantified in extracts of leaves 3 days after inoculation. **c,** *B. cinerea* infected area on leaves of *N. tabacum* wild-type plants (Wt) or transgenic *RLP30/SOBIR1* lines (left, shown are representative leaves) and determination of lesion diameter on day 2 after drop inoculation (right). **d,** Growth of *Phytophthora capsici* on leaves of *N. tabacum* wild-type plants (Wt) or transgenic *RLP30/SOBIR1* lines by determination of lesion size (right) of lesions observed under UV light (left, shown are representative leaves) on day 2 after drop inoculation. Data points are indicated as dots (n = 6 for a; n = 20 for b, n = 10 for c, d) and plotted as box plots (centre line, median; bounds of box, the first and third quartiles; whiskers, 1.5 times the interquartile range; error bar, minima and maxima). Statistically significant differences from wild-type (Wt) plants are indicated (two-sided Student's t-test, ***$P \leq 0.001$). Each experiment was repeated three times with similar results.

lines exhibited autoimmune phenotypes as mock treatment did not induce ethylene accumulation and no elevated expression of salicylic acid marker gene *PR-1a* or jasmonic acid marker gene *PDF1.2* could be detected in untreated plants (Fig. 12a and Supplementary Fig. 3a,d). In contrast to wild-type tobacco plants, *#49* and *#55* transgenic lines clearly responded to SCPs or SCP-like^{Psp} (Fig. 12a).

Next, the performance of RLP30 transgenic tobacco plants in infection assays were tested. When inoculated with the adapted bacterial pathogen *P. syringae pv. tabaci* (*Pta*), transgenic plants exhibited increased antibacterial immunity with less bacterial growth compared to wild-type plants (Fig. 12b). Moreover, RLP30-expression conferred resistance to the necrotrophic fungus *B. cinerea* in *N. tabacum* lines *#49* and *#55*. RLP30-transgenic lines showed less disease severity with significantly reduced lesion diameter upon *B. cinerea* inoculation compared to untransformed control plants (Fig. 12c). Similarly, disease-caused lesions developing after infection with the oomycete *Phytophthora capsici* were significantly smaller in leaves of RLP30-transgenic *N. tabacum* lines than those observed in wild-type plants (Fig. 12d). Taken together, stable, ectopic expression of RLP30 in *N. tabacum* conferred sensitivity to SCPs and SCP-like^{Psp} and rendered these transgenic plants more resistant to destructive bacterial, fungal, and oomycete pathogens.

4.7 Regulation of SCP^{Ss} signaling in *Arabidopsis*

4.7.1 BIR2 and BIR3 are negative regulators of RLP-induced immunity

BIR2 and BIR3 are negative regulators of RLK-mediated plant immunity by interacting with BAK1 to prevent FLS2–BAK1 complex formation in the non-induced state[82,83]. To examine

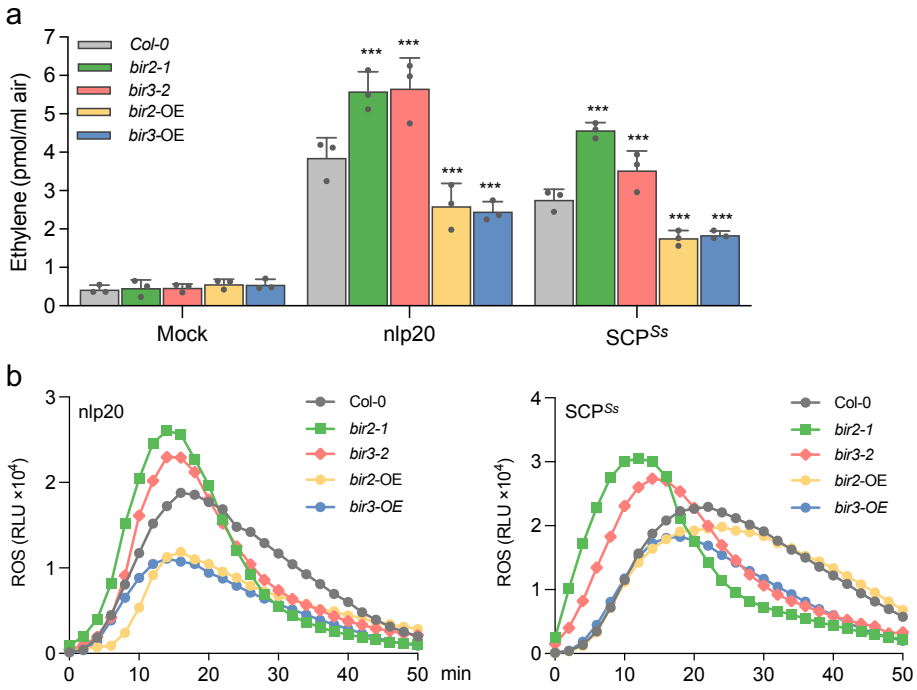

Fig. 13. BIR2 and BIR3 are negative regulators of RLP-induced immunity. a, Ethylene accumulation in Col-0 wild-type plants or bir2 and bir3 mutants or BIR2 and BIR3 overexpression lines 4 h after treatment with water

(mock), 1 µM nlp20, or 1 µM SCP^{Ss}. Data points are indicated as dots (n = 6) and plotted as box plots (centre line, median; bounds of box, the first and third quartiles; whiskers, 1.5 times the interquartile range; error bar, minima and maxima). Statistically significant differences from Col-0 plants are indicated (two-sided Student's t-test, ***P ≤ 0.001). **b,** ROS production in leaf pieces of *Arabidopsis* Col-0 wild-type plants or bir2 and bir3 mutants or BIR2 and BIR3 overexpression lines treated with 2 µM nlp20, or 2 µM SCP^{Ss}. Given are relative light units (RLU) ± SD (n=6). Statistically significant differences are indicated (two-sided Student's t-test, ***P ≤ 0.001).All experiments were repeated three times with similar results.

whether BIR2 and BIR3 also negatively regulate RLP-mediated immunity outputs, we measured SCP^{Ss}-induced PTI responses in the loss-of-function mutants (*bir2* and *bir3*) and the BIR2-OE and BIR3-OE overexpression plants (BIR2-OE and BIR3-OE)[82,83]. In *bir2* and *bir3* mutants, ethylene levels after SCP^{Ss} and nlp20 treatment were significantly higher than in the wild type, whereas elicitor-induced ethylene production was reduced in BIR2-OE and BIR3-OE plants (Fig. 13a). Consistent with the ethylene levels, SCP^{Ss}-induced production of ROS was significantly reduced by overexpression of BIR2 and BIR3, whereas elevated ROS levels were observed in the *bir2* and *bir3* mutants compared to wild-type plants (Fig. 31b). Hence, our results demonstrate that BIR2 and BIR3 negatively regulate RLP-mediated immunity.

4.7.2 The EDS1–PAD4–ADR1 node mediates SCP^{Ss}-triggered immunity

Recently, the *Arabidopsis* class VII RECEPTOR-LIKE CYTOPLASMIC KINASES (RLCKs) PBL30 and PBL31 were shown to mediate PTI triggered by RLPs ligands such as nlp20 or

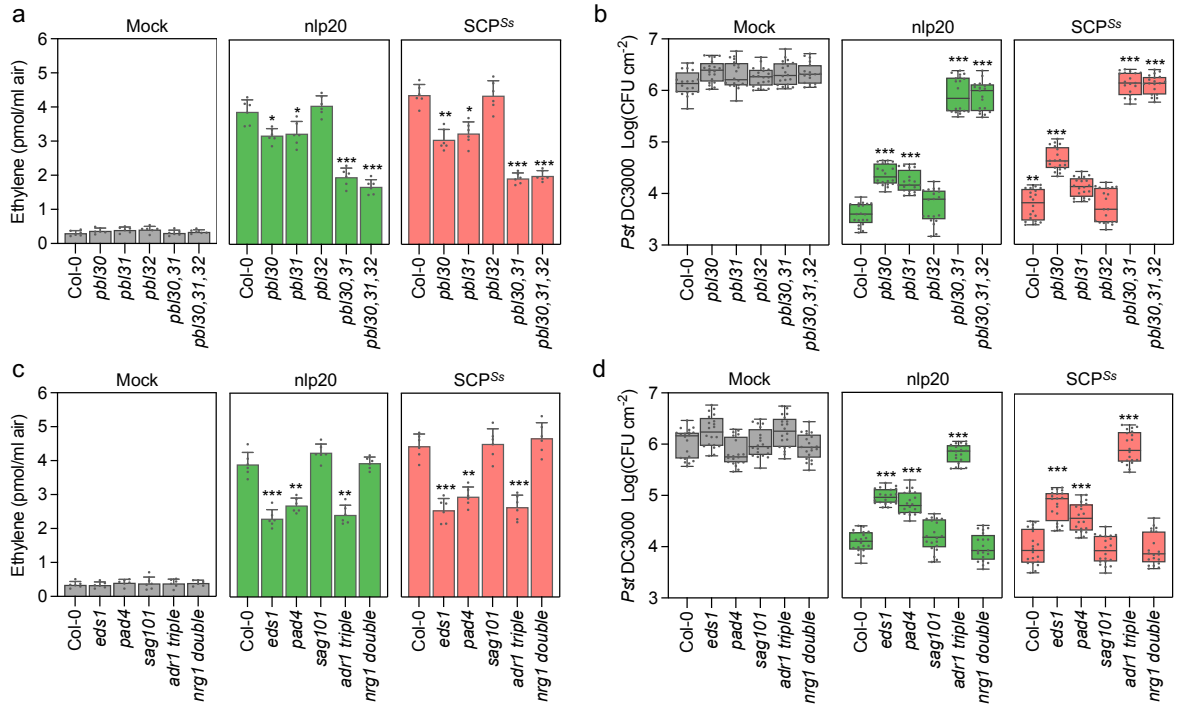

Fig. 14. Regulation of SCP^{Ss} signaling in *Arabidopsis*. a, Ethylene accumulation in *Arabidopsis* Col-0 wild-type plants, *pbl30*, *pbl31*, *pbl32* mutants, double or triple mutants 4 h after treatment with water (mock), 1 µM nlp20, or 1 µM *P. pastoris*-expressed SCP^{Ss}. **b,** Bacterial growth in plants (Col-0, *pbl30*, *pbl31*, *pbl32* mutants, double or

triple mutants) pre-treated with water (mock), 1 μM nlp20, or 1 μM SCP^{Ss} 24 h before infiltration of *Pst* DC3000. Bacteria (colony forming units, CFU) were quantified in extracts of leaves 3 days after inoculation. **c,** Ethylene accumulation in *Arabidopsis* Col-0, *eds1*, *pad4*, *adr1*, *sag101*, *adr1* triple or *nrg1* double mutants 4 h after treatment with water (mock), 1 μM nlp20, or 1 μM *P. pastoris*-expressed SCP^{Ss}. **d,** Bacterial growth in plants (Col-0, *eds1*, *pad4*, *adr1*, *sag101*, *adr1* triple or *nrg1* double mutants) pre-treated with water (mock), 1 μM nlp20, or 1 μM SCP^{Ss} 24 h before infiltration of *Pst* DC3000. Bacteria (colony forming units, CFU) were quantified in extracts of leaves 3 days after inoculation. Data points are indicated as dots (n = 6 for a, c; n = 20 for b, d) and plotted as box plots (centre line, median; bounds of box, the first and third quartiles; whiskers, 1.5 times the interquartile range; error bar, minima and maxima). Statistically significant differences from Col-0 plants are indicated (two-sided Student's t-test, *$P \leq 0.05$,**$P \leq 0.01$, ***$P \leq 0.001$). All assays were performed at least three times with similar results.

fungal polygalacturonases[9]. Ethylene accumulation triggered by SCP^{Ss} was slightly impaired in the *pbl30*, *pbl31* single mutants and significantly reduced in the *pbl30 pbl31* double mutants (Fig. 14a) Similarly, the *pbl30 pbl31* double mutant plants were unable to restrict the growth of *Pst* DC3000 after SCP^{Ss}-pretreatment (Fig. 14b).

PTI mediated by several RLPs (RLP23, RLP32, RLP42) depends on the ETI-components EDS1 and PAD4, and requires the helper NLR ADR1[79]. Consistently, SCP^{Ss}-triggered ethylene accumulation and SCP^{Ss}-induced resistance to *Pst* DC3000 was significantly reduced in *eds1*, *pad4* and *adr1* mutants compared to wild-type plants (Fig. 14c,d). In sum, RLP30-mediated SCP^{Ss} signaling in Arabidopsis is regulated by BIR2/3, PBL30/31 and EDS1, PAD4 and ADR1 family members.

4.8 Regulation of SCP^{Ss} signaling in *Nicotiana benthamiana*

4.8.1 EDS1 complexes are dispensable for SCP^{Ss} signaling in *N. benthamiana*

Although many studies have shown that PTI and ETI are interrelated in *Arabidopsis*[75-79], there is little information about the crosstalk between PTI and ETI in Solanaceae (such as *N. benthamiana*). EDS1, as a hub of signaling regulation, forms mutually exclusive heterodimers with PAD4 or SAG101[69]. While the EDS1-PAD4 complex together with ADR1 is required for TNL-mediated pathogen resistance and a subset of the immune responses triggered by RLPs in *Arabidopsi* [79], the EDS1/PAD4/NRG1 module regulates cell death[69]. To determine whether EDS1 complexes are also involved in RLP-mediated signaling in *N. benthamiana*, we tested ethylene accumulation elicited by SCP^{Ss} in a series of mutant lines deficient in EDS1 complexes. Intriguingly, *eds1*, *pad4*, *epss* (quadruple knockout mutant of *EDS1a*, *PAD4*, *SAG101a/b*, kindly obtained from the Johannes Stuttmann's Lab) and *adr1 nrg1*（knockout mutant of the two helper NLRs ADR1 and NRG1, kindly obtained from the Farid El Kasmi's Lab）mutants produced similar ethylene accumulation as the wild type in response to SCP^{Ss} (Fig. 15a). Similarly, ethylene production mediated by the RLK FLS2 was also not significantly reduced in these mutants compared to the wild-type plants (Fig. 15a).

Furthermore, EDS1-related immune modules were also not involved in SCP^{Ss}-induced late immune events such as induction of host cell death. We observed a strong hypersensitive

cell death triggered by SCP^{Ss} in wild-type plants but not in *nbsobir1/nbsobir1-like* mutant plants (*sobir1-Cas9*) (Fig. 15b). However, SCP^{Ss}-triggered cell death was not affected in EDS1 complex-deficient lines *eds1*, *pad4*, *epss* and *adr1 nrg1* (Fig. 15b). Next, we tested whether EDS1 complexes are also not involved in cell death formation mediated by other

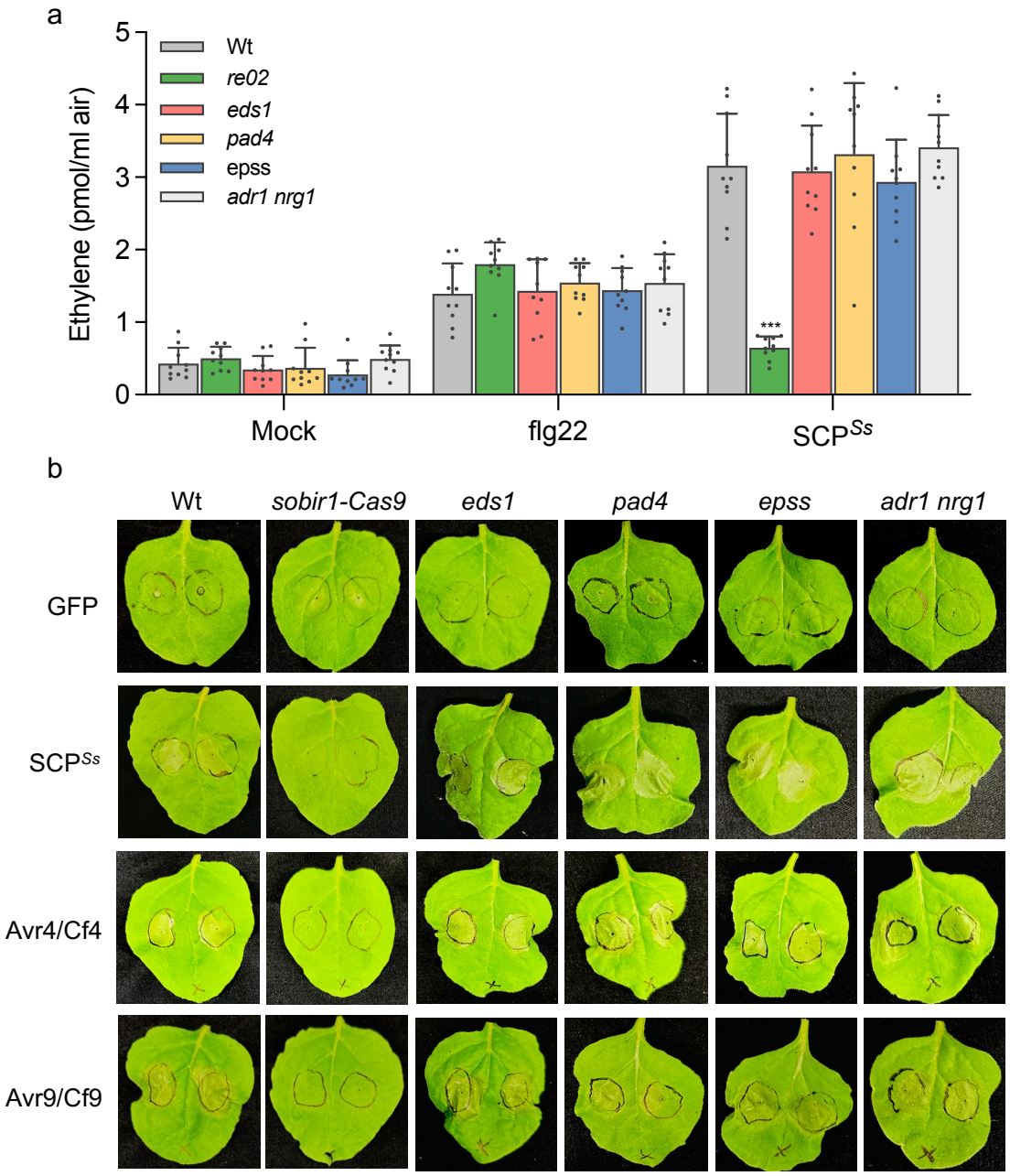

Fig. 15. EDS1-RNL modules are not involved in RLP-mediated immunity in *N. benthamiana*.

a, Ethylene accumulation in wild-type plants (Wt) or indicated mutants 4 h after treatment with water (mock), 2 μM flg22 or 1 μM SCP^{Ss}. Data points are indicated as dots (n = 9) and plotted as box plots (centre line, median; bounds of box, the first and third quartiles; whiskers, 1.5 times the interquartile range; error bar, minima and maxima). Statistically significant differences from Wt plants are indicated (two-sided Student's t-test, ***$P \leq 0.001$). **b,** Cell death induction upon transient expression of GFP, SCP^{Ss}, Avr4/Cf4 or Avr9/Cf9. All constructs were expressed by agroinfiltration (OD600 = 0.5) in the indicated *N. benthamiana* lines. Symptom (cell death) formation was documented 3 d postinfiltration (dpi). The experiment was conducted eight times with similar results.

RLPs in *N. benthamiana*. The tomato RLPs Cf4 and Cf9 can be activated and cause cell death by transient co-expression of their respective ligands Avr4 and Avr9 in *N. benthamiana*[84]. Similar to SCP-triggered cell death, we also did not observe significant differences in Avr4/Cf4 and Avr9/Cf9-triggered cell death between the wild type or *eds1*, *pad4*, *epss* and *adr1 nrg1* mutants. These results indicate that neither EDS1 dimers nor RNLs are required for RLP-triggered immune responses in *N. benthamiana* (Fig. 15b). Thus, we conclude that the dependence of PRR signaling on EDS1 complexes is not conserved between *Arabidopsis* and *N. benthamiana*.

4.8.2 SCP^{Ss}-induced cell death requires the NRC family in *N. benthamiana*

Since the RLP-mediated immune responses do not depend on EDS1-related modules in *N. benthamiana*, we hypothesized that other important ETI regulators might participate in SCP^{Ss}-induced immune signaling. So far, there are some clues pointing to the CC (coiled coil)-type NLR NRCs (NLR required for cell death) requirement for RLP Cf4 and EIX2-mediated immunity in Solanaceae[84,85]. We therefore speculated that NRCs might also be required for the immune response induced by SCP^{Ss}.

To test this hypothesis, deletion mutants of NRCs including *nrc23* (knockout mutant of *NRC2a*/*2b* and *NRC3*), *nrc4* (knockout mutant of *NRC4a/b/c*) and *nrc234* (knockout mutant of *NRC2a*/*2b*, *NRC3* and *NRC4a/b/c*, all kindly provided by the Sophien Kamoun's Lab, UK) were used to test the contribution of NRC helper NLRs in SCP^{Ss}-induced immune responses. We first monitored the production of ethylene in response to SCP^{Ss} and flg22. However, NRCs deletion did not affect SCP^{Ss}- or flg22-induced ethylene accumulation, which suggests that LRR-type receptor-mediated early immune responses may not require NRC helper NLRs (Fig. 16a). Interestingly, SCP^{Ss}-triggered cell death was significantly reduced in both the *nrc23* and *nrc234* mutant lines as compared to wild-type plants (Fig. 16b). Furthermore, while the negative control GFP and XopQ1 (an effector derived from *Xanthomonas*, induces the TNL Roq1 and EDS1-dependent cell death) did not cause cell death in these *nrc* plants, the cell death phenotypes mediated by the Avr4/Cf4 pair was abolished in *nrc23* mutants (Fig. 16b). These results indicate that NRC2/3 are involved in RLP-triggered cell death in *N. benthamiana*.

4.8.3 TIR enzymatic function is required for SCP^{Ss}-triggered cell death in *N. benthamiana*

A recent study demonstrated that the TNL SADR1 (Suppressor of ADR1-L2) is required for nlp20-induced resistance in *Arabidopsis*[86]. Inhibition of TIR enzymatic activity by nicotinamide (NAM) inhibits nlp20-driven defense priming[86], which suggests that the small molecules produced by activated TNLs are crucial for RLP-mediated defense. We therefore investigated whether the enzymatic activity of TNLs also participates in RLP-triggered immune signaling in *N. benthamiana*. Unlike in *Arabidopsis*, infiltration of *N. benthamiana* leaves with 50 mM NAM caused intense necrosis (data not shown). Testing a concentration gradient between 1 mM and 1000 mM indicated that 10 mM NAM does not cause spontaneous cell death (data not shown). However, 10 mM NAM is sufficient to inhibit TIR

enzymatic activity as shown by the absence of XopQ1/ROQ1 -dependent necrosis in the NAM-treated *N. benthamiana* leaves (Fig. 16d).

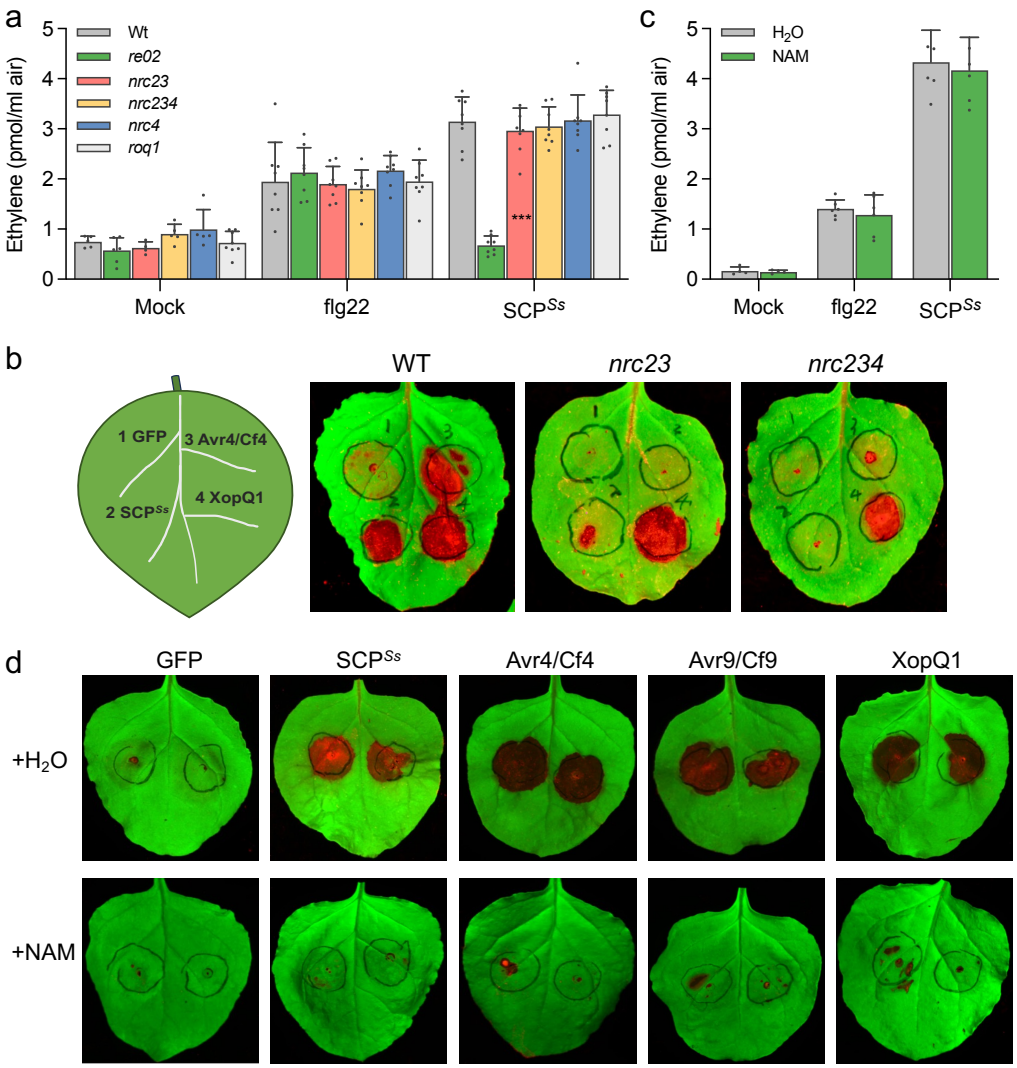

Fig. 16. Regulation of SCP^{Ss} signaling depends on the NRC family in *N. benthamiana*.

a, Ethylene accumulation in *N. benthamiana* wild-type plants (Wt) or indicated mutants 4 h after treatment with water (mock), 2 µM flg22 or 1 µM SCP^{Ss}. **b,d,** Cell death induction upon transient expression of GFP, SCP^{Ss}, Avr4/Cf4, Avr9/Cf9 or XopQ1. All constructs were expressed by agroinfiltration (OD600 = 0.5) in the indicated *N. benthamiana* lines. Cell death images were taken 3 d post-infiltration (dpi) under UV light using an Amersham ImageQuant 800 and an integrated Cy5 filter (GE Healthcare; Chalfont St. Giles, UK). The experiment was conducted ten times with similar results. **c,** Ethylene accumulation in wild-type plants (pretreated with H_2O or 10 mM NAM for 24 h) 4 h after treatment with water (mock), 2 µM flg22 or 1 µM SCP^{Ss}. The experiment was conducted eight times with similar results.

We then tested the effect of NAM treatment on SCP^{Ss}-induced ethylene accumulation and cell death. Interestingly, while 10 mM NAM didn't affect SCP^{Ss}-elicited ethylene production, SCP^{Ss}-triggered cell death was significantly reduced (Fig. 16c,d). Consistently, NAM treatment was ineffective in reducing flg22-induced ethylene accumulation. Moreover, we

also did not observe cell death formation mediated by Avr4/Cf4 and Avr9/Cf9 pairs in NAM-treated plants (Fig. 16d). Overall, TIR enzymatic function is required for RLP-mediated cell death in *N. benthamiana*. Therefore, we conclude that the NRC family as well as the unknown TNL members are involved in RLP-mediated late immune responses such as cell death in *N. benthamiana*.

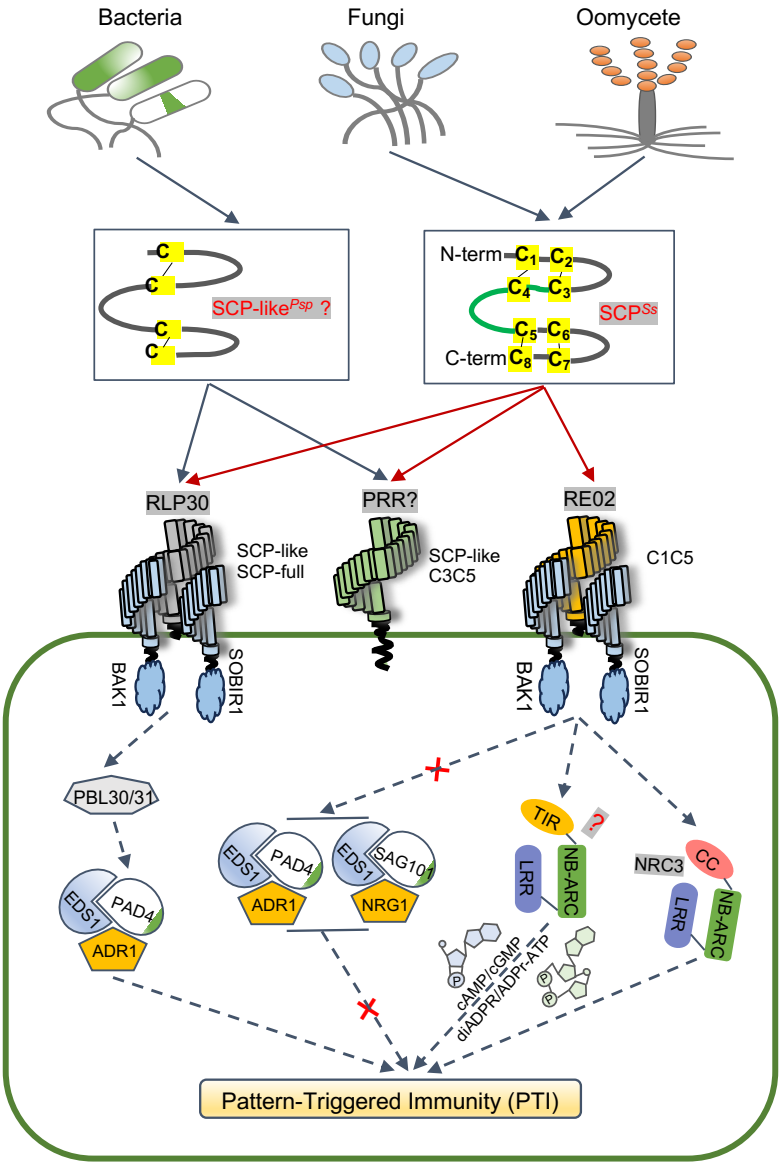

Fig. 17. Schematic model of RLP30 and RE02-mediated pattern recognition and signaling in plants. RLP30 recognizes SCP^{Ss} and its homologs from different fungi and oomycetes, as well as an SCP^{Ss}-unrelated and conserved pattern from *Pseudomonas* (SCP-like^{Psp}). RE02, an RLP non-homologous to RLP30, mediates SCP^{Ss} recognition in *N. benthamiana*. Unlike RLP30-mediated recognition of entire SCP^{Ss} in *A. thaliana*, Brassica species and Solanaceae perceive a small immunogenic epitope and a disulfide-bond containing peptide of SCP^{Ss}, C3C5 and C1C5, respectively. While RLP30 signals through the EDS1–PAD4–ADR1 node in *Arabidopsis*, EDS1-RNLs modules are dispensable for SCP^{Ss}-triggered immunity in *N. benthamiana.* Instead, TIR enzymatic function of unknown TNLs and the helper NLR NRC3 are involved in SCP^{Ss}-induced cell death, but not early immune events such as ethylene production in *N. benthamiana*.

5. Discussion

5.1 A Single PRR can detect patters from microorganisms of three kingdoms

Plants deploy pattern-triggered immunity (PTI) mediated by Pattern Recognition Receptors (PRRs) to counter harmful pathogen infection. However, the characterization of these large numbers of potential receptor genes in plants is strictly dependent on knowledge of the respective ligands. Employing mass spectrometry, reverse genetics and biochemical assays we identified here the ligand of the previously described RLP30 as a secreted, small cysteine-rich protein (SCP^{Ss}).

RLP30 is a bona-fide SCP^{Ss}-receptor based on the following findings: (i) SCP^{Ss} fails to trigger immune responses in *rlp30* mutants, (ii) RLP30 confers sensitivity to SCP^{Ss}-insensitive *N. tabacum*, (iii) RLP30 specifically binds SCP^{Ss}, (iv) SCP^{Ss} triggers complex formation of RLP30/SOBIR1 with SERK family members, and (v) *rlp30* mutants fail to restrict pathogen growth upon pretreatment with SCP^{Ss}. Single nucleotide polymorphism analyses of RLP30 in SCP^{Ss}-insensitive accessions and SCP^{Ss} binding assays suggest that the single amino acids L307, R433, N561, G563, and F760 are important for RLP30 functionality as point mutations in insensitive *Arabidopsis* accessions render these mutated receptors non-functional. Hence, SNP-based analysis provides a tool for the prediction of RLP-ligand binding sites as long as crystal structures of ligand-bound RLPs have not been solved.

The genomes of filamentous plant pathogenic fungi encode numerous, potentially secreted, small cysteine-rich proteins (SCRPs) which are generally defined as small proteins (less than 300 aa) with high cysteine content (number of cysteines exceeds 5% of the mature protein)[87]. With eight cysteine residues and 147 amino acids, SCP^{Ss} is thus a classical SCRP. However, the absence of any previously characterized protein domains hampers the prediction of its possible biological function. SCRPs often function as elicitors of plant immune responses or as virulence factors with multiple strategies or as both. In contrast to other known conserved SCRPs, such as Ecp proteins, cerato-platanin proteins or Avr proteins which rather act as effectors with or without additional PAMP activity[88–92], SCP^{Bc} and VmE02 don't contribute to virulence in *Botrytis cinerea* and *Valsa mali*, respectively[80,81]. Unlike above mentioned SCRPs, SCP^{Ss} is widely distributed across fungi and oomycete species, making SCP^{Ss} unique among so far described SCRPs. Two SCP^{Ss} homologs, SCP^{Bc} and SCP^{Pi} from *Botrytis cinerea* and *Phytophthora infestans*, respectively, can induce RLP30-dependent immunity (Fig. 17).

SCP^{Ss}-like sequences are not found in bacteria, yet RLP30 confers recognition of an SCP-like protein from both pathogenic and beneficial *Pseudomonas* strains and *rlp30* mutants are more susceptible to infection with *Pseudomonas phaseolicola*[93]. Hence, unlike RLP23, which detects conserved nlp20 sequences derived from NLPs across three microbial kingdoms, RLP30 is a unique receptor that can recognize unrelated ligands from fungi, bacteria and oomycetes (Fig. 17).

5.2 Convergent and rapid evolution of plant pattern recognition receptors

Notably, the functionality of known RLP-type PRRs is restricted to the plant species they were initially identified in or to closely related plant species. In *Arabidopsis*, these receptors include RLP1, RLP23, RLP32 and RLP42. Likewise, RLPs identified in solanaceous plants such as tomato ETHLYENE-INDUCING XYLANASE RECEPTOR EIX2, or Cf proteins detecting effectors from *Cladosporium fulvum* have not been found outside this plant species. However, RLP30-mediated SCP^{Ss} recognition systems are present in both Brassicaceae and Solanaceae, which is similar to FLS2 occurrence in various plant genera[28] and suggest that RLP30 is distinct from other identified immune-related RLPs.

Whereas RLP30-mediated perception in *Arabidopsis* requires intact SCP^{Ss}, Solanaceae receptors sense the N-terminal part containing two disulfide bonds, suggesting an independent evolution of the two distinct SCP^{Ss}-binding specificities in Brassicaceae and Solanaceae. Similarly, *Arabidopsis* FLS2 and tomato FLS2 and FLS3 detect immunogenic flagellin epitopes with different lengths. Surprisingly, unlike RLP30-mediated recognition of intact SCP^{Ss} in *Arabidopsis*, *Brassica* species sense a small immunogenic epitope independently of its tertiary structure. In general, such large differences of sensor systems occurs rather in remotely related plant families. Thus, the perception diversity for SCP^{Ss} in closely related species within the same plant genera reflects a rapid evolution of RLPs in Brassicaceae. Another example would be PG perception in *A. thaliana*, *A. arenosa* and *Brassica rapa*, which perceive immunogenic PG fragments pg9(At), pg20(Aa) and pg36(Bra), respectively. To date, we identified three distinct SCP^{Ss} sensing mechanisms in *Arabidopsis*, Brassica and Solanaceae.

The recognition of the same ligand SCP^{Ss} by two receptors (RLP30 and RE02) with low sequence similarity may be the result of convergent evolution. To investigate RLP30 and RE02 evolution, we analyzed the phylogenetic distribution of receptor proteins related to RLP30. In collaboration with Prof. Annette Becker, we calculated a detailed phylogeny based on a dataset comprising *A. thaliana* protein sequences, those of other Brassicaceae, Fabaceae, Solanaceae, grape vine (*Vitis vinifera*, member of the sister lineage to rosids and asterids), and *Amborella trichopoda* (the sister species to all other angiosperms) (Supplemental Fig. 4). Our data show a strong support for a sister group relationship of the RE02-like subfamily and the RLP30 subfamily with both subfamilies including members of *Amborella*. This indicates a split of the RLP30 and RE02 subfamilies in the lineage leading to the most recent common ancestor of all flowering plants, allowing these subfamilies to evolve independently for least 140 Million years[94]. Hence, SCP recognition arose from convergent evolution and evolved at least two times independently.

Moreover, RE02 and RLP30 have different protein structures with RE02 harboring 28 LRR motifs versus 21 LRRs in RLP30 and both proteins have highly divergent island domains. Based on the motif features within the island domain, RE02 (Kx_5Y motif) and RLP30 (Hx_8KG motif) are classified into two different clades[95]. Notably, the island domain of plant LRR-proteins was shown to participate in ligand binding, explaining the different structural

requirements of RLP30 and RE02 for SCP^{Ss} perception and the ability of RLP30 to recognize a bacterial SCP-like pattern.

Interestingly, the RE02-like subfamily does not include any malvid protein sequences, suggesting that malvids lost *RE02*-like genes, while in contrast RE02-like genes were copied multiple times in grape vine (Supplemental Fig. 4). Thus, compared to the Solanaceae, immunity against microbial pathogens in malvids, including Brassicaceae or Fabaceae, relies more strongly on *RLP30*-related genes. Unlike the RE02-like subfamily, members of the RLP30-like subfamily were retained in all species analyzed and show lineage-specific expansions, as predicted previously by pre-computed phylogenetic trees from PhyloGene[94]. Within the Brassicaceae, 30 *RLP30*-like genes are encoded by the *A. thaliana* genome. They form a monophyletic clade with other Brassicaceae genes supported by maximum bootstrap support, suggesting that they originate from a single gene copy in the lineage leading to Brassicaceae. Nested within the Brassicaceae-specific RLP30-related clade, the genes most closely related to RLP30 are found (RLP11, 12, 31, 36, 37, 38) which are also candidates for SCP recognition based on sequence similarity.

Although EIX2 and EIX1 are the two RLPs most homologous to RE02 in tomato[18], they cannot respond to SCP^{Ss} stimulation. We also tested several other candidates with high similarity to RE02, none of which are SCPs receptors. (data not shown), suggesting that different types or less similar receptors may drive recognition of the same SCP^{Ss} immune epitope in Solanaceae.

5.3 Engineering crops using RLPs

Transforming plant immune receptors into susceptible plants is an effective strategy for improving crop resistance. Some of the widely studied PRR and NLR-type receptors have been transferred to crops to improve their resistance. NLR receptors usually confer pathogen race-specific resistance, which means that the rapid evolution of most pathogens aims at evading recognition by plants carrying these NLRs and render these plants useless. Thus, stacking multiple NLR genes is a viable approach to engineer resistance, however, evolving pathogens remain a major threat to the effectiveness of transgenic NLRs.

In comparison, PRRs confer basal and broad resistance to pathogens since they recognize pathogen-derived molecular patterns that are generally thought to be conserved. As these PAMPs are often important for microbial lifestyle they are less prone to evolutionary changes. Therefore, it is feasible that interfamily transfer of PRRs across plant families might constitute a widely applicable strategy for improving immunity. This strategy is supported by previous reports on increased resistance to bacterial infections in wheat, apple, tomato and sweet orange plants expressing the *Arabidopsis* EFR receptor[96–99]. Unlike EFR, another widely studied RLK FLS2 is conserved in several plant species, and the perception of flg22 by FLS2 homologs varies among species, thus limiting its potential for engineering crop immunity. In addition to RLKs, many RLPs were also shown to have application potential, such as transfer of the elicitin receptor ELR from wild potato into cultivated potato which results in enhanced resistance to *P. infestans* infection[23]. Interfamily transfer of RXEG1 from *N. benthamiana* into

wheat confers Fusarium head blight resistance by sensing glycoside hydrolase 12 (GH12) family proteins secreted by *F. graminearum*[100]. However, these receptors only mediate the pattern recognition from specific pathogens, for example, while ELR and FLS only detect bacterial-derived PAMPs, ELR and XEG1 are involved in the recognition of patterns from fungi or oomycetes. Therefore, these receptors can only confer a specific single resistance to the respective stably transformed plants.

Two so far unique receptors, RLP23 and RLP30, mediate sensing of molecular patterns from three microbial kingdoms. Such a broad detection range predestined RLP30 and RLP23 as valuable genetic tools to boost crop immunity. Indeed, RLP23 transgenic potato plants exhibit more resistance to infection with the fungal pathogen *Sclerotinia sclerotiorum* and the oomycete *Phytophthora infestans*[5]. Our results demonstrate that expression of RLP30 in *N. tabacum* confers not only responsiveness to SCP^{Ss} and SCP-like, but also broad-spectrum resistance to bacterial, fungal and oomycete infections. Thus, enhanced broad-spectrum resistance may be engineered as compared to expressing single PRRs alone.

Notably, as co-expression with RLP30 and the co-receptor SOBIR1 confers enhanced immune output, we propose that co-expression of heterologous PRR/co-receptor pairs may be deployed to overcome putative incompatibilities of ectopically expressed PRRs. Incompatibilities between ectopically expressed PRRs and co-receptors from a different plant species may also explain the failure of many PRR transfers which are likely not due to the limitation of PRR immune function, but because they are not fully integrated into the immune system of the transformed host.

Overexpression of immune-related receptors often leads to autoimmune phenotypes, such as dwarfism, early flowering, and reduced yield. For example, SOBIR1 overexpression in *N. benthamiana* has been shown to induce autoimmune symptoms such as cell death. Neither of the two RLP30 transgenic lines exhibit autoimmune phenotypes as mock treatment did not induce ethylene accumulation and no elevated expression of salicylic acid or jasmonic acid marker genes could be detected in wildtype plants. However, we can't rule out that there are differences in other autoimmune events or that co-expression with other RLPs and SOBIR1 might cause autoimmunity.

Another strategy for improving the efficiency of engineering crop immunity is to deploy chimeric RLP receptor proteins generated by the fusion of a ligand binding domain of the target RLP and the transmembrane and/or cytoplasmic domain of a host or host-related RLP. Such approach would allow the hybrid receptor to utilize the host co-receptors. This hypothesis is supported by a study on Arabidopsis RLP1 which was only functional in *N. benthamiana* when expressed as a hybrid RLP made of *Arabidopsis* RLP1 and tomato EIX2[8]. Thus, for the long-term consideration of engineering crop immunity, especially ectopic expression of RLPs, we need to further understand the function of RLPs. Transfer of chimeric RLP-typed receptors into transgenic plants might not only confer a broad-spectrum resistance without autoimmune responses but may also improve functionality.

5.4 PTI and ETI crosstalk differs in *Arabidopsis* and *N. benthamiana*

PRR-mediated immunity and intracellular NLR-mediated immunity constitute the two major branches of the innate immune system in plants. Although their signaling pathways were initially thought to be qualitatively distinct, recent findings suggest a degree of crosstalk[75,76,78,79]. Here we show that SCP^{Ss}-induced signaling in *Arabidopsis* is dependent on the EDS1-PAD4–ADR1 node which has been previously reported to be involved in RLP23-, RLP32-, and RLP42-mediated immune responses, further solidifying that RLP-mediated defenses rely on ETI components (Fig. 17).

However, RE02-mediated early and late immune responses in *N. benthamiana*, as far as tested, do not require EDS1 complexes and RNLs. This is similar to an earlier report that EDS1 complexes are dispensable for Avr4/Cf4 signaling[101]. Dependence on the EDS1-RNL modules for RLP signaling might only be present in *Arabidopsis* and potentially other Brassicaceae species. Alternatively, EDS1-RNL modules in *N. benthamiana* could affect other SCP^{Ss}-induced defense responses apart from ethylene accumulation and cell death, but which were not tested here.

PTI-ETI crosstalk is largely associated with evolutionary trajectories and expansion of immune receptors, as the number of receptor genes encoding cell surface and intracellular immune receptors is predicted to be strongly correlated[102]. Intriguingly, while *Arabidopsis* possesses a large number of TNLs, *N. benthamiana* has relatively few TNLs but an expanded NRC family, implying that PRR-mediated signaling might be associated with NRCs. Indeed, our data together with a previous report demonstrate that NRC family is specifically required for cell death initiated by RLPs in *N. benthamiana*. NRCs is conserved in solanaceous species, suggesting that the association of RLP-mediated cell death signaling with the NRCs involved in ETI is conserved in Solanaceae. In tomato, SlNRC4a is required for xylanase-induced immunity and able to associate with its receptor EIX2[83]. Apart from the cell death response, NRCs seem not to be involved in PRR-mediated early immune responses, such ethylene accumulation and ROS burst[82,103]. This also equips Solanaceae with more defense selectivity against pathogen infections, such as NRC-dependent and NRC-independent immune responses.

Additionally, NRCs are structurally rather related to CNLs because they share a similar structure with the known CNL ZAR1. The pentameric “resistosome” assembled by ZAR1 acts as a Ca^{2+} channel, and a recent study has also shown that the predicted α1-helix of NRC3 can be functionally replaced by the ZAR1 α1-helix, which raises the possibility that induction of cell death downstream of RLP immune signaling involves an activated “resistosome”. Whether the activation of RLPs induces the formation of the NRC3 resistosome needs, however, to be demonstrated. Furthermore, SGT1, a core component of the CC-NLR-mediated hypersensitive cell death, is involved in RE02-mediated cell death but not for RLK signaling in *N. benthamiana*, further enhancing the possibility that the CNLs are involved in RLP immunity. This is consistent with the involvement of CC-type NRC3 in RE02 signaling instead of RLK-signaling by for instance FLS2.

Nicotinamide inhibits TIR enzymatic function while abolishing cell death induced by SCP^{Ss} or Avr4 and Avr9, suggesting that RLP-mediated cell death requires TIR enzymatic activity. A suite of small molecules produced by TNL oligomerization bind and activate the EDS1 complex, leading to the recruitment and activation of “helper” NLRs. Interestingly, RLP signaling does not depend on EDS1-RNL modules but the CC-typed “helper” NRCs. But the question remains, how the unknown TNL and the CNL NRCs do connect and mediate cell death signaling triggered by some RLPs (Fig. 17)?

The identification of which TNL(s) are involved in RLP signaling in *N. benthamiana* could be achieved by screening mutant libraries of TNLs. In *Arabidopsis*, loss of the TNL *sadr1* (Suppressor of ADR1-L2 1) completely suppresses stunted growth and defense gene expression activation induced by the autoactive ADR1-L2 DV protein by regulating the activity of ADR1-L2 DV at the level of Ca^{2+} influx. Strikingly, inhibition of TIR NADase function with NAM not only reduces Ca^{2+} level in TNL-RNL signaling but also affects CNL-induced Ca^{2+} level such as ZAR1. NRCs can form a pentameric resistosome similar to ZAR1, suggesting that the NRC3 resistosome might also function as Ca^{2+} channel. Therefore, we speculate that NAM inhibits TIR NADase function to prevent the production of small signaling molecules, thereby affecting Ca^{2+} influx mediated by the NRC resistosomes and resulting in the absence of a cell death response. This may explain why RLP signaling requires TNL-derived small molecules but not EDS1 that binds these small molecules. Interestingly, in animals cADPR, a small molecule substance catalyzed by the TIR domain, can regulate Ca^{2+} levels by modulating ryanodine receptors, a class of Ca^{2+} channels involved in calcium-induced calcium release[104]. Similarly, despite the absence of ryanodine receptors in plants, cADPR is also involved in Ca^{2+} regulation [105–107]. Notably, TIR domains are the only known proteins with ADPR cyclase activity in plants[108]. Finally, we hypothesize that *Arabidopsis* RLP signaling requires the EDS1-PAD4-ADR1 node, in contrast to *N. benthamiana* where a TNL-CNL tandem pathway regulates RLP-mediated cell death.

6 References

1. Jones, J. D. G. & Dangl, J. L. The plant immune system. *Nature* 444, 323–329 (2006).

2. Ngou, B. P. M., Ding, P. & Jones, J. D. G. Thirty years of resistance: Zig-zag through the plant immune system. *The Plant Cell* 34, 1447–1478 (2022).

3. Gust, A. A. & Felix, G. Receptor like proteins associate with SOBIR1-type of adaptors to form bimolecular receptor kinases. *Current Opinion in Plant Biology* 21, 104–111 (2014).

4. DeFalco, T. A. & Zipfel, C. Molecular mechanisms of early plant pattern-triggered immune signaling. *Molecular Cell* 81, 3449–3467 (2021).

5. Albert, I. *et al.* An RLP23–SOBIR1–BAK1 complex mediates NLP-triggered immunity. *Nature Plants* 1, 15140 (2015).

6. Zhang, L. *et al.* Distinct immune sensor systems for fungal endopolygalacturonases in closely related Brassicaceae. *Nat. Plants* 7, 1254–1263 (2021).

7. Zhang, W. *et al. Arabidopsis* RECEPTOR-LIKE PROTEIN30 and Receptor-Like Kinase SUPPRESSOR OF BIR1-1/EVERSHED Mediate Innate Immunity to Necrotrophic Fungi. *The Plant Cell* 25, 4227–4241 (2013).

8. Jehle, A. K. *et al.* The Receptor-Like Protein ReMAX of *Arabidopsis* Detects the Microbe-Associated Molecular Pattern eMax from *Xanthomonas*. *The Plant Cell* 25, 2330–2340 (2013).

9. Fan, L. *et al.* Genotyping-by-sequencing-based identification of Arabidopsis pattern recognition receptor RLP32 recognizing proteobacterial translation initiation factor IF1. *Nat Commun* 13, 1294 (2022).

10. Ghanbarnia, K. *et al.* Rapid identification of the Leptosphaeria maculans avirulence gene AvrLm2 using an intraspecific comparative genomics approach. *Molecular Plant Pathology* 16, 699–709 (2015).

11. Larkan, N. J. *et al.* The Brassica napus blackleg resistance gene LepR3 encodes a receptor-like protein triggered by the Leptosphaeria maculans effector AVRLM1. *New Phytologist* 197, 595–605 (2013).

12. Dixon, M. S., Golstein, C., Thomas, C. M., van der Biezen, E. A. & Jones, J. D. G. Genetic complexity of pathogen perception by plants: The example of Rcr3, a tomato gene required specifically by Cf-2. *Proceedings of the National Academy of Sciences* 97, 8807–8814 (2000).

13. Thomas, C. M. *et al.* Characterization of the tomato Cf-4 gene for resistance to Cladosporium fulvum identifies sequences that determine recognitional specificity in Cf-4 and Cf-9. *The Plant Cell* 9, 2209–2224 (1997).

14. Ron, M. & Avni, A. The Receptor for the Fungal Elicitor Ethylene-Inducing Xylanase Is a Member of a Resistance-Like Gene Family in Tomato. *The Plant Cell* 16, 1604–1615 (2004).

15. Bar, M., Sharfman, M., Ron, M. & Avni, A. BAK1 is required for the attenuation of ethylene-inducing xylanase (Eix)-induced defense responses by the decoy receptor LeEix1. *The Plant Journal* 63, 791–800 (2010).

16. Hegenauer, V. *et al.* The tomato receptor CuRe1 senses a cell wall protein to identify Cuscuta as a pathogen. *Nat Commun* 11, 5299 (2020).

17. Yin, Z. *et al. Nicotiana benthamiana* LRR-RLP NbEIX2 mediates the perception of an EIX-like protein from *Verticillium dahliae*. *J. Integr. Plant Biol* 63, 949–960 (2021).

18. Nie, J. *et al.* A receptor-like protein from Nicotiana benthamiana mediates VmE02 PAMP-triggered immunity. *New Phytologist* 229, 2260–2272 (2021).

19. Chen, Z. *et al.* Convergent evolution of immune receptors underpins distinct elicitin recognition in closely related Solanaceous plants. *The Plant Cell* 35, 1186–1201 (2023).

20. Wang, Y. *et al.* Leucine-rich repeat receptor-like gene screen reveals that Nicotiana RXEG1 regulates glycoside hydrolase 12 MAMP detection. *Nat Commun* 9, 594 (2018).

21. Sun, Y. *et al.* Plant receptor-like protein activation by a microbial glycoside hydrolase. *Nature* 610, 335–342 (2022).

22. Steinbrenner, A. D. *et al.* A receptor-like protein mediates plant immune responses to herbivore-associated molecular patterns. *Proceedings of the National Academy of Sciences* 117, 31510–31518 (2020).

23. Du, J. *et al.* Elicitin recognition confers enhanced resistance to Phytophthora infestans in potato. *Nature Plants* 1, 15034 (2015).

24. Dufayard, J.-F. *et al.* New Insights on Leucine-Rich Repeats Receptor-Like Kinase Orthologous Relationships in Angiosperms. *Frontiers in Plant Science* 8, (2017).

25. Zipfel, C. *et al.* Perception of the Bacterial PAMP EF-Tu by the Receptor EFR Restricts Agrobacterium-Mediated Transformation. *Cell* 125, 749–760 (2006).

26. Zipfel, C. *et al.* Bacterial disease resistance in Arabidopsis through flagellin perception. *Nature* 428, 764–767 (2004).

27. Sun, Y. *et al.* Structural Basis for flg22-Induced Activation of the Arabidopsis FLS2-BAK1 Immune Complex | Science 342, 624–628 (2013)

28. Hind, S. R. *et al.* Tomato receptor FLAGELLIN-SENSING 3 binds flgII-28 and activates the plant immune system. *Nat. Plants* 2, 16128 (2016).

29. Luu, D. D. *et al.* Biosynthesis and secretion of the microbial sulfated peptide RaxX and binding to the rice XA21 immune receptor. *Proceedings of the National Academy of Sciences* 116, 8525–8534 (2019).

30. Lei, W. *et al.* The pattern-recognition receptor CORE of Solanaceae detects bacterial cold-shock protein. *Nat. Plants* 2, 16185 (2016).

31. Ortiz-Morea, F. A. *et al.* Danger-associated peptide signaling in Arabidopsis requires clathrin. *Proceedings of the National Academy of Sciences* 113, 11028–11033 (2016).

32. Yamaguchi, Y., Huffaker, A., Bryan, A. C., Tax, F. E. & Ryan, C. A. PEPR2 Is a Second Receptor for the Pep1 and Pep2 Peptides and Contributes to Defense Responses in Arabidopsis. *The Plant Cell* 22, 508–522 (2010).

33. Hou, S. *et al.* The Secreted Peptide PIP1 Amplifies Immunity through Receptor-Like Kinase 7. *PLOS Pathogens* 10, e1004331 (2014).

34. Hou, S. *et al.* The Arabidopsis MIK2 receptor elicits immunity by sensing a conserved signature from phytocytokines and microbes. *Nat Commun* 12, 5494 (2021).

35. Rhodes, J. *et al.* Perception of a divergent family of phytocytokines by the Arabidopsis receptor kinase MIK2. *Nat Commun* 12, 705 (2021).

36. Wang, L. *et al.* The systemin receptor SYR1 enhances resistance of tomato against herbivorous insects. *Nature Plants* 4, 152–156 (2018).

37. Miya, A. *et al.* CERK1, a LysM receptor kinase, is essential for chitin elicitor signaling in Arabidopsis. *Proceedings of the National Academy of Sciences* 104, 19613–19618 (2007).

38. Cao, Y. *et al.* The kinase LYK5 is a major chitin receptor in Arabidopsis and forms a chitin-induced complex with related kinase CERK1. *eLife* 3, e03766 (2014).

39. Shimizu, T. *et al.* Two LysM receptor molecules, CEBiP and OsCERK1, cooperatively regulate chitin elicitor signaling in rice. *The Plant Journal* 64, 204–214 (2010).

40. Hayafune, M. *et al.* Chitin-induced activation of immune signaling by the rice receptor CEBiP relies on a unique sandwich-type dimerization. *Proceedings of the National Academy of Sciences* 111, E404–E413 (2014).

41. Chen, D. *et al.* Extracellular ATP elicits DORN1-mediated RBOHD phosphorylation to regulate stomatal aperture. *Nat Commun* 8, 2265 (2017).

42. Laohavisit, A. *et al.* Quinone perception in plants via leucine-rich-repeat receptor-like kinases. *Nature* 587, 92–97 (2020).

43. Gouhier, C. *et al.* Signalling of Arabidopsis thaliana response to Pieris brassicae eggs shares similarities with PAMP-triggered immunity. *Journal of Experimental Botany* 64, 665–674 (2013).

44. Alexander, K. *et al.* Bacterial medium-chain 3-hydroxy fatty acid metabolites trigger immunity in Arabidopsis plants. *Science* 364, 178–181 (2019)

45. Brutus, A., *et al*. A domain swap approach reveals a role of the plant wall-associated kinase 1 (WAK1) as a receptor of oligogalacturonides. *Proceedings of the National Academy of Sciences* 107, 9452–9457 (2010).

46. Gong, S. *et al.* The hijacking of a receptor kinase–driven pathway by a wheat fungal pathogen leads to disease. *Science* 2, 178–181 (2016)

47. Yuan, M. *et al.* PTI-ETI crosstalk: an integrative view of plant immunity. *Current Opinion in Plant Biology* 62, 102030 (2021).

48. Hai, C. *et al.* Effector-Triggered Immunity: From Pathogen Perception to Robust Defense | *Annual Review of Plant Biology* 66, 487-511 (2015).

49. Schultink, A., Qi, T., Lee, A., Steinbrenner, A. D. & Staskawicz, B. Roq1 mediates recognition of the Xanthomonas and Pseudomonas effector proteins XopQ and HopQ1. *The Plant Journal* 92, 787–795 (2017).

50. Botella, M. A. *et al.* Three Genes of the Arabidopsis RPP1 Complex Resistance Locus Recognize Distinct Peronospora parasitica Avirulence Determinants. *The Plant Cell* 10, 1847–1860 (1998).

51. Martin, R. *et al.* Structure of the activated ROQ1 resistosome directly recognizing the pathogen effector XopQ. *Science* 370, eabd9993 (2020).

52. Ma, S. *et al.* Direct pathogen-induced assembly of an NLR immune receptor complex to form a holoenzyme. *Science* 370, eabe3069 (2020).

53. Wan, L. *et al.* TIR domains of plant immune receptors are NAD+-cleaving enzymes that promote cell death. *Science* 365, 799–803 (2019).

54. Yu, D. *et al.* TIR domains of plant immune receptors are 2',3'-cAMP/cGMP synthetases mediating cell death. *Cell* 185, 2370-2386.e18 (2022).

55. Bhattacharjee, S., Halane, M. K., Kim, S. H. & Gassmann, W. Pathogen effectors target Arabidopsis EDS1 and alter its interactions with immune regulators. *Science* 334, 1405–1408 (2011).

56. Shi, H. *et al.* Identification and receptor mechanism of TIR-catalyzed small molecules in plant immunity. *Science* 377, Issue 6605 (2022)

57. Ao, J. *et al.* TIR-catalyzed ADP-ribosylation reactions produce signaling molecules for plant immunity. *Science* 377, Issue 6605 (2022)

58. Wang, G. *et al.* The Decoy Substrate of a Pathogen Effector and a Pseudokinase Specify Pathogen-Induced Modified-Self Recognition and Immunity in Plants. *Cell Host Microbe* 18, 285–295 (2015).

59. Wang, J. *et al.*Reconstitution and structure of a plant NLR resistosome conferring immunity. *Science* 364, Issue 3645 (2019) |

60. Bi, G. *et al.* The ZAR1 resistosome is a calcium-permeable channel triggering plant immune signaling. *Cell* 184, 3528-3541.e12 (2021).

61. Salcedo, A. *et al.* Variation in the AvrSr35 gene determines Sr35 resistance against wheat stem rust race Ug99. *Science* 358, 1604–1606 (2017).

62. Förderer, A. *et al.* A wheat resistosome defines common principles of immune receptor channels. *Nature* 610, 532–539 (2022).

63. Saile, S. C. & El Kasmi, F. Small family, big impact: RNL helper NLRs and their importance in plant innate immunity. *PLoS Pathog* 19, e1011315 (2023).

64. Ngou, B. P. M. *et al.* Estradiol-inducible AvrRps4 expression reveals distinct properties of TIR-NLR-mediated effector-triggered immunity. *Journal of Experimental Botany* 71, 2186–2197 (2020).

65. Sun, X. *et al.* Pathogen effector recognition-dependent association of NRG1 with EDS1 and SAG101 in TNL receptor immunity. *Nat Commun* 12, 3335 (2021).

66. Peart, J. R., Mestre, P., Lu, R., Malcuit, I. & Baulcombe, D. C. NRG1, a CC-NB-LRR Protein, together with N, a TIR-NB-LRR Protein, Mediates Resistance against Tobacco Mosaic Virus. *Current Biology* 15, 968–973 (2005).

67. Lapin, D., Bhandari, D. D. & Parker, J. E. Origins and Immunity Networking Functions of EDS1 Family Proteins. *Annu. Rev. Phytopathol.* 58, 253–276 (2020).

68. Zönnchen, J. *et al.* EDS1 complexes are not required for PRR responses and execute TNL-ETI from the nucleus in Nicotiana benthamiana. *New Phytologist* 236, 2249–2264 (2022).

69. Jacob, P. *et al.* Plant “helper” immune receptors are Ca^{2+} -permeable nonselective cation channels. *Science* 373, 420–425 (2021).

70. Wu, C.-H. *et al.* NLR network mediates immunity to diverse plant pathogens. *Proc. Natl. Acad. Sci. U.S.A.* 114, 8113–8118 (2017).

71. Wu, C.-H., Derevnina, L. & Kamoun, S. Receptor networks underpin plant immunity. *Science* 360, 1300–1301 (2018).

72. Adachi, H. *et al.* An N-terminal motif in NLR immune receptors is functionally conserved across distantly related plant species. *eLife* 8, e49956 (2019).

73. Contreras, M. P. *et al.* Sensor NLR immune proteins activate oligomerization of their NRC helpers in response to plant pathogens. *The EMBO Journal* 42, e111519 (2023).

74. Chang, M., Chen, H., Liu, F. & Fu, Z. Q. PTI and ETI: convergent pathways with diverse elicitors. *Trends in Plant Science* 27, 113–115 (2022).

75. Ngou, B. P. M., Ahn, H.-K., Ding, P. & Jones, J. D. G. Mutual potentiation of plant immunity by cell-surface and intracellular receptors. *Nature* 592, 110–115 (2021).

76. Yuan, M. *et al.* Pattern-recognition receptors are required for NLR-mediated plant immunity. *Nature* 592, 105–109 (2021).

77. Pruitt, R. N. *et al*. Plant immunity unified. *Nature Plants* 7, 382–383 (2021).

78. Tian, H. *et al.* Activation of TIR signalling boosts pattern-triggered immunity. *Nature* 598, 500–503 (2021).

79. Pruitt, R. N. *et al.* The EDS1–PAD4–ADR1 node mediates Arabidopsis pattern-triggered immunity. *Nature* 598, 495–499 (2021).

80. Nie, J., Yin, Z., Li, Z., Wu, Y. & Huang, L. A small cysteine-rich protein from two kingdoms of microbes is recognized as a novel pathogen-associated molecular pattern. *New Phytologist* 222, 995–1011 (2019).

81. Leisen, T. *et al.* Multiple knockout mutants reveal a high redundancy of phytotoxic compounds contributing to necrotrophic pathogenesis of Botrytis cinerea. *PLoS Pathog* 18, e1010367 (2022).

82. Halter, T. *et al.* The Leucine-Rich Repeat Receptor Kinase BIR2 Is a Negative Regulator of BAK1 in Plant Immunity. *Curr. Biol* 24, 134–143 (2014).

83. Imkampe, J. *et al*. The Arabidopsis Leucine-Rich Repeat Receptor Kinase BIR3 Negatively Regulates BAK1 Receptor Complex Formation and Stabilizes BAK1. *Plant Cell* 29, 2285–2303 (2017).

84. Kourelis, J. *et al.* The helper NLR immune protein NRC3 mediates the hypersensitive cell death caused by the cell-surface receptor Cf-4. *PLOS Genetics* 18, e1010414 (2022).

85. Leibman-Markus, M. *et al.* The intracellular nucleotide-binding leucine-rich repeat receptor (SlNRC4a) enhances immune signalling elicited by extracellular perception. *Plant Cell Environ.* 41, 2313–2327 (2018).

86. acob, P. *et al.* Broader functions of TIR domains in Arabidopsis immunity. *Proc. Natl. Acad. Sci.* 120, e2220921120 (2023).

87. Stergiopoulos, I. & De Wit, P. Fungal Effector Proteins. *Annual review of phytopathology* 47, 233–63 (2009).

88. van Esse, H. P., Bolton, M. D., Stergiopoulos, I., de Wit, P. J. G. M. & Thomma, B. P. H. J. The chitin-binding Cladosporium fulvum effector protein Avr4 is a virulence factor. *Mol Plant Microbe Interact* 20, 1092–1101 (2007).

89. Joosten, M. H., Vogelsang, R., Cozijnsen, T. J., Verberne, M. C. & De Wit, P. J. The biotrophic fungus Cladosporium fulvum circumvents Cf-4-mediated resistance by producing unstable AVR4 elicitors. *Plant Cell* 9, 367–379 (1997).

90. Ronnie, J. *et al.* Conserved Fungal LysM Effector Ecp6 Prevents Chitin-Triggered Immunity in Plants. *Science* 329, 953-955 (2010).

91. Frías, M., González, C. & Brito, N. BcSpl1, a cerato-platanin family protein, contributes to Botrytis cinerea virulence and elicits the hypersensitive response in the host. *New Phytol* 192, 483–495 (2011).

92. Yang, G. *et al.* A cerato-platanin protein SsCP1 targets plant PR1 and contributes to virulence of Sclerotinia sclerotiorum. *New Phytol* 217, 739–755 (2018).

93. Wang, G. *et al.* A Genome-Wide Functional Investigation into the Roles of Receptor-Like Proteins in Arabidopsis. *Plant Physiol.* 147, 503–517 (2008).

94. Zhang, P. *et al.* PhyloGenes: An online phylogenetics and functional genomics resource for plant gene function inference. *Plant Direct* 4, e00293 (2020).

95. Snoeck, S., Garcia, A. GK. & Steinbrenner, A. D. Plant Receptor-like proteins (RLPs): Structural features enabling versatile immune recognition. *Physiological and Molecular Plant Pathology* 125, 102004 (2023).

96. Lu, F. *et al.* Enhancement of innate immune system in monocot rice by transferring the dicotyledonous elongation factor Tu receptor EFR: EFR confers bacterial disease resistance in monocot rice. *J. Integr. Plant Biol.* 57, 641–652 (2015).

97. Lacombe, S. *et al.* Interfamily transfer of a plant pattern-recognition receptor confers broad-spectrum bacterial resistance. *Nat Biotechnol* 28, 365–369 (2010).

98. Mitre, L. K. *et al*. The Arabidopsis immune receptor EFR increases resistance to the bacterial pathogens Xanthomonas and Xylella in transgenic sweet orange. *Plant Biotechnology Journal* 19, 1294–1296 (2021).

99. Schwessinger, B. *et al.* Transgenic Expression of the Dicotyledonous Pattern Recognition Receptor EFR in Rice Leads to Ligand-Dependent Activation of Defense Responses. *PLoS Pathog* 11, e1004809 (2015).

100. Wang, Z. *et al.* Recognition of glycoside hydrolase 12 proteins by the immune receptor RXEG1 confers Fusarium head blight resistance in wheat. *Plant Biotechnology Journal* 21, 769–781 (2023).

101. Zönnchen, J. *et al.* EDS1 complexes are not required for PRR responses and execute TNL-ETI from the nucleus in *Nicotiana benthamiana*. *New Phytologist* 236, 2249–2264 (2022).

102. Ngou, B. P. M., Heal, R., Wyler, M., Schmid, M. W. & Jones, J. D. G. Concerted expansion and contraction of immune receptor gene repertoires in plant genomes. *Nat. Plants* 8, 1146–1152 (2022).

103. Wu, C.-H. *et al. NRC4* Gene Cluster Is Not Essential for Bacterial Flagellin-Triggered Immunity. *Plant Physiol.* 182, 455–459 (2020).

104. Woll, K. A. & Van Petegem, F. Calcium-release channels: structure and function of IP_3 receptors and ryanodine receptors. *Physiological Reviews* 102, 209–268 (2022).

105. Allen, G. J., Muir, S. R. & Sanders, D. Release of Ca2+ from individual plant vacuoles by both InsP3 and cyclic ADP-ribose. *Science* 268, 735–737 (1995).

106. Calum, L. *et al.* Abscisic acid-induced stomatal closure mediated by cyclic ADP-ribose. *PNAS* 95, 15837–15842 (1998).

107. Navazio, L., Mariani, P. & Sanders, D. Mobilization of Ca2+ by Cyclic ADP-Ribose from the Endoplasmic Reticulum of Cauliflower Florets. *Plant Physiology* 125, 2129–2138 (2001).

108. Abdul-Awal, S. M. *et al.* NO-Mediated [Ca2+] cyt Increases Depend on ADP-Ribosyl Cyclase Activity in Arabidopsis1. *Plant Physiol* 171, 623–631 (2016).

109. Huang, W. R. H., Schol, C., Villanueva, S. L., Heidstra, R. & Joosten, M. H. A. J. Knocking out SOBIR1 in Nicotiana benthamiana abolishes functionality of transgenic receptor-like protein Cf-4. *Plant Physiology* 185, 290–294 (2020).

7 Supplementary

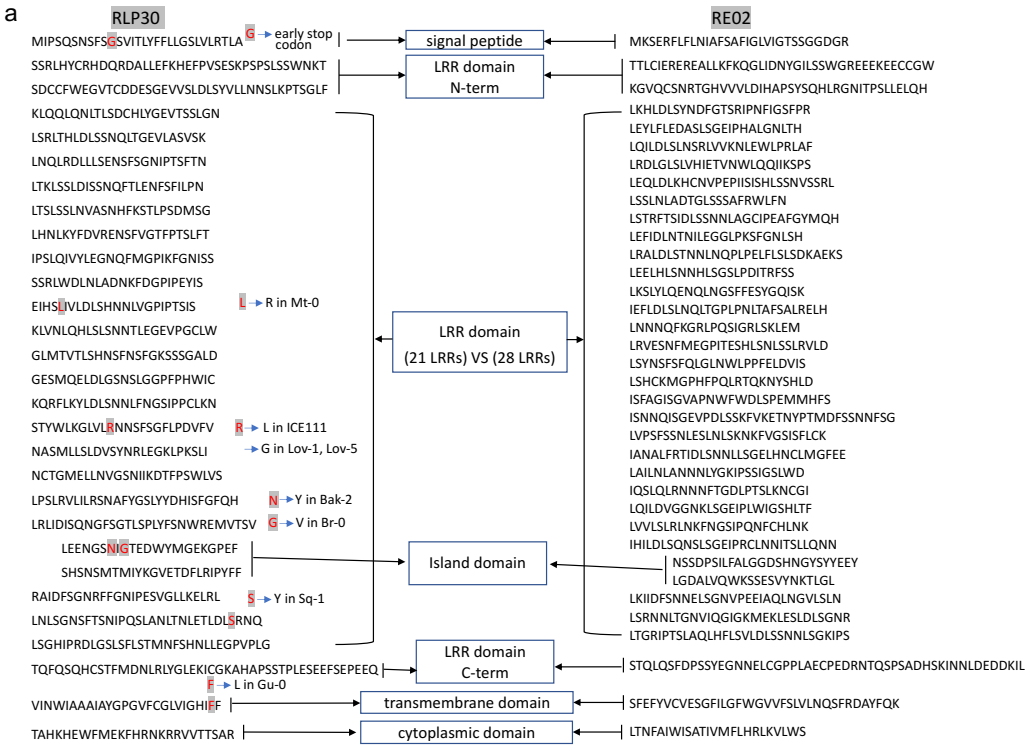

Supplementary Figure 1. Comparison of RLP30 and RE02 protein sequences.

a Protein sequence display of RLP30 and RE02. Amino acids marked in red in the RLP30 sequence indicate amino acid changes in accessions that are insensitive to SCP^{Ss}. b Protein sequence alignment performed by ClustalW, conserved residues between RLP30 and RE02 are shown in red.

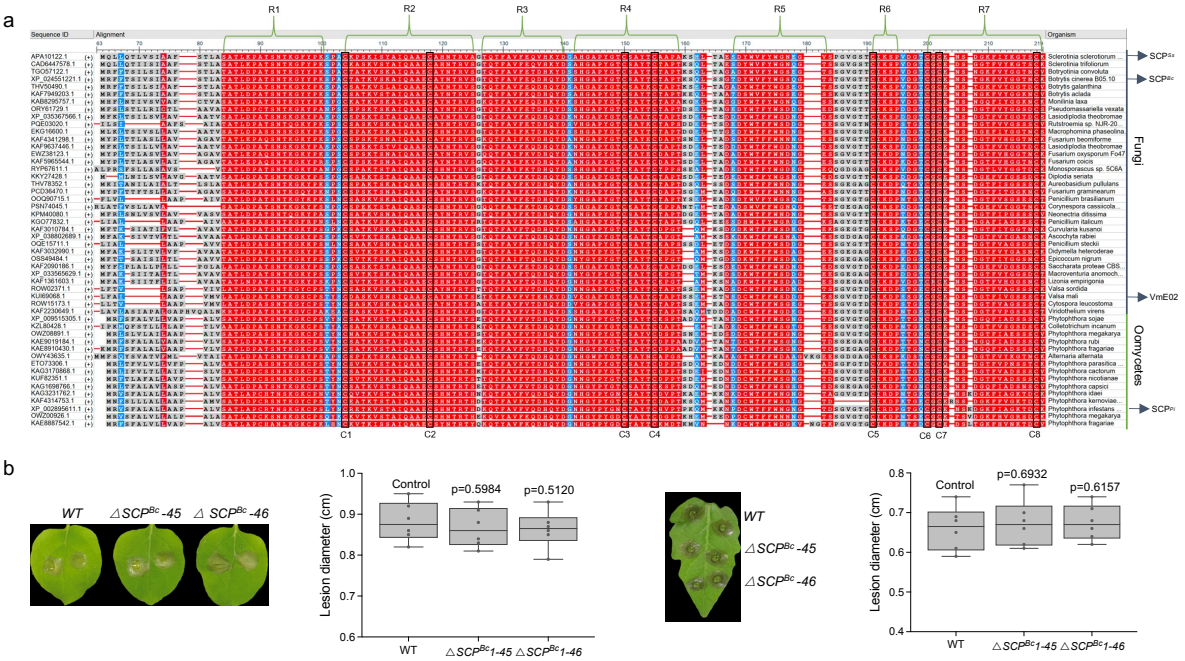

Supplementary Figure 2. SCP^{Ss} is conserved in fungi and oomycetes and not involved in pathogenicity. a, Amino acid alignment of SCP^{Ss} (top sequence) and its homologous sequences (Protein IDs given on the left) from the species indicated on the right. Conserved regions in red and conserved cysteine residues are numbered at the top (R1 to R7) and bottom (C1 to C7), respectively. **b,** Lesion formation of two independent *B. cinerea* depletion mutants of *SCP^{Bc}* (also named *Bcplp1*[81]) on *N. benthamiana* or tomato leaves 48 hours post inoculation and determination of lesion size.

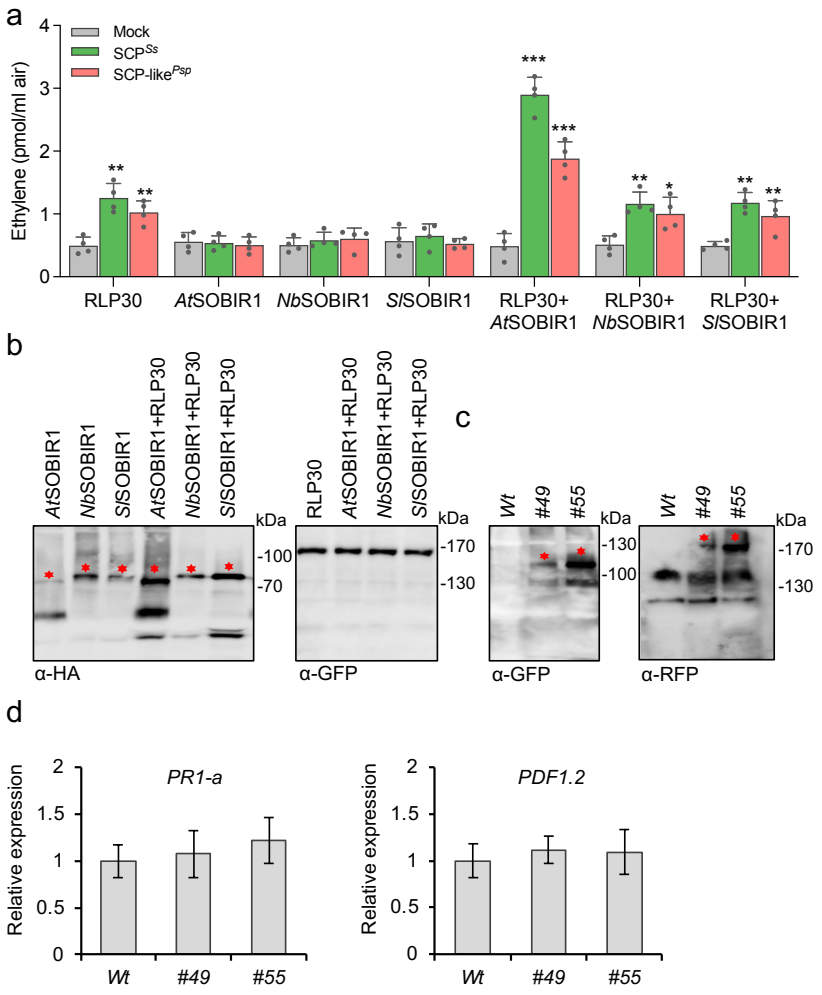

Supplementary Figure 3. AtSOBIR1 co-expression enhances RLP30 function in *N. tabacum*.

a, Ethylene accumulation in *N. tabacum* plants transiently expressing RLP30-GFP and/or SOBIR1 from *Arabidopsis* (*At*), *N. benthamiana* (*Nb*) *or S. lycopersicum* (*Sl*), either alone or in the indicated combination and treated for 4 h with water (mock), 1 µM SCP^{Ss}, or 1.5 µg/ml SCP-like^{Psp}. Data points are indicated as dots (n = 6) and plotted as box plots (centre line, median; bounds of box, the first and third quartiles; whiskers, 1.5 times the interquartile range; error bar, minima and maxima). Statistically significant differences from mock treatments in the respective plants are indicated (two-sided Student's t-test, *$P \leq 0.05$, **$P \leq 0.01$, ***$P \leq 0.001$). **b** Western Blot analysis with protein extracts from *N. tabacum* leaves transiently expressing RLP30-GFP and/or AtSOBIR1-HA, NbSOBIR1-HA or SlSOBIR1-HA as shown in (**a**) using an anti-GFP antibody for RLP30 detection and an anti-HA antibody for SOBIR1 detection. **c** Western Blot analysis with protein extracts from two independent *N. tabacum* lines (*#49* and *#55*) stably expressing RLP30-RFP and AtSOBIR1-GFP using tag-specific antisera. The asterisks indicate the position of epitope-tagged proteins. **d** RT-qPCR analysis in tobacco lines #49 and #55 stably expressing RLP30-RFP and AtSOBIR1-GFP using gene specific primers for indicated defense-related marker genes. Expression of marker genes was normalized to the levels of *NtACT9* transcript and are presented relative to the wild-type control which was set to 1. Statistically significant differences were determined using a two-sided Student's t-test, differences were not significant. All experiments were repeated three times with similar results.

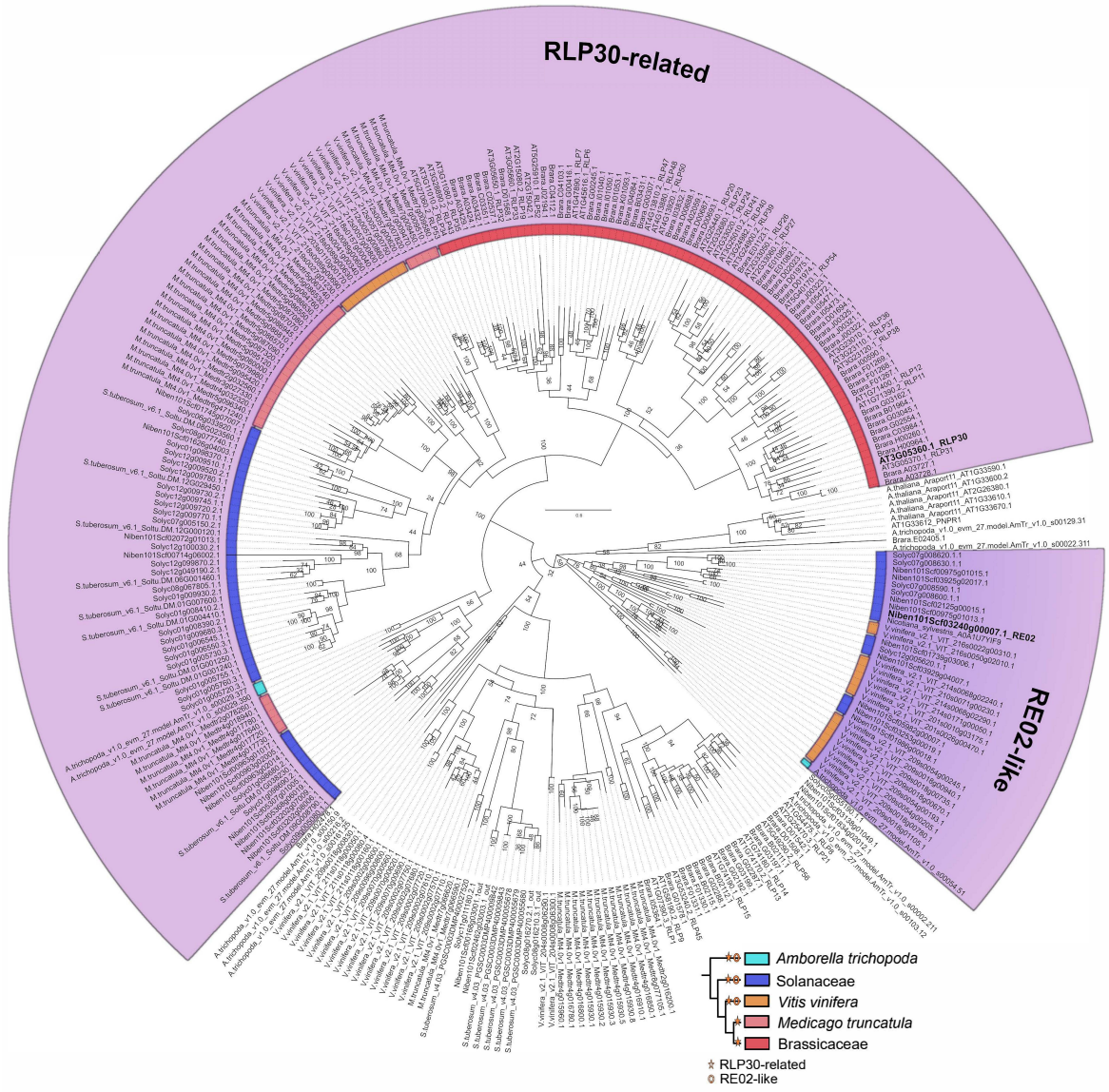

Supplementary Figure 4. Evolutionary relation of RLP30 and RE02.

The Midpoint rooted Maximum-likelihood phylogeny includes sequences of *A. trichopoda, S. lycopersicum, S. tuberosum, N. benthamiana, N. sylvestris, V. vinifera, M. tuncatula, B. rapa* and *A. thaliana*. The least deep node that includes sequences of *A. trichopoda*, indicating independent evolution for more than 140 mya, defines clades of RLP30-related and RE02-like proteins. The evolutionary history of *RLP30*-related genes is highly complex due to several lineage specific gene duplications and likely losses; since our phylogeny only covers a limited number of taxa, we named the clade that includes RLP30 as RLP30-related. The phylogenetic tree was generated and explained by Mr. Clemens Rössner and Prof. Annette Becker.

Tables

Table 1: *Arabidopsis* lines used in the thesis

Line (*Arabidopsis*)	Description	Reference
rlp30-2	Insertion, SALK_008911	7
sobir1-12	Insertion, SALK_050715, *sobir1-12*	5
bak1-5 bkk1-1	Double mutant of bak1-5 and SALK_044334	5
bir2	Insertion, GK-793F12	82
bir2-OE	*bir2*, complemented with YFP-tagged BIR2	82
bir3	Insertion, Salk_116632	83
bir3-OE	*bir3*, complemented with YFP-tagged BIR3	83
pbl30	Insertion, SAIL_296_A06, also known as cst-2	79
pbl31	Insertion, SAIL_273_C01	79
pbl32	Insertion, SALK_113804	79
pbl30,31	Insertions, SAIL_296_A06, SAIL_273_C01	79
pbl30,31,32	Insertions, SAIL_296_A06, SAIL_273_C01, SALK_113804	79
eds1	Polymorphism 1009135505, eds1-2, introgressed into Col-0	79
pad4	Polymorphism, 4770301, pad4-1	79
sag101	Insertion, *sag101*-2	79
adr1 triple	Insertions, *adr1-1* (SAIL_842_B05), *adr1-L1-1* (SAIL_302_C06) and *adr1-L2-4* SALK_126422)	79
nrg1 double	NRG1.1 and NRG1.2 CRISPR/Cas9 deletion mutant	79
30-2/RLP30-YFP	*rlp30-2*, complemented with YFP-tagged RLP30	This study
30-2/NbRE02-GFP	*rlp30-2*, complemented with GFP-tagged NbRE02	This study
30-2/SlEIX1-GFP	*rlp30-2*, complemented with GFP-tagged SlEIX1	This study
30-2/SlEIX2-GFP	*rlp30-2*, complemented with GFP-tagged SlEIX2	This study
fls2 efr	Double mutant of SAIL_691_C4 and SALK_044334	9
rlp32-2	Insertion, SM_3_33092	9
rlp23-1	At2g32680, Insertion, SALK_034225	5

Table 2: *N. benthamiana* lines used in the thesis

Line (*N. benthamiana*)	Description	Reference
sobir1/sobir1-like	knockout of SOBIR1 and SOBIR1 like	109
eds1	EDS1 CRISPR/Cas9 deletion mutant	101
pad4	PAD4 CRISPR/Cas9 deletion mutant	101
epss	knockout of EDS1, PAD4, SAG101a and SAG101b	101
adr1 nrg1	ADR1 and NRG1 CRISPR/Cas9 deletion mutant	101
nrc2/3-1.3.1	knockout of NRC2 and NRC3 line 1.3.1	84
nrc2/3-3.3.1	knockout of NRC2 and NRC3 line 3.3.1	84
nrc2/3/4-4.3.1	knockout of NRC2, NRC3 and NRC4 line 4.3.1	84
nrc2/3/4-5.5.1	knockout of NRC2, NRC3 and NRC4 line 5.5.1	84
nrc4-1.2.1	knockout of NRC4 line 1.2.1	84

Table 3: Primers used for cloning

Template	Expression in	Primer name	Primer sequence (5' – 3')
NbRE02	*rlp30-2* *N. tabacum,* *N. benthamiana*	B_RE02-F	tatggtctcatctgaacaATGAAAAGTGAGAGATTT
		D_RE02-R	ttggtctctccttACTCCAGAGCACCTTCAATCTGTG
RLP30, *All accessions*	*N. tabacum,* *N. benthamiana*	RLP30-F	ATGATTCCAAGCCAATCTAATTCC
		RLP30-R	ACGAGCACTTGTGGTGACTAC
SCP^{Ss}	*N. benthamiana* apoplast	SCP-N_F	CATTTACGAACGATAGGGTACCCCCATGCAACTCCTCCAAACCC
		SCP-N_R	TGCTCACCATGGATCCGTCGACCCCTTTACAAGAAGTCCCCTTGTAGATAAAC
SCP^{Ss} *SCP^{Ss}* (C1-7S)	*Pichia pastoris*	SCP-P_F	CGGAATTCATGACCCTCAAACCCGCTACCTC
		SCP-P_R	GCTCTAGACCTTTACAAGAAGTCCCCTTGTAGATAAACTTACC
SCP^{Ss} (C8S)	*Pichia pastoris*	SCP$^{C8\text{-}S}$-P_F	GCGGAATTCATGACCCTCAAACCCGCTACCTC
		SCP$^{C8\text{-}S}$-P_R	GCTCTAGACCTTTAGAAGAAGTCCCCTTGTAGATAAACTTACC
SCP^{Ss} *SCP^{Ss}* (C1-7-S)	*N. benthamiana*	SCP-N_F	CATTTACGAACGATAGGGTACCCCCATGCAACTCCTCCAAACCC
		SCP-N_R	TGCTCACCATGGATCCGTCGACCCCTTTACAAGAAGTCCCCTTGTAGATAAAC
SCP^{Ss} (C8S)	*N. benthamiana*	SCP$^{C8\text{-}S}$-_F	CATTTACGAACGATAGGGTACCCCCATGCAACTCCTCCAAACCC
		SCP$^{C8\text{-}S}$-_R	TGCTCACCATGGATCCGTCGACCCCTTTAGAAGAAGTCCCCTTGTAGATAAACTTACC
SCP^{Bc}	*Pichia pastoris*	SCP^{Bc}-P_F	CGGAATTCATGCTCGACCCCGCTACCTCAAAC
		SCP^{Bc}-P_R	GCTCTAGACCCTTGCAGTTCGTTCCTCCATAAACAAAC
SCP^{Pi}	*Pichia pastoris*	SCP^{Pi}-P_F	CGGAATTCATGGCTCCTTGCCGCACCAATAG

		SCP^{Pi}-P_R	GCTCTAGACCTTTGCAGTCCGTCTTGCCG
SCP^{Ss} (C1C5)	*Pichia pastoris*	SCP^{C1C5}P_F	CGGAATTCATGACCCTCAAACCCGCTACCTC
		SCP^{C1C5}P_R	GCTCTAGACCAATACAAGTCGAGCCCACACCA
SCP^{Ss} (C3C8)	*Pichia pastoris*	SCP^{C3C8}P_F	CGGAATTCATGACTTGTTCCGCTTATACCTGTGCT
		SCP^{C3C8}P_R	GCTCTAGACCTTTACAAGAAGTCCCCTTGTAGATAAACTTACC
SCP^{Ss} (C1C4)	*Pichia pastoris*	SCP^{C1C4}P_F	CGGAATTCATGGCTTGCAAACCAAGCAAAATCTCC
		SCP^{C1C4}P_R	GCTCTAGACCAGCACAGGTATAAGCGGAACAAG

Table 4: Constructs used in the thesis

Constructs	Tag	Description
ppizαZA-SCP^{Ss} , SCP$^{C\text{-}S}$, SCP^{C1C5} or SCP^{C3C8}	His	Expression of SCP from *S. sclerotiorum*, SCP^{Ss} with individual cysteine to serine mutations, C1C5 or C3C8 peptides in *Pichia pastoris*
ppizαZA-A-SCP^{Bc} or SCP^{Pi}	His	Expression of SCP from *B. cinerea* and *P. infestans* in *Pichia pastoris*
pBIN-SCP^{Ss}	GFP	Expression of SCP^{Ss} in *N. benthamiana*
Pfec006- SCP^{Ss}	Myc	Expression of SCP^{Ss} in *N. benthamiana*
pB7FWG2-RLP23	GFP	Expression in *N. benthamiana*
pGWB5-RLP30	GFP	Expression in *A. thaliana, N. benthamiana* and *N. tabacum*
pGWB14-AtSOBIR1, NbSOBIR1 or SlSOBIR1	HA	Expression in *N. tabacum*
pB7RWG2.0-RLP30	RFP	Stable transformation in *N. tabacum* and *A. thaliana*
pGWB5-SOBIR1	GFP	Stable transformation in *N. tabacum*
pGWB5-RLP30 (From SCP-insensitive ecotypes)	GFP	Expression in *N. benthamiana*
LII_F_1-2_-_BB10-RE02, SlEIX1 or SlEIX2	GFP	Expression in *N. benthamiana* or Stable transformation in *A. thaliana*
pBIN-avr4	no	Expression in *N. benthamiana*
pBIN-Cf4	no	Expression in *N. benthamiana*
pBIN-avr9	no	Expression in *N. benthamiana*
pBIN-Cf9	no	Expression in *N. benthamiana*
pGGA1:XopQ	GFP	Expression in *N. benthamiana*

Table 5: Ms data of SCFE1

Protein ID	detected unique peptides per protein	Sequence coverage [%]	Mol. weight [kDa]	Sequence length [amino acid count]	signal peptide present	cysteines	Cysteine content [cysteines/seq.length in %]
Sscle06g048920	2	17	15,481	147	yes	8	5,4
Sscle10g077860	2	18,8	21,712	191	no	1	0,5
Sscle12g090490	2	6,5	26,041	245	yes	5	2
Sscle06g050580	2	13,4	26,089	238	yes	4	1,7
Sscle01g009200	2	12,1	28,531	273	yes	5	1,8
Sscle16g108160	6	19,9	34,201	327	yes	3	0,9
Sscle09g073350	2	5,3	37,229	339	yes	10	2,9
Sscle16g108170	3	3,7	37,672	380	yes	8	2,1
Sscle10g080050	6	12,6	40,184	358	yes	4	1,1
Sscle14g099090	5	16,5	41,639	375	no	4	1,1
Sscle03g030530	8	21,9	42,399	397	no	3	0,8
Sscle04g040020	2	4,8	48,544	475	yes	11	2,3
Sscle03g028450	9	17,3	49,123	445	yes	4	0,9
Sscle02g017490	2	1,8	62,841	605	yes	8	1,3
Sscle11g085960	2	5,2	66,699	611	yes	6	1
Sscle10g080270	19	30,2	67,026	616	yes	10	1,6
Sscle08g063080	13	23,9	67,41	610	yes	8	1,3
Sscle15g106280	3	6,2	68,529	632	yes	6	0,9
Sscle14g100060	2	4,9	69,742	613	no	9	1,5
Sscle06g050510	3	6,7	72,965	669	yes	9	1,3
Sscle07g057170	2	5,2	99,173	907	yes	12	1,3
Sscle09g074570	4	4,2	109,64	1012	yes	2	0,2

Protein ID	MS intensity (iBAQ) in SCFE1 fraction B9	MS intensity (iBAQ) in SCFE1 fraction B11	MS intensity (iBAQ) in SCFE1 fraction B12	MS intensity (iBAQ) in SCFE1 fraction B13	MS intensity (iBAQ) in SCFE1 fraction B15
Sscle06g048920	0	3349300	10808000	10764000	0
Sscle10g077860	0	1958400	626520	1260200	0
Sscle12g090490	47343000	273220000	102210000	116290000	0
Sscle06g050580	0	0	270780	1350500	0
Sscle01g009200	769810	178500	0	0	638100
Sscle16g108160	790000000	584600000	326300000	376090000	13573000
Sscle09g073350	0	1079300	113530	267700	0
Sscle16g108170	0	121680000	5940700	4476100	810830
Sscle10g080050	525860	162740000	384270000	1745000000	730920000
Sscle14g099090	977170	1847300	1657100	1846100	3282500
Sscle03g030530	290420	303070000	151640000	695190000	24978000
Sscle04g040020	0	3365600	2651900	4968400	0
Sscle03g028450	0	4928200	6765900	19093000	0
Sscle02g017490	0	747520	879350	2244900	0
Sscle11g085960	0	6739000	0	10596000	0
Sscle10g080270	12583000	245180000	423460000	570200000	16638000
Sscle08g063080	28634000	109240000	61576000	80709000	6074600
Sscle15g106280	583570	1179100	1547600	4099900	490000
Sscle14g100060	104900	556270	943020	2439600	1364000
Sscle06g050510	0	242100	0	1844300	1419800
Sscle07g057170	0	36568	0	370790	0
Sscle09g074570	0	1325600	1280500	1194200	0

8 List of Abbreviations

aa	Amino Acid
ADP	Adenosine Diphosphate
ATP	Adenosine Triphosphate
ADR1	Activated Disease Resistance 1
Avr4/Avr9	Avirulence 4/9
BAK1	Brassinosteroid Insensitive 1 - Associated Receptor Kinase 1
BIR2/3	Bak1-Interacting Receptor-Like Kinase 1/2/3
cADPR	Cyclic ADP-Ribose
CEBiP	Chitin Oligosaccharide Elicitor-Binding Protein
CERK1	Chitin Elicitor Receptor Kinase 1
Cf4/9	*Cladosporium Fulvum* Resistance Protein 4/9
CNL	Coiled-Coil (CC)-Nucleotide-Binding LRR (NLR)
CORE	Cold Shock Protein Receptor
CuRe1	Cuscuta Receptor 1
cryo-EM	Cryo-Electron Microscopy
DAMP	Damage Associated Molecular Pattern
DMSO	Dimethylsulfoxide
DTT	Dithiothreitol
EC50	Half-Maximal Response
EDS1	Enhanced Disease Susceptibility 1
EFR	Elongation Factor Tu Receptor
EF-Tu	Elongation Factor Tu
EIX1/2	Ethylene-Inducing Xylanase Receptor 1/2
ELR	Elicitin Response Protein
eMAX	Enigmatic MAMP In Xanthomonas
ETI	Effector-Tiggered Immunity
ETS	Effector-Triggered Susceptibility
flg22	22 aa Peptide of Bacterial _Agellin Protein
FLS2	Flagellin Sensing 2
FLS3	Flagellin Sensing 3
FPLC	Fast-Protein Liquid Chromatography
GC	Gas Chromatography
GFP	Green Fluorescent Protein
HAMP	Herbivore Associated Molecular Pattern

HopQ1	The Hrp Outer Protein Q
HR	Hypersensitive Response
IF1	Translation Initiation Factor 1
INF1	*Phytophthora Infestans* Elicitin *1*
INR	Inceptin Receptor
LORE	Lipooligosaccharide-Specific Reduced Elicitation
LRR	Leucine-Rich Repeat
LYK	Lysm Containing Receptor-Like Kinase
LysM	Lysin Motif
MAMP	Microbe-Associated Molecular Pattern
MAPK	Mitogen-Activated Protein Kinase
MIK2	Male Discoverer 1-Interacting Receptor-Like Kinase 2
MS	Mass Spectrometry;
NLP	Necrosis and Ethylene-Inducing Peptide 1-Like Proteins
NLR	Nucleotide-Binding Leucine-Rich Repeat
NRG1	Nrequirement Gene 1
OG	Oligogalacturonide
PAD4	Phytoalexin Defect 4
PAGE	Polyacrylamid-Gelelektrophorese
PAMP	Pathogen-Associated Molecular Pattern
PG	Polygalacturonase
PBL1	PBS1-Like Kinase
PEPR1	Pep1 Receptor1
PRR	Pattern Recognition Receptor
PTI	PAMP-Triggered Immunity
RKS1	Resistance Related Kinase 1
RLCK	Receptor-Like Cytoplasmic Kinase
RLK	Receptor Like Kinase
RLP	Receptor Like Protein
RNL	RPW8-Like Coiled-Coil (CC_R) Domain NLR
ROQ1	Recognition of Xopq 1
ROS	Reactive Oxygen Species
RPP1	Recognition of *Peronospora Parasitica*1
RXEG1	Response To XEG1
SAG101	Senescence-Associated Gene 101
SALK	Salk Institute Genomic Analysis Laboratory
SCFE1	*Sclerotinia* Culture Filtrate Elicitor1

SCOOP	Serine-Rich Endogenous Peptides
SDS	Sodium Dodecyl Sulfate
SGT1	Suppressor of G2 Allele of Skp1
SERK	Somatic Embryogenesis Receptor
SOBIR1	Suppressor of Bir1 (Bak1-Interacting Receptor-Like Kinase 1)
Sr35	Stem Rust Resistance Gene 35
SYR	Systemin Receptor
TIR	Toll-Interleukin 1 Receptor
TNL	TOLL-INTERLEUKIN 1 RECEPTOR (TIR)-NLR Receptor
VmE02	*Valsa Mali* Elicitor 2
WAK1	Wall-Associated Kinase 1
XA21	*Xanthomonas* Resistance 21
XopQ 1	*Xanthomonas* Outer Protein Q
ZAR1	Hopz-Activated Resistance 1
2′,3′-cAMP	2′,3′-Cyclic Adenosine Monophosphate
2′,3′-cGMP	2′,3′-Cyclic Guanosine Monophosphate

9 List of figures

10 Acknowledgments

On the occasion of the completion of my thesis, I would like to express my sincerest gratitude to all those who have helped and encouraged me during my four-year doctoral career.

First of all, I am very grateful to my supervisor, Dr. Andrea Gust, who gave me an opportunity to do doctoral training and showcase my scientific research talents. The achievements I achieved during my Ph.D would have ceased to exist without her guidance, help, encouragement and affirmation. She always believed in me, gave me opportunities to participate in the review of publications, made me the corresponding author and gave me sufficient academic freedom, which is crucial for my future independent scientific research career. I still remember and often think back to the scene when I first met her at Stuttgart Airport on October 22, 2019. I am very proud to be her Ph.D in the beautiful city of Tübingen.

As a member of Prof. Thorsten Nürnberber's team, I am very grateful for his every guidance and advice. His academic insights and passion for scientific research have always inspired me. The first paper on the plant-microbe interaction that I read in my scientific career in 2016 was his article on RLP23 published in Nature Plants. How incredible and amazing I joined this team three years later and worked together on plant immunity.

I would like to especially thank our technician, Mrs. Birgit Löffelhardt. She always does a lot of work for us silently, preparing culture media, constructing plasmids, transforming plants, etc., even though she often communicates with me in German inadvertently, haha. We are very lucky to have such a versatile technician. I would also express my gratitude to every member of our team, former or current colleagues. They gave me a lot of suggestions and discussions, and also learned a lot from them. We spent a lot of happy time together, such as hiking, BBQ, drinking, and cooking.

Thanks to the ZMBP facilities team for helping me a lot, for example our secretary Mrs. Liane Schön who helped prepare the work contracts and financial work, Mr. Dieter Steinmetz who handled all the computer problems easily, Mrs. Caterina Brancato who helped me with tomato transformation and our gardeners who prepare the soil, harvests seeds, cares for my plants, etc. With their contributions, I can focus more on my research.

I am also grateful to my collaborators who provided me with tremendous support and help. They are Dr. Christina E. Steidele, Prof. Georg Felix, Prof. Matthias Hahn, Prof. Paulo J.P.L. Teixeira, etc. I also would like to thank the researchers who have shared experimental materials with us.

Finally, I am very grateful to my family. Regardless of success, failure, happiness, or loss, they are my strongest supporters and give me their unreserved and selfless love. I feel so guilty that I haven’t been with them these past four years due to the COVID-19 pandemic. I would also like to thank my wife, who is my spiritual support and the source of my efforts. She always believed that I could become an excellent scientist. In the last words at the end of this thesis, I would like to express my gratitude to myself. No matter the failure of the experiment, the discomfort of living in a foreign country, or the loneliness of being far away from my relatives, I persevered and turned it into the motivation to face life and scientific research positively.